Aus dem Veterinärwissenschaftlichen Department
der Tierärztlichen Fakultät der Ludwig-Maximilians-Universität München

Arbeit angefertigt unter der Leitung von Univ.-Prof. Dr. med. vet. Eckhard Wolf

Angefertigt an der Fakultät für Chemie und Pharmazie, Lehrstuhl für Pharmazeutische Biotechnologie der Ludwig-Maximilians-Universität München

(Univ.-Prof. Dr. Ernst Wagner)

Innovative cancer therapeutics based on polymers or biogenic drugs evaluated in murine tumor models

Inaugural-Dissertation

zur Erlangung der tiermedizinischen Doktorwürde

der Tierärztlichen Fakultät

der Ludwig-Maximilians-Universität München

von

Laura Schreiner

aus

Saarlouis

München 2013

Gedruckt mit der Genehmigung der Tierärztlichen Fakultät

der Ludwig-Maximilians-Universität München

Dekan: Univ.-Prof. Dr. Joachim Braun

Referent: Univ.-Prof. Dr. Eckhard Wolf

Korreferenten: Univ.-Prof. Dr. Hermann Ammer
Univ.-Prof. Dr. Kaspar Matiasek
Univ.-Prof. Dr. Johannes Hirschberger
Priv.-Doz. Dr. Sabine André

Tag der Promotion: 09. Februar 2013

Meiner Familie

TABLE OF CONTENTS

I. INTRODUCTION

Cancer is a major cause of morbidity and mortality worldwide. In 2008, more than 7 million people died in consequence of their tumor burden[1] and the incidence of cancer is even predicted to increase over the next few years.[2, 3] There is a range of therapeutic options including conventional methods like surgery, chemotherapy and radiotherapy, but also immunotherapy, hormone therapy, hyperthermia and other supportive treatments. However, the unsatisfying cure rate and the occurring side effects of established treatment methods propel the research in cancer therapy. The aim is to improve common therapies, to combine them with more innovative therapeutics, and to evaluate novel medical techniques and drug technologies against cancer.

Therefore, we investigated three promising anticancer approaches *in vivo*: specific and targeted polymer based siRNA therapy; novel nature-derived anticancer compounds; and polymer conjugated chemotherapeutics. Each of these therapeutic concepts generated promising *in vitro* results, before it was further evaluated in different mouse models. The experiments and results presented in this thesis have promise for further improvements in the fight against cancer.

1. Tumor targeted siRNA delivery

1.1. Nucleic acid therapy

Various diseases are caused by an alteration of the genetic material of single cells. In consequence, the encoded proteins can lose their functionality, entailing genetic diseases. Medicinal nucleic acids have been developed over the last decades[4] in order to treat diseases caused by altered genes, like cardiovascular,[5] neurological[6] and infectious[7] disorders as well as cancer.[8, 9] With these agents, genetically altered cells can be manipulated or cured through nucleic acid delivery. Thus, a mutated gene can be replaced or a new gene can be introduced by plasmid DNA (pDNA) or a gene can be silenced by RNA delivery or inactivated by antisense oligonucleotides.

During the past 20 years, oligonucleotide and gene therapy has been strongly explored and many clinical trials, with a focus on cancer diseases, have been carried out.[10] Within cancer therapy, the translation of messenger RNA (mRNA), responsible for tumor growth and metastasis or essential for cell survival, can be blocked. On the other hand, genes, encoding growth and migration hampering proteins, can be introduced or upregulated by affecting their opponent proteins.

Gene therapy has already been successful, for example, in the treatment of patients with a blood-coagulation disorder (hemophilia B) or with a degenerative eye disease, called Leber congenital amaurosis (LCA).[11, 12] However, the main difficulty in nucleic acid therapy and therefore, the reason for its still limited therapeutic use lies within the delivery of the nucleic acids.[13]

1.2. siRNA therapy

RNA delivery leads to a post transcriptional inhibition of gene expression by genetic interference.[14] For this purpose, a specific double-stranded RNA (dsRNA) can be introduced into cells.[15] In 2001, 21-nucleotide RNA duplexes, called small interfering RNA (siRNA), were identified as gene-specific therapeutics, which do not (or to a much lesser extent) induce inflammatory responses like long dsRNA does.[16]

Nowadays, the single steps of RNA interference (RNAi) and the resulting gene silencing are very well explored.[17] After entering the cell, the antisense strand of siRNA is incorporated by the so called RNA-induced silencing complex (RISC), whereas the sense strand is released and degraded.[18] The antisense strand enables

RISC to identify the complementary mRNA, resulting in its cleavage by an activated RNase (Figure 1).[19] Therefore, siRNAs can be used as a tool for sequence-specific knockdown and thus, they are a promising instrument in cancer therapy.

In 2002, the therapeutic potential of siRNA was shown for the first time in an *in vivo* experiment.[20] siRNA itself has an untargeted distribution, is rapidly degraded in the bloodstream[21] and cleared by the kidneys.[22] Additionally, the negative charge of siRNA hinders the crossing of cellular membranes. Therefore, safe delivery systems have to be developed for effective siRNA therapy.[23]

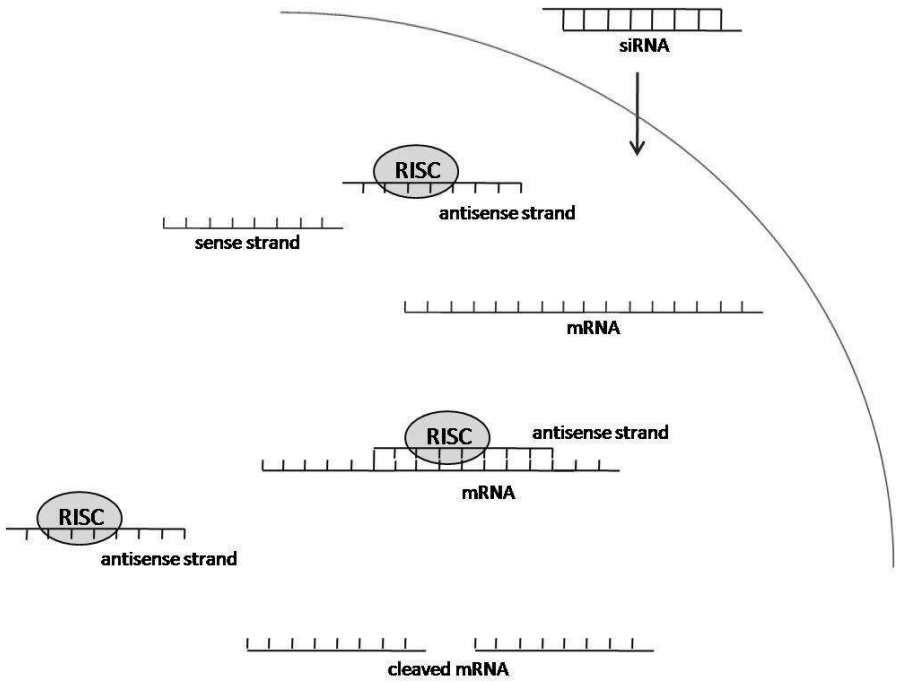

Figure 1: Mechanism of gene silencing by siRNA. In the cytosol, siRNA is incorporated into the RISC complex and the dsRNA is spliced into single strands. The sense strand is released and degraded. The antisense strand enables RISC to identify and cleave a complementary mRNA. The RISC-antisense strand complex remains stable during this process and can attach to a new corresponding mRNA.

1.3. Obstacles in nucleic acid delivery

To overcome the problems of oligonucleotide delivery and to enable the medical use of nucleic acids, various carriers have been investigated in recent years. Delivery systems have to overcome several extracellular and intracellular obstacles. In the extracellular environment, vectors have to protect the nucleic acids against degradation and must form stable complexes. After systemic injection, they need to shield the nucleic acids from interactions with diverse

blood components, for example albumin, erythrocytes, immune cells and enzymes. At the same time, the complexes have to circulate without being directly cleared by the kidneys or liver.[24] The carrier system has to target specific cell types, like tumor cells, and overcome the cell membrane for being internalized. Intracellular, the complexes have to escape out of the endosome and the nucleic acid has to be released from the vector for being active in the cytoplasm or nucleus, in case of pDNA. Additionally, the carrier systems have to be non-toxic, non-immunogenic and non-pathogenic.[25]

1.4. The range of delivery systems

Carriers are primarily categorized into viral and synthetic vectors.[26] Viruses can be utilized as nucleic acid transporters by replacing part of their genome with a therapeutic gene. They are very efficient delivery systems with the highest potency concerning gene transfection. Nevertheless, their therapeutic use is limited by several negative characteristics, especially their inflammatory, safety and immunogenic effects.[27] The restricted payload capacity of viruses and the complexity of production are additional disadvantages.[28] Therefore, the synthesis of non-viral vectors for oligonucleotide delivery is the main focus in this part of research.

To benefit from the positive properties of both, viruses and synthetic vectors, virus-like carrier systems are investigated.[29-31] The most promising artificial viruses are liposomes[32] and polymers.[28, 33] Liposomes are synthetic vesicles, consisting of a hydrophilic core enclosed in one or more lipid bilayers. Cationic polymers bind nucleic acids through electrostatic interactions with the negatively charged phosphate backbone. Polycations, like the gold standard linear polyethylenimine (LPEI),[34] are commonly utilized in nucleic acid delivery. After endocytosis, these polyplexes reach the cytoplasm through endosomal disruption, caused by the so called proton sponge effect.[35] These initial polyplexes bear several problems, like activation of the immune system[36] and quick detection by the reticuloendothelial system.[37] Additionally, they have toxic side effects caused by their molecular weight, as well as their cationic charge,[38] and a lack of efficiency compared to viral vectors. The functionality and safety of polyplexes can be improved by adding several substructures for shielding, targeting and endosomal escape to the polymeric backbone.[39] Figure 2 shows the critical delivery steps of such polyplexes.

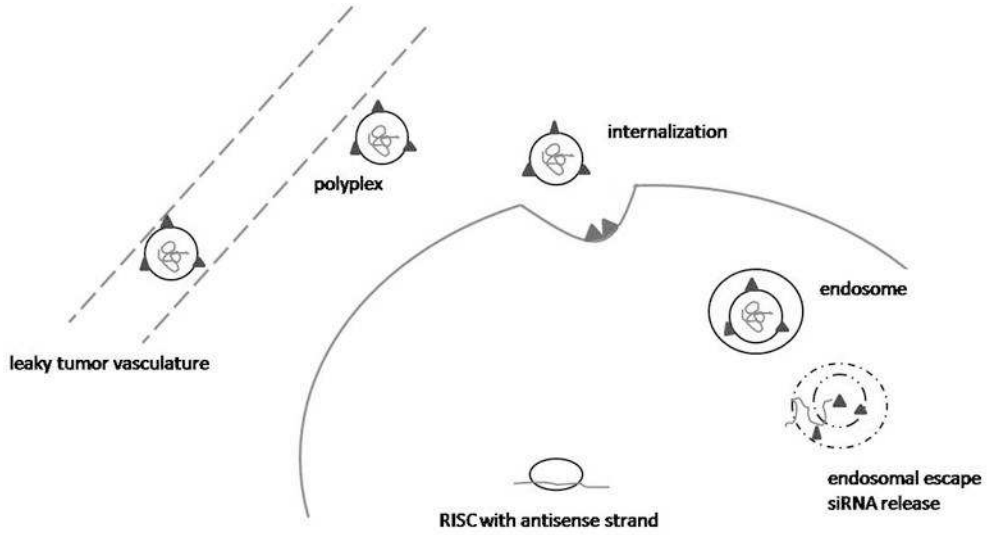

Figure 2: Steps of siRNA delivery by shielded and targeted polyplexes. After systemic injection, polyplexes reach the tumor site through the leaky vasculature and their active targeting. By local application, polyplexes directly reach the extracellular environment of the tumor tissue. The targeting ligands bind to the appropriate receptors and lead to internalization of the polyplexes into the tumor cell. Polyplexes induce endosomal disruption and the siRNA is released into the cytosol and can be incorporated into the RISC complex.

1.5. Precise multifunctional polycations

The difficulty in polymer development is to build a carrier system, which is precise, highly efficient and can be reproducibly synthesized, and is at the same time multifunctional. It was a huge progress in precise vector synthesis, when Hartmann *et al.* designed defined polycationic structures and further on, libraries of polycations with clear structure-activity relationships were generated.[40-42] The functionality of these polymers was improved by the work of Dohmen *et al.*, adding several substructures to the polycationic backbone or the siRNA itself. Figure 3 shows the synthesized polymer under investigation in the current thesis.

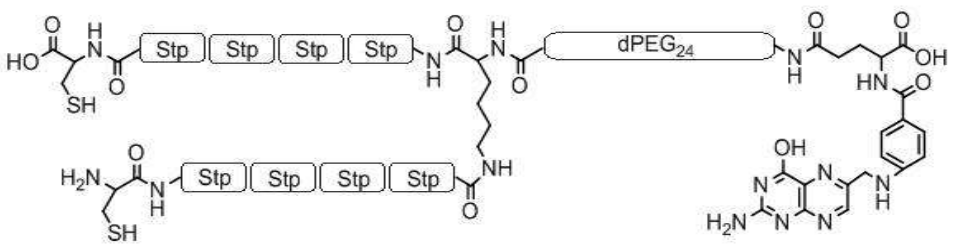

Figure 3: Folic acid targeted defined polymer. FolA-PEG_{24}-K(Stp_4-C)$_2$.

The synthesis was based on a linear backbone consisting of polyamino-amides, using Stp (16-amino-4-oxo-5,8,11,14-tetraaza-hexadecanoic acid) as building block.[41] Cysteines were incorporated to increase polyplex stability by disulfide formation. For shielding, and therefore preventing unwanted interactions of the polyplexes in the body, polyethylene glycol (PEG) was attached by means of a branching lysine. To target the synthesized vectors to folate receptor overexpressing tumor cells, folic acid was incorporated as target ligand. The endosomolytic domain Inf7,[43] which is highly lytic at endosomal pH, was covalently bound to the siRNA itself to ensure the endosomal escape of the polyplexes. These modifications led to nano sized multifunctional polyplexes for receptor mediated siRNA delivery.[44]

2. Myxobacterial compounds as natural anticancer drugs

2.1. Natural products as pharmaceutical compounds

Natural products play an important role in drug discovery and have been the origin of more than 80% of therapeutic drugs in former times.[45, 46] Despite the increase of alternative drug discovery methods nowadays, natural products are still of particular importance and are basis for every second approved drug since 1994.[47]

They are used for the production of various pharmaceuticals, in particular of anticancer and anti-infective drugs like doxorubicin, paclitaxel and penicillin.[48] The benefits of natural compounds are their broad therapeutic effects, their diversity of chemical structures and their increased absorption compared to synthetic drugs. The disadvantages are among other things, the difficulty of a continuous supply and their chemical complexity.[47]

Natural products derive from animals, plants or microbial sources. Within microbes, fungi and terrestrial actinomycetes are the best-studied source, producing a wide range of secondary metabolites.[49] However, looking for novel natural products, various microbes are investigated in recent decades with a growing interest in cyanobacteria,[50] marine actinomycetes[51, 52] and myxobacteria.[53]

2.2. Myxobacteria and their bioactive secondary metabolites

Myxobacteria are gram-negative bacteria and belong to the delta group of proteobacteria. These microbes are able to live in various habitats including the sea,[54, 55] but are mainly residing in soil.[56, 57] Myxobacteria have special characteristics, like the ability to move actively by gliding on a surface[58] and to form multicellular fruiting bodies, when resources are becoming scarce.[59] Another remarkable characteristic is the production of a wide range of secondary metabolites, which are well explored these days.[53]

In 1947, it was first described that myxobacteria have an antibiotic activity.[60] Thirty years later, in 1977, the first secondary metabolite, ambruticin, was isolated from a myxobacterium.[61] Through the work of Reichenbach and Hoefle, myxobacteria have gained increasing attention during the last two decades as producers of several biological active secondary metabolites.[62] These products often have unusual structural elements and target cell structures, which are rarely or not targeted by other metabolites.[63] Therefore, they often own a complete novel mode of action.[64] There need to be further investigations on why myxobacteria produce this range of secondary metabolites, but it is assumed that they protect their habitat in the highly competitive terrestrial environment.[65]

To date, there are more than 60 families of myxobacterial compounds identified.[64] Besides their antifungal (54%) and antibacterial (29%) bioactivity, myxobacterial metabolites are also cytotoxic towards mammalian cells.[66] Therefore, myxobacterial products are of great interest in cancer therapy.

They are the research topic of the DFG network FOR 1406 (Prof. Vollmar/Prof. Müller "Exploiting the Potential of Natural Compounds: Myxobacteria as Source for Leads, Tools, and Therapeutics in Cancer Research") to which our lab (Prof. Wagner) contributes.

Most of the reported cytostatic metabolites of myxobacteria interact with the eukaryotic cytoskeleton. They can promote (e.g. epothilone[67]) or inhibit (e.g. tubulysin[68]) tubulin polymerization or interfere with actin polymerization (e.g. chondramide[69]). Other compounds, for example apicularen or archazolid, are cytotoxic, as they inhibit vacuolar ATPases (V-ATPases) of mammalian cells.[70, 71]

2.2.1. Archazolid

Archazolid (Figure 4) is a macrolactone, isolated from the myxobacteria *Archangium gephyra and Cystobacter violaceus*.[71]

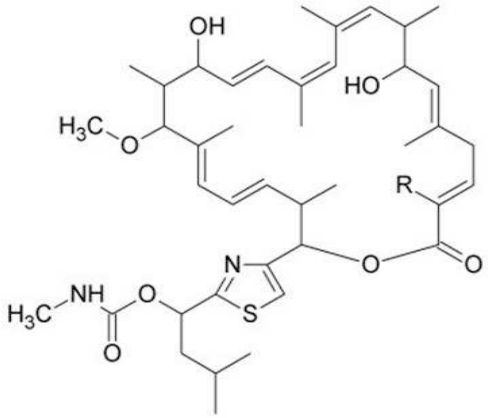

Figure 4: Chemical structure of archazolid A and B. Archazolid A, R = CH_3; archazolid B, R = H.

Archazolid targets V-ATPases of eukaryotic cells. These ATP-dependent proton pumps are ubiquitous in endomembranes and often occur in cell plasma membranes. They regulate the proton concentration in the intracellular acidic compartments and the cytoplasm of diverse cells. V-ATPases consist of a membrane bound V_0 domain for proton translocation and a catalytic V_1 domain that is directed towards the cytosol.[72] Beside cytoplasmic pH homeostasis, V-ATPases are involved in various cellular processes, including receptor mediated endocytosis and intracellular transport.[73]

Additional to their normal incidence, these proton pumps are overexpressed within the plasma membrane of various malignant tumor types, acidifying the extracellular space.[74] Several tumor cells degrade the extracellular matrix through the secretion of lysosomal enzymes. These enzymes have a significant higher activity in an acidic environment. Therefore, the V-ATPase is suspected to be involved in tumor invasiveness and migration.[73, 75]

Before archazolid was identified, potent V-ATPase inhibitors like the plecomacrolides bafilomycin and concanamycin were already discovered in the early eighties.[76-78] Archazolid inhibits V-ATPases very specific and effective with IC_{50} values in the low nanomolar range.[72] Its efficacy is comparable to the efficacy of these two well established compounds named above.

In vitro, archazolid impairs as well tumor cell proliferation as tumor cell migration through the inhibition of V-ATPases.[79, 80] These results are promising for further *in vivo* investigations of this myxobacterial compound.

2.2.2. Pretubulysin

Pretubulysin (Figure 5) is a precursor of the myxobacterial product tubulysin, which is produced by *Archangium gephyra* and *Angiococcus disciformis*.[49]

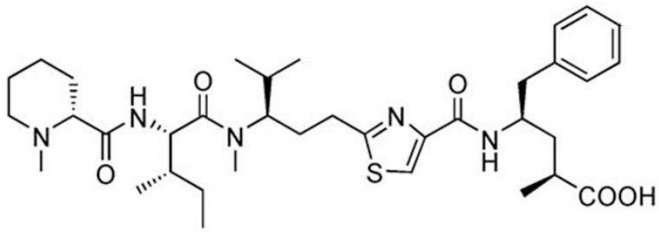

Figure 5: Chemical structure of pretubulysin.

Tubulysins are a family of nine myxobacterial products that interact with the eukaryotic cytoskeleton.

The yield of the synthetic production of pretubulysin is higher compared to tubulysin, as it has a less complex structure. This reduces the supply problems, which are typical for natural compounds due to their high chemical complexity. Fortunately, despite this structural simplification, pretubulysin loses only little efficacy in the inhibition of cell proliferation and migration compared to tubulysin and still has a subnanomolar activity.[81]

The cytotoxicity of pretubulysin is based on the inhibition of the polymerization of tubulin to microtubules.[82] Microtubules form the spindle apparatus and are therefore essential for the separation of chromosomes during mitosis. Besides mitosis, microtubules are also necessary for intracellular transports and cell movements. Thus, hampering tubulin polymerization leads to a reduction of cell proliferation and migration.

Compared to other tubulin interfering natural compounds, like epothilones and taxol, tubulysins even have a 20- till 100-fold higher efficacy on hampering cell growth.[81] Epothilones have already been demonstrated to be effective *in vivo* against multidrug resistant tumors.[83] In 2012, the Vollmar group together with our group (Rath *et al.*) first proved the efficacy of pretubulysin concerning tumor growth inhibition in a murine HuH7 tumor model.[84]

2.2.3. Chondramide

Chondramides (Figure 6) are peptides, produced by the myxobacteria *Chondromyces crocatus*.[69]

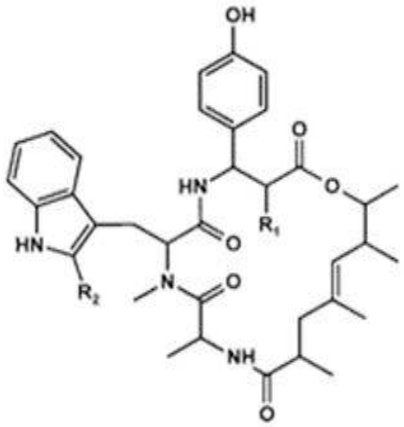

Figure 6: Chemical structure of chondramide. Chondramide A, R^1 = OMe, R^2 = H; chondramide B, R^1 = OMe, R^2 = Cl; chondramide C, R^1 = H, R^2 = H; chondramide D, R^1 = H, R^2 = Cl.

These peptides induce the polymerization of the multi-functional protein actin. Actin polymerization and depolymerization is not only necessary for the process of chemotaxis, but also for cytokinesis. Interfering with these procedures leads to a dysfunction in cell migration and proliferation. After epothilone[85] and rhizopodin,[86, 87] the chondramides had been the third class of myxobacterial metabolites that interfere with the cytoskeleton of eukaryotic cells.[88]

Closer related are the chondramides to jasplakinolide, a natural compound, isolated from marine sponges of the genus *Jaspis*[89] that induces actin polymerization. Already years ago, chondramide was identified to reduce cell growth of different cell lines *in vitro*.[69] Sasse *et al.* compared the efficacy of chondramide and jasplakinolide on cell growth inhibition and showed that the IC_{50} values of these two compounds are relatively similar and in the nanomolar range.[88] As jasplakinolides have already shown to hamper tumor metastasis in animal experiments,[90] this could be a hint that chondramide has an *in vivo* anticancer efficacy as well.

3. Polymer formulations of chemotherapeutics

3.1. The drawbacks of chemotherapeutics

Cytostatic drugs play an important role in cancer therapy, but their clinical use is still limited. Conventional chemotherapeutics distribute randomly in the body when injected systemically and have poor tumor selectivity. This leads to a low therapeutic efficacy and strong toxic side effects, restricting their application and preventing an increase in cancer cure rate in recent years.[91, 92] The underlying cause is that most cytostatic drugs, being low-molecular-weight substances, are able to diffuse out of the blood circulation into any tissue, where they hamper cell division (mitosis). Fast dividing cells of the bone marrow, the digestive tract and hair follicle are especially affected besides tumor cells, leading to typical toxicity like myelosuppression, mucositis and hair loss. For a safe and more effective application, chemotherapeutics need to be guided to the tumor tissue. Besides active targeting, anticancer drugs can be targeted passively[93, 94] through the attachment to a polymeric carrier. Consequently, the molecular weight of the drug is increased and the pharmacokinetics change radically.[95] This enables tumor-specific targeting and reduces the access to healthy tissue due to the "enhanced permeability and retention" (EPR) effect.[96]

Another obstacle, limiting the efficacy of chemotherapy, is the development of chemoresistance. Resistance to anticancer drugs can be intrinsic and exist before the treatment, or tumors can become resistant during chemotherapeutic application. When resistance is acquired, tumors may become resistant not only to the currently used drug, but also to other therapeutics with different modes of action.[97] There are diverse mechanisms of drug resistance, including active efflux of chemotherapeutics out of the tumor cell through ABC transporters, alteration of drug-target interaction and changes in cellular response like increased DNA repair mechanisms, tolerating stress conditions and defects in apoptotic pathways. [98-100] An individual tumor can use one or more of these mechanisms against chemotherapeutics, making their administration ineffective. It is believed that chemoresistance is responsible for about 90% of therapeutic failure in metastatic cancer treatment.[97]

3.2. EPR effect

In 1986 Matsumura and Maeda first reported the EPR effect (Figure 7).[101]

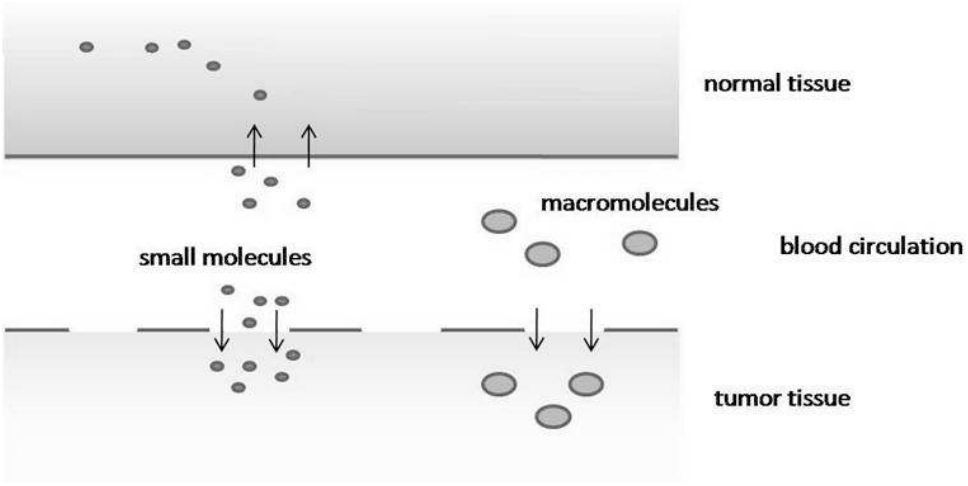

Figure 7: Passive tumor targeting due to the EPR effect. Small molecules are able to diffuse out of the blood circulation into any tissue. Macromolecules however, can only pass leaky tumor endothelium, missing the ability to diffuse through normal endothelial cells. Reaching the tumor, macromolecules accumulate and remain in this tissue, as tumors have an impaired lymphatic drainage.

This effect is based on a special morphology of tumor vessels. As tumors are rapidly growing, they need an increased amount of nutrients and oxygen. To ensure a sufficient supply, tumors possess several pathophysiological characteristics, like intense angiogenesis,[102, 103] hypervasculature with defective, leaky vessels and a reduced lymphatic drainage.[104] These characteristics enable macromolecules to reach the tumor site through leaky vessels and accumulate in the tumor tissue due to the impaired lymphatic drainage. As macromolecules are unable to penetrate through tight endothelial junctions of normal vessels and are not rapidly cleared by the kidneys due to their large size, these tumor characteristics can be used for passive tumor targeting.[105, 106] Small molecules in contrast, pass through the endothelium of normal blood vessels into any tissue. This leads to an unspecific body distribution and a short plasma half-life due to fast renal clearance.

To benefit from the EPR effect, low-molecular-weight anticancer drugs are conjugated to polymers, enhancing the efficacy of the drugs and decreasing their side effects. Additionally, the polymeric conjugation reduces the renal clearance and prolongs the circulation time, which plays an important role for passive drug

targeting.[107, 108] Thus, the drug concentration in the tumor tissue can reach a 10-30 times higher level than in the blood circulation.

Since its first description, the EPR effect is basis for modifications of diverse anticancer therapeutics,[109-111] including several drugs that are already evaluated in clinical trials.[112, 113]

3.3. Polymer-anticancer drug conjugates

The term polymer therapeutics[114] includes polymeric drugs, polyplexes, polymeric mycelles, polymer-protein conjugates and polymer-drug conjugates.[112] Thereby, the polymer has always the function of guiding its binding partner to its therapeutic target.

Ringsdorf first described polymer-anticancer drug conjugates in 1975.[115] These conjugates always include a water soluble polymeric carrier, a biodegradable linker and an antitumor drug.[116] The polymeric conjugation enhances the solubility of hydrophobic drugs[117] and improves their pharmacokinetic characteristics.[118] The circulation time is prolonged, the clearance hampered and the drug passively targeted to the tumor tissue through the EPR effect. Additionally, the polymer can protect the drug against degradation[119] and can overcome multidrug resistance (MDR), as macromolecules can accumulate in tumor cells without being recognized by the permeability glycoprotein (P-glycoprotein), one of the main mediators of multidrug resistance.[120]

To ensure an improvement of the drugs' efficacy, polymers need to meet several requirements. They have to be non-toxic, non-immunogenic and to carry an appropriate drug payload, bound over a stable linker that releases the drug at the target are. In addition, their molecular weight has to be high enough to enable a long circulation time.[121] If these prerequisites are fulfilled, an active targeting ligand can be introduced[122, 123] but is not absolutely necessary.

Since the first synthetic polymer-anticancer conjugate entered clinical trial in 1994,[116] several more have followed.[124-126] Anticancer conjugates, containing for example doxorubicin,[127] paclitaxel[128] or camptothecin,[129] are the most investigated conjugates in clinical trials.[130] Despite this fact, none of these structures is on the market until now.

3.4. Polymer-melphalan conjugates

Chemotherapy formerly started with the discovery of the cytotoxic effect of nitrogen mustards at Yale in 1942.[131] Nitrogen mustards, including the chemotherapeutic melphalan hydrochloride, are nonspecific DNA alkylating agents. Melphalan was first introduced more than 50 years ago and has a wide spectrum of antitumor activity.[132, 133] It is used for the treatment of various tumors, but bears several disadvantages, like nonspecific distribution, low bioavailability, drug resistance and side effects including bone marrow suppression, vomiting and hair loss. The first synthesized polymer-drug conjugates already contained, among some other drugs, melphalan. Since then, various melphalan conjugates have been developed.[134, 135]

Polymers with repeating phosphoester in the backbone are highly biocompatible and similar to bio-macromolecules such as nucleic acids, and therefore popular in polymeric conjugate synthesis.[136-138] Thus, melphalan was covalently or non-covalently bound to three biodegradable and water soluble polyphosphoesters (Figure 8 - Figure 10) for the current study. In Conjugate 1, melphalan was covalently immobilized by reacting with poly(oxyethylene H-phosphonate). Complex 2 consisted of electrostatic complexes of negatively charged polyphosphodiester poly(hydroxyoxyethylene phosphate) and positively charged protonated melphalan. In Complex 3, melphalan was hydrogen-bonded to the polyphosphotriester poly(methyloxyethylene phosphate).

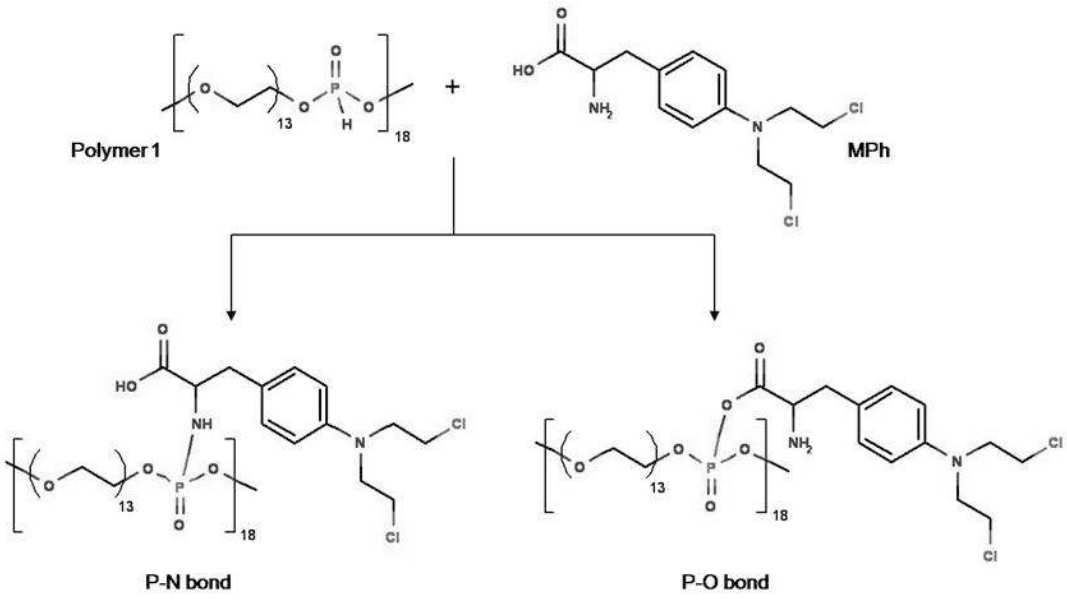

Figure 8: Conversion of polyphosphonate and melphalan into Conjugate 1 (formation of P-N and P-O covalent bonds).

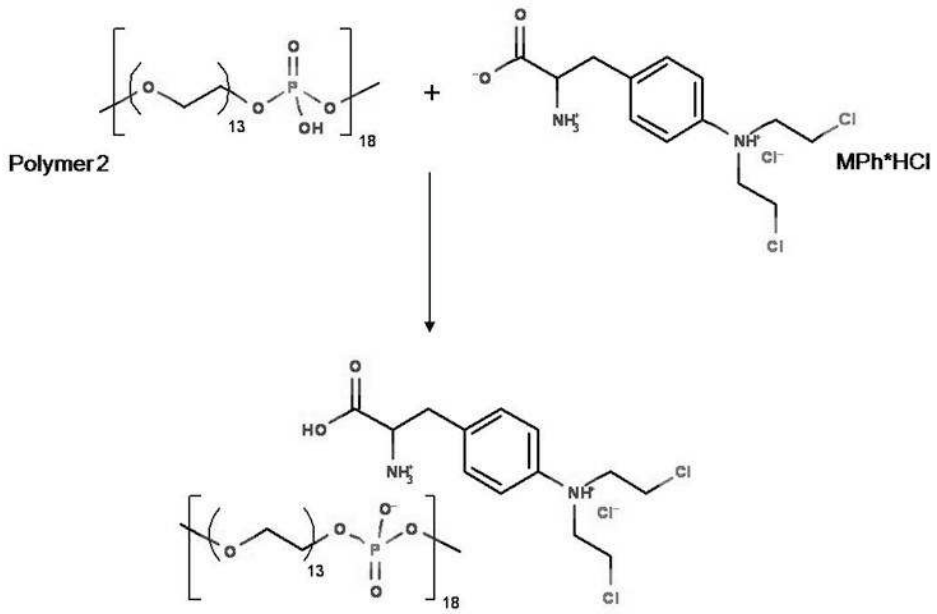

Figure 9: Salt formation of melphalan hydrochloride with polyphosphodiester into ionic Complex 2.

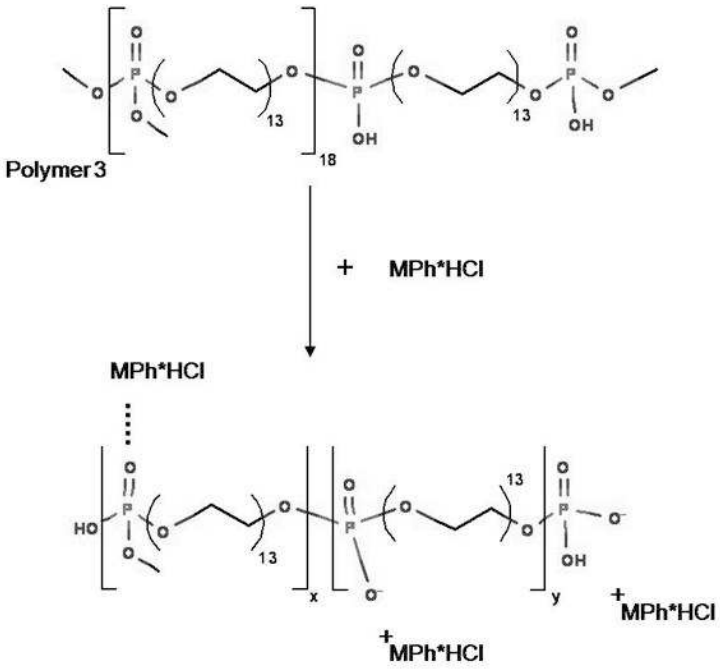

Figure 10: Immobilization of melphalan hydrochloride with polyphosphotriester into hydrogen-bonded Complex 3.

4. Aims of the thesis

4.1. siRNA delivery

The aim of this part of the thesis was to analyze the synthesized and *in vitro* tested multifunctional polycations described above (Figure 3) in different *in vivo* trials and to improve them for being more efficient in animal experiments. Evaluation of the polymers should be done in combination with fluorescent (Cy7-) labeled siRNA and with Inf7 conjugated siRNA. The aim was, to analyze the functionality of the targeted carrier, investigating the cell attachment and internalization of the polyplexes and the siRNA's silencing effect *in vivo*. In the next step it was purposed to analyze and, if applicable, to improve the characteristics of the polyplexes after intravenous injection to achieve a well-tolerated, function nucleic acid therapy method for *in vivo* assays.

4.2. Myxobacterial compounds

Each of the three myxobacterial compound families archazolid, pretubulysin and chondramide is cytotoxic towards mammalian cells. It has been shown that they inhibit tumor cell proliferation and migration in different *in vitro* assays.

In vivo however, only pretubulysin had been analyzed before concerning its effect on tumor angiogenesis and tumor growth, but not on tumor metastasis. About archazolid and chondramide, there were no *in vivo* data published at all.

Therefore, one aim of this study as subproject of the FOR 1406 network was, to continue the evaluation of these compounds and to investigate if these secondary metabolites have the potential to hamper tumor growth and tumor metastasis *in vivo*. Additionally, we aimed to gather important information about the toxicity of the compounds after systemic injection.

4.3. Polymer-melphalan formulations

Within this thesis, the three novel polymeric analogues of melphalan first had to be analyzed concerning their effects on cell proliferation and viability. The polymer-melphalan conjugate, if effective, was subsequently to be evaluated in two animal experiments. The aim was to improve the antitumoral efficacy of pure melphalan especially *in vivo* by its polymeric immobilization, taking advantage of the typical characteristics of polymer-drug conjugates. These include an improved solubility and possibly the protection of the drug against degradation, as well as a

reduction of chemoresistance, a delayed release of the conjugated drug and the benefit of the EPR effect.

II. MICE, MATERIALS AND METHODS

1. Mice

1.1. Strains

1.1.1. NMRI nude mice

Female Rj:NMRI-Foxn1^{nu}/Foxn1^{nu} mice (Janvier, Le Genest-St-Isle, France) belong to a mutant strain, which has its origin in an outbred colony of albino mice. These animals lack a thymus, are unable to produce T cells, and therefore are immunodeficient. Thus, they were used for xenograft tumor models.

1.1.2. BALB/c mice

Female BALB/cByJRj mice belong to an inbred strain and were purchased from Janvier, Le Genest-St-Isle, France. These albino mice have a competent immune system and thus, were used in a syngeneic tumor model.

1.1.3. SCID mice

Female SCID mice (CB17/Icr-*Prkdc*^{scid}/IcrCrl) were purchased from Charles River. These mice have a severe combined immunodeficiency involving B and T lymphocytes. Therefore, they were used for xenograft tumor models.

1.2. Housing

Mice were housed under specific pathogen-free conditions in individually ventilated cages (IVC type II long). They were kept within a 12 h day/night cycle, with food and water *ad libitum*. Mice were purchased with an age of five weeks and experiments were started after one week of acclimatization. All animal experiments were performed according to the guidelines of the German law for protection of animal life and approved by the local ethics committee.

2. Materials

2.1. Cell culture

KB cells	ATCC (Wesel, Germany)
4T1-Luc cells	Caliper (Alamenda, CA, USA)

SKBR3 cells	ATCC (Wesel, Germany)
U87MG cells	ATCC (Wesel, Germany)
HuH7 cells	HSRRB (Tokyo, Japan)
RPMI 1640 medium	Invitrogen (Karlsruhe, Germany)
Ham's F12 medium	Invitrogen (Karlsruhe, Germany)
DMEM medium	Invitrogen (Karlsruhe, Germany)
FCS (fetal calf serum)	Invitrogen (Karlsruhe, Germany)
TE (Tris, EDTA)	Biochrom (Berlin, Germany)
PBS (phosphate buffered saline)	Biochrom (Berlin, Germany)
Cell culture plates, flasks	TPP (Trasadingen, Switzerland)
Penicillin-Streptomycin	Biochrom (Berlin, Germany)
L-alanyl-L-glutamine	Biochrom (Berlin, Germany)

2.2. *In vitro* experiments

MTT bromide	Sigma-Aldrich (Steinheim, Germany)
Dimethyl sulfoxide (DMSO)	Sigma-Aldrich (Steinheim, Germany)
Trypsin	Biochrom (Berlin, Germany)
EDTA	Sigma-Aldrich (Steinheim, Germany)
Hoechst 33342	Sigma-Aldrich (Steinheim, Germany)
Boric acid	Sigma-Aldrich (Steinheim, Germany)
Trisma® Base	Sigma-Aldrich (Steinheim, Germany)
GelRed	Biotium Inc. (Hayward, USA)
TCEP = Tris(2-carboxyethyl) phosphine	Sigma-Aldrich (Steinheim, Germany)
Glycerine	Sigma-Aldrich (Steinheim, Germany)
Xylene cyanol	Sigma-Aldrich (Steinheim, Germany)
Hepes	Biomol (Hamburg, Germany)
LabTek chamber slide	NUNC (Wiesbaden, Germany)

2.3. *In vivo* experiments

Luciferin	Promega (Mannheim, Germany)
Forene®	Abbott GmbH & Co. KG (Wiesbaden, Germany)
Bepanthen®	Bayer Vital GmbH (Leverkusen, Germany)
Syringes, needles	BD Consumer Healtcare (Heidelberg, Germany)

2.4. *Ex vivo* experiments

Mayer's haematoxylin solution	Sigma-Aldrich (Steinheim, Germany)
Eosin Y	Sigma-Aldrich (Steinheim, Germany)
Tissue-Tek® Cryomold	Sakura Finetek (Heppenheim, Germany)
Tissue-Tek® O.C.T. Compound	Sakura Finetek (Heppenheim, Germany)
Tissue-Tek® Mega-Casette	Sakura Finetek (Heppenheim, Germany)
Superfrost ultraplus®	Menzel GmbH (Braunschweig, Germany)
DAPI	Sigma-Aldrich (Steinheim, Germany)
Heparin (25.000 I.E./5mL)	Ratiopharm GmbH (Ulm, Germany)

2.5. Instruments

Luminometer Centro LB 960	Berthold Technologies (Bad Wildbad, Germany)
IVIS Lumina	Caliper Life Science (Rüsselsheim, Germany)
Shaver	Aesculap Suhl GmbH (Suhl, Germany)
DIGI-MET Calliper	Preisser (Gammertingen, Germany)
LSM 510 Meta	Zeiss (Jena, Germany)
Olympus BX41	Olympus (Hamburg, Germany)
Leica CM3050 S	Leica Microtechnologies (Bensheim, Germany)
Leica EG1150 H	Leica Microtechnologies (Bensheim, Germany)
Leica RM2265	Leica Microtechnologies (Bensheim, Germany)
Axiovert 200	Zeiss (Jena, Germany)
Plate reader	Tecan (Groedig, Austria)

2.6. Software

Graph Pad Prism 5 software	Graph Pad Software (San Diego, USA)
Living Image 3.2	Caliper Life Science (Rüsselsheim, Germany)

2.7. siRNA

siCtrl	Axolabs (formerly Roche Kulmbach, Germany) AuGuAuuGGccuGuAuuAG dTsdT CuAAuAcAGGCcAAuAcAU dTsdT
siEG5	Axolabs (formerly Roche Kulmbach, Germany) ucGAGAAucuAAAcuAAcu dTsdT AGUuAGUUuAGAUUCUCGA dTsdT
siAHA1-Cy7	Axolabs (formerly Roche Kulmbach, Germany) GGAuGAAGuGGAGAuuAGu dTsdT (Cy7)(NHC_6)ACuAAUCUCcACUUcAUCC dTsdT

Capital letters refer to standard RNA ribonucleotides; small letters (u, c) refer to 2'-O-methyl-ribonucleotides; dT refers to DNA building block deoxy-thymidine; s refers to stabilizing phosphorothioate linkage.

2.8. Peptides

Inf 7 (influenza HA2 – derived)	Biosyntan (Berlin, Germany)

2.9. Polycations

Polycations were synthesized by Dr. Christian Dohmen (PhD thesis 2012, LMU).

FolA-PEG_{24}-K(Stp_4-C)$_2$

FolA-PEG_{48}-K(Stp_4-C)$_2$

FolA-PEG_{72}-K(Stp_4-C)$_2$

A-PEG_{120}-K(Stp_4-C)$_2$

A-PEG_{192}-K(Stp_4-C)$_2$

C-Y3-Stp_4-K(Stp_4-Y3-C)-PEG_{24}-FolA

C-K(K-$CapA_2$)-Stp_4-K(Stp_4-K(K-$CapA_2$)-C)-PEG_{24}-FolA

C-K(K-$SteA_2$)-Stp_4-K(Stp_4-K(K-$SteA_2$)-C)-PEG_{24}-FolA

2.10. Polyphosphoesters

Polyphosphoesters and melphalan formulations were synthesized by Dr. Anita Bogomilova (LMU guest scientist 2011).

poly(oxyethylene H-phosphonate)

poly(hydroxyoxyethylene phosphate)

poly(methyloxyethylene phosphate)

2.11. Myxobacterial compounds/melphalan

Archazolid A	Helmholtz-Institut für Pharmazeutische Forschung Saarland (Prof. Rolf Müller)
Pretubulysin	Helmholtz-Institut für Pharmazeutische Forschung Saarland (Prof. Rolf Müller)
Chondramide B	Helmholtz-Institut für Pharmazeutische Forschung Saarland (Prof. Rolf Müller)
Melphalan hydrochloride	Sigma-Aldrich (Steinheim, Germany)

3. Methods

3.1. Cell culture

KB (human cervix carcinoma), SKBR3 (human breast adenocarcinoma) and 4T1-Luc (luciferase expressing murine breast adenocarcinoma) cells were grown in RPMI 1640 medium. U87MG (human glioblastoma-astrocytoma) cells were cultured in DMEM, HuH7 (human hepatocellular carcinoma) cells were cultured in DMEM/Ham's F12. All media were supplemented with 10% FCS and 4 mM stable glutamine. 1% penicillin-streptomycin was supplemented to the medium for cells cultured for *in vitro* assays.

3.2. Cell viability assay

HuH7, SKBR3 and U87MG cells were seeded into 96 well plates ($1x10^4$ cells/well). After 24 h, culture medium was replaced with 80 µL fresh growth medium containing 10% FCS and cells were treated with 20 µL of several dilutions of the novel formulations, equivalent concentration of pure melphalan or with the polymeric carriers alone. A 20 µL buffer solution was used as control. After 48 h, 10 µL/well MTT (3-(4,5-dimethylthiazol-2-yl)-2,5-diphenyltetrazolium bromide) were added with a final concentration of

0.5 mg/mL. After 1 h of incubation, unreacted dye and medium were removed. Plates were frozen at -80 °C. After defrosting, 200 µL dimethyl sulfoxide were added to each well and the purple formazan product was quantified by a plate reader at 590 nm with background correction at 630 nm. The relative cell viability (%) relative to control wells was calculated by [A] test / [A] control × 100.

3.3. Proliferation assay

HuH7, SKBR3 and U87MG cells were seeded into 96 well plates ($1x10^4$ cells/well). After 24 h, culture medium was replaced with 80 µL fresh growth medium containing 10% FCS and cells were treated with 20 µL of several dilutions of the novel conjugates, equivalent concentration of pure melphalan or with the polymeric carriers alone. 20 µL buffer was used as control. After 48 h, cells were washed with 200 µL PBS per well and 40 µL trypsin/EDTA-solution was added into each well. Plates were frozen at -80 °C. After defrosting, 200 µL Tris-NaCl-EDTA-buffer and the DNA stain H33342 (final concentration: 1 µg/mL) were added per well. After 15 min of incubation without light irradiation, 200 µL of the solutions were pipetted onto a 96 well multititer plate. Fluorescence was measured by a plate reader and the relative cell proliferation (%) was calculated relative to control wells by [A] test / [A] control × 100.

3.4. Gel electrophoresis of polyplexes

A 2.5% agarose gel was prepared by dissolving agarose in TBE buffer (trizma base 10.8 g, boric acid 5.5 g, disodium EDTA 0.75 g, and 1 L of water) and boiling everything up to 100 °C. After cooling down to about 50 °C and addition of GelRed, the agarose gel was casted in the electrophoresis unit. Polyplexes containing 500 ng of siRNA in 20 µl HBG and loading buffer (prepared from 6 mL of glycerine, 1.2 mL of 0.5 M EDTA, 2.8 mL of H2O, 0.02 g xylene cyanol) were placed into the sample pockets. Electrophoresis was performed at 120 V for 40 min.

3.5. Fluorescence correlation spectroscopy (FCS)

The particle size of polyplexes was measured by fluorescence correlation spectroscopy using an Axiovert 200 microscope with a ConfoCor2 unit. A HeNe laser (633 nm, average power of 50 µW at the sample) was used for excitation. The objective was a 40x (NA = 1.2) water immersion apochromat. Particles were formed in a volume of 10 µL of HEPES with a final concentration

of 14.8 µM Inf7-siRNA, including 50 nM Cy5-labeled Inf7-siRNA at indicated N/P ratios. After polyplex formation, the particles were filled up with 200 µL of HEPES and transferred to eight-well LabTek I chamber slides for measurement. Three experimental replicates were measured.

3.6. *In vivo* experiments

For intravenous applications, injection volumes did not exceed 250 µL. Intratumoral injections were performed, using 50 µL of the solutions. All siRNA experiments were carried out with 50 µg siRNA per injection and with an N/P of 16.

3.6.1. Intratumoral polyplex retention

KB cells ($5x10^6$ per mouse) were injected subcutaneously in 150 µL PBS into the nape of 15 anesthetized NMRI nude mice. Anesthesia was performed with 3% isoflurane in oxygen. On day eleven after tumor inoculation, mice were divided into three groups and anesthetized with isoflurane. Targeted (FolA-PEG_{24}-K(Stp_4-C)$_2$) and untargeted (A-PEG_{24}-K(Stp_4-C)$_2$) polyplexes, containing 50 µg Cy7-labeled siRNA, or pure Cy7-labeled siRNA, were injected intratumorally in 50 µL HBG. Near infrared (NIR) imaging was performed with a CCD camera 0 h, 4 h, 24 h, 48 h, 72 h, 96 h and 120 h after injection. For evaluation of the images, the efficiency of the fluorescence signals was analyzed. The efficiency number for each pixel stands for the fraction of fluorescent photons relative to each incident excitation photon. For image interpretation, color bar scales were equalized, using a minimum of 4.7e-7 and a maximum of 1.0e-5 fluorescent photons/incident excitation photon. For quantification of the tumor retention of the polyplexes, Regions of Interest (ROIs) were defined and total signals per ROI were calculated as total efficiency/area with Living Image software 3.2. The average signal intensities per group were compared over time (mean ± S.E.M. of five mice per group). Pictures were taken with an exposure time of 5 s and medium binning.

3.6.2. Intratumoral EG5 gene silencing after local polyplex application

KB cells ($5x10^6$ per mouse) were injected in 150 µL PBS subcutaneously into the nape of twelve anesthetized NMRI nude mice. On day eleven after tumor inoculation, mice were divided into two groups. Mice were anesthetized with 3% isoflurane in oxygen. FolA-PEG_{24}-K(Stp_4-C)$_2$ combined with 50 µg Inf7-siEG5 or with 50 µg Inf7-siCtrl was injected intratumorally. After 24 h, mice were

euthanized by cervical dislocation and tumors were harvested. Tumors were fixed in formalin and embedded into paraffin. Tumors were cut with a microtome into 4.5 µm slices and stained with hematoxylin (2 min) and eosin (5 min). Results were evaluated and documented, using an Olympus BX41 microscope.

3.6.3. Systemic distribution of the initial and modified polyplexes

KB cells ($5x10^6$ per mouse) were injected in 150 µL PBS subcutaneously into the nape of anesthetized NMRI nude mice. Anesthesia was performed with 3% isoflurane in oxygen. On day 13 after tumor inoculation, the initial folate targeted polyplex, polyplexes with extended PEG spacers (2 PEG, 3 PEG) or with hydrophobic modifications (tyrosine, caprylic acid, stearyl acid) containing Cy7-labeled siRNA, were injected intravenously in 250 µL HBG. Untargeted polyplexes with 5 PEG or 8 PEG chains were injected into tumor free NMRI nude mice. Each polymer was injected intravenously into three animals, with only one exception. The stearyl acid containing polyplexes were only injected in one mouse, as this mouse died after the application.

NIR fluorescence measurement was started immediately after polyplex injection and repeated after 0.25 h, 1 h, 4 h and 24 h (polyplexes with 1 PEG, 2 PEG, 3 PEG, tyrosine, caprylic acid or stearyl acid) or after 0.25 h, 0.5 h and 1 h (polyplexes with 5 PEG and 8 PEG). For evaluation, the efficiency of the fluorescence signals was presented, using equalized color bar scales for each group. Pictures were taken with an exposure time of 5 s and medium binning.

3.6.4. Intratumoral EG5 gene silencing after systemic polyplex application

KB cells ($5x10^6$ per mouse) were injected in 150 µL PBS subcutaneously into the nape of 18 anesthetized NMRI nude mice. Anesthesia was performed with 3% isoflurane in oxygen. On day 13, mice were treated i.v. with FolA-PEG_{24}-K(Stp_4-C)$_2$ containing Inf7-siEG5, FolA-PEG_{24}-K(Stp_4-C)$_2$ containing Inf7-siCtrl or A-PEG_{24}-K(Stp_4-C)$_2$ containing Inf7-siEG5 on two consecutive days. 24 hours after the last injection, mice were euthanized through cervical dislocation. Tumors were harvested, embedded into Tissue-Tek and stored at -20°C. The following day, tumors were cut into 5 µm slices, using a cryotom. Afterwards, they were dried, fixed with paraformaldehyde and stained with DAPI. Results were interpreted and documented with a Zeiss Axiovert 200 fluorescence microscope.

3.6.5. Gel electrophoresis of urine samples

Tumor free NMRI nude mice were treated intravenously with FolA-PEG_{24}-$K(Stp_4\text{-}C)_2$ containing Cy7-labeled siRNA (n = 2), FolA-PEG_{72}-$K(Stp_4\text{-}C)_2$ containing Cy7-labeled siRNA (n = 2) or pure Inf-siEG5 (n = 1). At 4 h after application, mice were anesthetized with 3% isoflurane in oxygen and placed in dorsal position. Bladders were blindly punctured with an insulin syringe. Urine samples were analyzed in a 2.0% (w/v) agarose gel in TBE buffer (800 mM Tris, 3.8 M boric acid, 2 mM EDTA) without further dilution. For staining, GelRed was added to the liquid gel. Where indicated, 2 µL of a 0.5 M TCEP solution and 2 µL of a heparin solution were added. Gel electrophoresis was performed using an electric tension of 80 V for 60 min.

3.6.6. Effect of myxobacterial compounds on tumor colonization

In the colonization experiments with archazolid A, 20 BALB/c mice were divided into two groups (treatment and control) and inoculated with 1 x 10^5 4T1-Luc cells (stably transfected with the luciferase gene) *via* the tail vein. 24 h and 4 h before tumor cell injection, the treatment group was premedicated intravenously with 1 mg/kg archazolid A in 5% DMSO/PBS. On day eight after tumor cell inoculation, mice were anesthetized with 2% isoflurane in oxygen and 6 mg Na-luciferin were injected intraperitoneally. 15 min later, bioluminescence imaging of the still anesthetized mice was performed using the IVIS Lumina system with Living Image software 3.2. Thereafter, mice were sacrificed through cervical dislocation. Lungs were harvested, imaged separately and weighed. Images of the mice and the lungs were taken with a CCD camera. They were interpreted with equalized color bar scales, measuring the photon emission of the mice. For quantification of the lung signals, the images of the harvested lungs were analyzed. Regions of Interest (ROIs) were defined and total signals per ROI were calculated as photons/second/cm^2 (total flux/area). Pictures were taken with an exposure time of 5 s and medium binning. During the experiment, mice were weighed every second till third day.

Pretubulysin and chondramide B were evaluated concerning their effect on tumor colonization side by side in one experiment. 30 BALB/c mice were divided into three groups. Mice were pretreated with 0.1 mg/kg pretubulysin or 0.5 mg/kg chondramide B in 5% DMSO/PBS. The control group was injected with equal amounts of 5% DMSO/PBS. The experiment was performed with the same

settings as the archazolid A experiment.

3.6.7. Effect of myxobacterial compounds on tumor growth

Regarding the effect of myxobacterial compounds on tumor growth, archazolid A, pretubulysin and chondramide B were evaluated side by side in one trial. BALB/c mice (n = 32) were locally shaved before the injection of $2x10^6$ 4T1-Luc cells subcutaneously into the flank. Three days after tumor inoculation, mice were divided into four groups. Mice were treated with 3 mg/kg archazolid A, 0.1 mg/kg pretubulysin or 0.5 mg/kg chondramide B in 5% DMSO/PBS. Control mice were injected equal amounts of 5% DMSO/PBS. The treatment was done on day 3, 5, 7, 10, 12, 14 and 17 after tumor inoculation. Tumors were measured every two to three days with a caliper, using the formula $a \times b^2/2$ with a as the widest side of the tumor and b the widest side vertical to a. The average tumor volumes of the four groups were compared over time. After the second treatment, four of the eight archazolid A treated mice were taken out of the experiment, because of edema and inflammation on the injection site. On day 18, mice were sacrificed through cervical dislocation. Tumors and lungs were harvested.

In the second tumor growth experiment, 20 BALB/c mice were locally shaved and $2x10^6$ 4T1-Luc cells were injected subcutaneously into the flank of each mouse. Mice were divided into two groups and treated with 3 mg/kg archazolid A in 5% DMSO/PBS or equal amounts of 5% DMSO/PBS. Treatment was done on day 2, 3, 4, 5, 6, 9, 13 and 17 after tumor inoculation. Tumors were measured every two to three days with a caliper, using the formula $a \times b^2/2$ with a as the widest side of the tumor and b the widest side vertical to a. The average tumor volumes of the two groups were compared over time. On day 18, mice were sacrificed through cervical dislocation. Tumors and lungs were harvested.

3.6.8. *In vivo* evaluation of polymer-melphalan conjugates

3.6.8.1. Short-time experiment

HuH7 cells ($5x10^6$ per mouse) were injected subcutaneously into the left shaved flank of ten SCID mice. On day five, mice were divided into two groups. They were treated i.v. 5, 7, 9, 12 and 14 days after tumor cell inoculation with the polymer melphalan conjugate (Conjugate 1) or the equivalent amount of unmodified melphalan (6 mg/kg in PBS). Tumor volumes were monitored by caliper measurement every second to third day, using the formula

a x $b^2/2$ with a as the widest side of the tumor and b the widest side vertical to a. On day 16, mice were sacrificed through cervical dislocation and tumors were harvested. The average tumor volumes of both groups were compared over time and at the end of the trial (mean ± S.E.M. of five mice per group). Mice were weighed every second to third day. Weight of five mice per group was compared over time (mean ± S.E.M.).

3.6.8.2. Long-term experiment

SCID mice (n = 32) were injected $5x10^6$ HuH7 cells subcutaneously into the left shaved flank. On day five, they were divided into four groups. They were treated intravenously with Conjugate 1, the equivalent amount of unmodified melphalan (6 mg/kg in PBS), the polymeric carrier alone or pure PBS. Injections were carried out on day 5, 7, 9, 12, 14 and 16 after tumor cell inoculation. Tumor volumes were monitored by caliper measurement using the formula a x $b^2/2$ with a as the widest side of the tumor and b the widest side vertical to a. Each mouse was sacrificed through cervical dislocation, when its tumor reached a volume of 1500 mm^3 or the mouse lost more than 15% of its body weight. The experiment was terminated 120 days after tumor cell inoculation and all surviving mice were sacrificed. The average tumor volumes of the groups were compared over time (mean ± S.E.M.). As the tumors of the Conjugate 1 treated mice and of the melphalan treated mice were successfully treated after six injections, regrowth of the single tumors was compared over time. Mice were weighed at least once a week. Weight of eight mice per group was compared over time (mean ± S.E.M.).

3.7. Statistical analysis

Results are expressed as mean value ± S.E.M. Unpaired Students t-tests (one-tailed) were performed using GraphPadPrism™. P-values < 0.05 were considered as significant.

III. RESULTS

1. Tumor targeted siRNA delivery

The *in vitro* efficacy of the folate targeted polymer FolA-PEG_{24}-$K(Stp_4\text{-}C)_2$ in combination with endosomolytic Inf7-siRNA conjugate had already been demonstrated and is described in Dr. Christian Dohmen's PhD thesis. The following studies deal with the *in vivo* characteristics and modification of these polyplexes. The experiments were performed with Daniel Edinger (PhD student, LMU) in NMRI nude mice and folate receptor overexpressing KB tumors.

1.1. Functionality of the folic acid targeted carrier system

To analyze the functionality of the folate targeted carrier system, FolA-PEG_{24}-$K(Stp_4\text{-}C)_2$ in combination with Cy7-labeled siRNA was injected into subcutaneous KB tumors. Its retention effect was compared to fluorescent labeled untargeted polyplex (A-PEG_{24}-$K(Stp_4\text{-}C)_2$) and pure Cy7-labeled siRNA. Analysis was done using near infrared (NIR) imaging of the mice. Figure 11 represents one mouse per group over the first 120 h after polyplex injection.

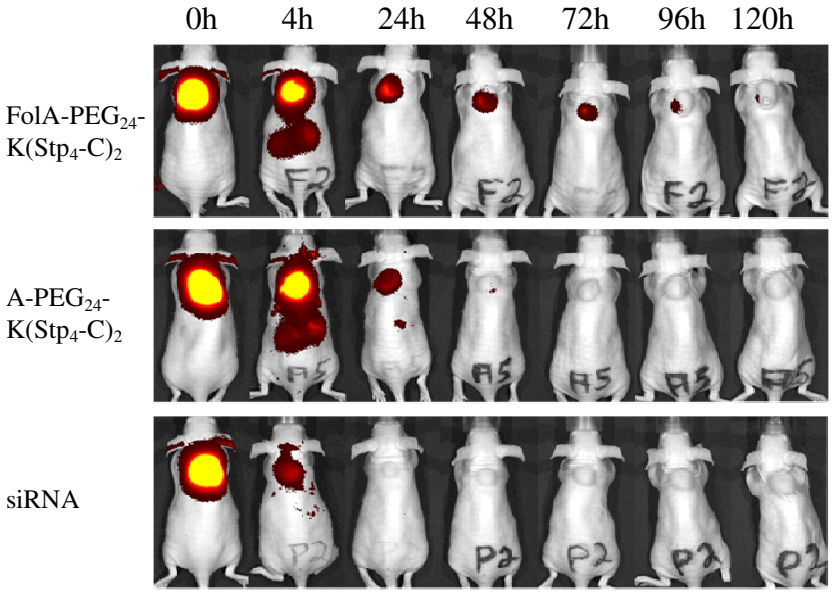

Figure 11: Retention of polyplexes and pure siRNA in the tumor tissue. Targeted polyplexes (top) and untargeted polyplexes (middle), both containing Cy7-labeled siRNA, and pure Cy7-labeled siRNA (bottom) were injected intratumorally. NIR imaging was performed at different points in time till 120 h after polyplex/siRNA application. Pictures represent one mouse per group over time. The color scale (efficiency) had a minimum of 4.7e-7 and a maximum of 1.0e-5 fluorescent photons/incident excitation photon.

The FolA-PEG_{24}-K(Stp_4-C)$_2$ injected mice had a strong fluorescent signal in the tumor, visible over 120 h. In comparison, the signal of the non-targeted nanoparticles disappeared after 48 h, representing a decreased retention in the tumor tissue. In contrast, pure siRNA was already cleared after very short time; no signal could be detected after 24 h. The signal caudal to the tumor (4 h after injection) represents targeted and untargeted polyplexes in the kidneys. Pure siRNA injected mice did not have any renal signal within this setting.

In Figure 12, the fluorescence signals of all 15 mice are presented from 24 h till 120 h after injection as total efficiency/area. The graph reveals the prolonged tumor retention of the folate targeted polyplex compared to the untargeted polyplex, and the fast clearance of free siRNA within all mice of the groups. The 0 h values were almost identically, which can be seen in Figure 11, but are not presented in this graphic.

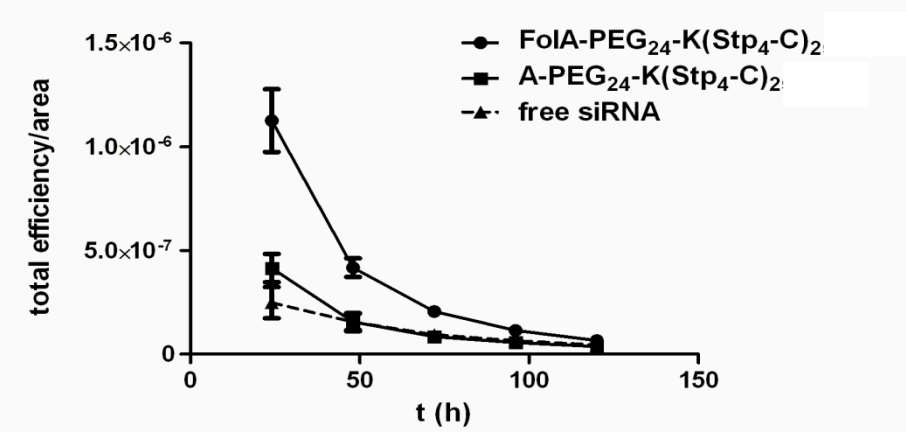

Figure 12: Fluorescence signals of Cy7-labeled siRNA in tumors. After intratumoral injection of FolA-PEG_{24}-K(Stp_4-C)$_2$ or A-PEG_{24}-K(Stp_4-C)$_2$ combined with Cy7-labeled siRNA or pure labeled siRNA, fluorescence signals of the tumors were determined as total efficiency/area. Represented is the mean ± S.E.M. of five mice per group.

1.2. Intratumoral gene silencing after local polyplex application

The NIR images proved the increased tumor retention of the targeted polyplexes. The intracellular uptake and the activity of the siRNA could not been demonstrated within this experiment. For evaluation of the gene silencing effect, targeted polyplexes containing Inf7-siEG5 were injected intratumorally. EG5 is a protein, which is active in spindle formation during mitosis. Silencing of the EG5 gene leads to a mitotic arrest of the affected cells and thus to mitotic figures, so called “asters”. These formations are detectable by means of microscopy.

Targeted polyplexes containing Inf7-siCtrl were injected as negative control. Figure 13 exemplifies the increased number of mitotic figures in tumors treated with FolA-PEG_{24}-K(Stp_4-C)$_2$ containing Inf7-siEG5, compared to tumors treated with Inf7-siCtrl including polyplexes.

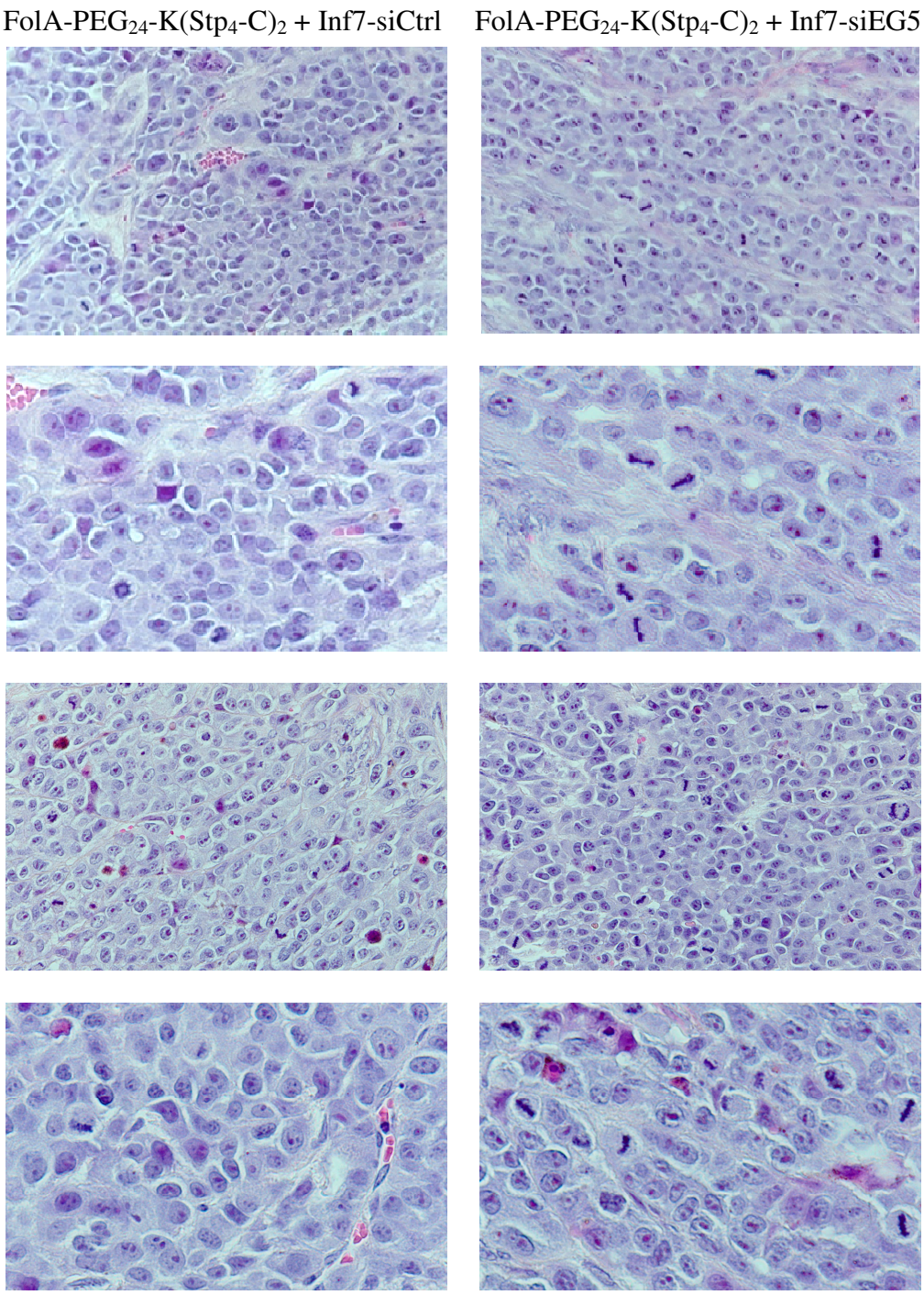

Figure 13: Intratumoral EG5 mRNA knockdown by targeted siRNA. FolA-PEG_{24}-K(Stp_4-C)$_2$ polyplexes containing Inf7-siCtrl (left side) or Inf7-siEG5 (right side) were injected intratumorally. 24 h after application, tumors were harvested and stained with haematoxylin and eosin. Right pictures represent more mitotic figures than left pictures.

1.3. Biodistribution of the initial polymer

In the following experiments, polyplexes were injected intravenously to evaluate the biodistribution and clearance of siRNA in combination with the targeted polymer. FolA-PEG_{24}-$K(Stp_4\text{-}C)_2$ containing Cy7-labeled siRNA was applicated into the tail veins of the mice and its distribution in the body was observed through NIR imaging. Polyplexes had a similar distribution in all mice (n = 3); pictures of one mouse are shown in Figure 14.

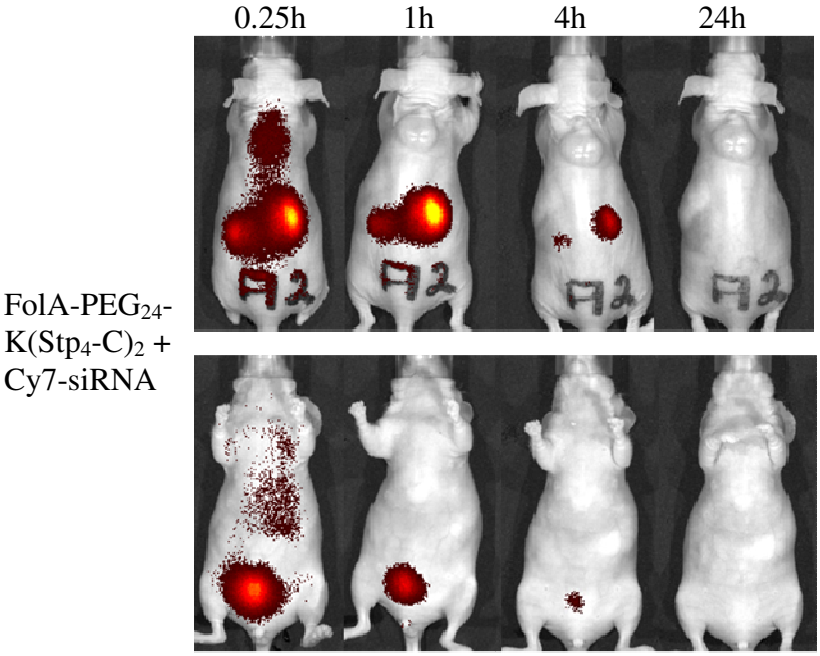

Figure 14: Biodistribution of i.v. injected FolA-PEG_{24}-$K(Stp_4\text{-}C)_2$ bound siRNA. FolA-PEG_{24}-$K(Stp_4\text{-}C)_2$ combined with Cy7-labeled siRNA was injected intravenously into tumor bearing mice. NIR imaging was performed at several points in time (15 min, 1 h, 4 h, 24 h). Images represent the polyplex biodistribution in one mouse in ventral (top) and dorsal (bottom) position over time. The color scale had a minimum of 3.7e-7 and a maximum of 2.47e-6 fluorescent photons/incident excitation photon.

After 15 min, the strongest fluorescence signal was observed in the kidneys and in the bladder of the animals. The tumor tissue (nape) was the only fluoresce tissue beside the genitourinary system. 4 h after injection, most of the polyplexes were cleared. In spite of systemical application, polyplexes did not accumulate in any other tissue than the tumor and were completely cleared by the kidneys. Mice were clinically monitored during the experiment and did not show any medical condition.

1.4. Biodistribution of modified polymers

1.4.1. Polymers with extended PEG spacer

FolA-PEG_{24}-$K(Stp_4\text{-}C)_2$/siRNA polyplexes have a hydrodynamic radius of only 2.8 nm, causing a relatively fast renal clearance. In the following experimental setups, the size of the polymers was enlarged (Table 1), using additional precise PEG_{24} molecules with the objective of obtaining a prolonged circulation time of the siRNA and to increase the EPR effect.

Table 1: Hydrodynamic radius [nm] of the siRNA polyplexes. Hydrodynamic radius of polyplexes, using Cy5-labeled Inf7-siRNA at N/P 16. Determined by Dr. Christian Dohmen and Christina Troiber (LMU) through fluorescent correlation spectroscopy.

Polymer	r_h [nm]
FolA-PEG_{24}-$K(Stp_4\text{-}C)_2$	2.8 ± 0.1
FolA-PEG_{48}-$K(Stp_4\text{-}C)_2$	3.2 ± 0.1
FolA-PEG_{72}-$K(Stp_4\text{-}C)_2$	4.4 ± 0.1
A-PEG_{120}-$K(Stp_4\text{-}C)_2$	5.8 ± 0.2
A-PEG_{192}-$K(Stp_4\text{-}C)_2$	25.4 ± 0.9

Precise prolonged polyplexes, containing FolA-PEG_{48}-$K(Stp_4\text{-}C)_2$ and FolA-PEG_{72}-$K(Stp_4\text{-}C)_2$ combined with Cy7-labeled siRNA, were injected intravenously into mice and NIR images were taken. Figure 15 represents one mouse per group. Compared to FolA-PEG_{24}-$K(Stp_4\text{-}C)_2$, no difference was seen in the distribution and clearance of the modified polymers.

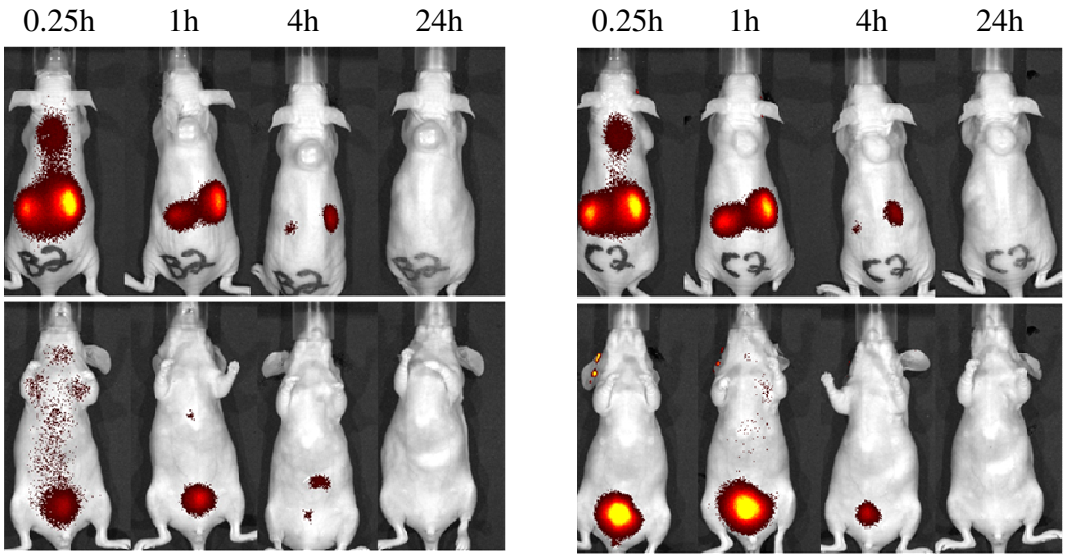

Figure 15: Biodistribution of i.v. injected, polymeric bound siRNA. Cy7-labeled siRNA was injected systemically in combination with FolA-PEG_{48}-$K(Stp_4\text{-}C)_2$ (left) or FolA-PEG_{72}-$K(Stp_4\text{-}C)_2$ (right) into tumor bearing mice. NIR imaging was performed in ventral (upper panel) and dorsal (lower panel) position over the following 24 h. The color scale had a minimum of 3.7e-7 and a maximum of 2.47e-6 fluorescent photons/incident excitation photon.

In the next step, polymers were synthesized with five (A-PEG_{120}-$K(Stp_4\text{-}C)_2$) and eight (A-PEG_{192}-$K(Stp_4\text{-}C)_2$) monodisperse PEG_{24} chains. These polymers did not include folic acid, as the focus of this experiment was put on the impact on circulation time and not on tumor targeting. Nanoparticles, now reaching a hydrodynamic radius of 5.8 nm and 25.4 nm, were analyzed in their distribution properties as before. Figure 16 represents one mouse per group. The measurement was stopped after 1 h due to the weak signals at later points in time in previous trials. Both modified polyplexes still had a fast renal clearance, but showed a better tissue distribution in the first 30 min compared to the initial polyplexes. The polyplex with 5 PEG spacers had the most extensive distribution at all points in time, especially after 15 min and 30 min.

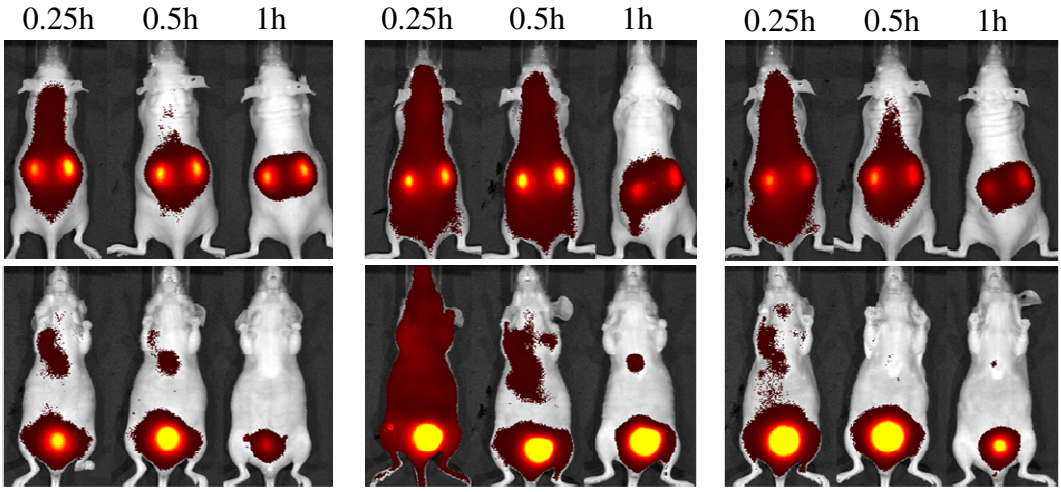

Figure 16: Biodistribution of i.v. injected siRNA linked to untargeted 5 PEG and 8 PEG containing polyplexes. Cy7-labeled siRNA was combined with A-PEG_{120}-K(Stp_4-C)$_2$ (middle) or A-PEG_{192}-K(Stp_4-C)$_2$ (right) and injected intravenously into tumor free mice. As control, the initial polyplex containing FolA-PEG_{24}-K(Stp_4-C)$_2$ was injected intravenously (left). NIR imaging was performed in ventral (upper panel) and dorsal position (lower panel) 15 min, 30 min and 60 min after application. The color scale had a minimum of 1.0e-6 and a maximum of 9.6e-6 fluorescent photons/incident excitation photon.

1.4.2. Polymers with hydrophobic modifications

As the enlargement of the polymers by additional PEG spacers was limited, polymers were synthesized containing hydrophobic domains like tyrosines, caprylic acids or stearic acids. The hydrophobic modification with tyrosine did not influence particle size, whereas caprylic acids and stearic acids increased the polyplex size (Table 2).

Table 2: Hydrodynamic radius [nm] of polyplexes with hydrophobic modified polymers. Hydrodynamic radius of polyplexes, using Cy5-labeled Inf7-siRNA at N/P 16. Determined by Dr. Christian Dohmen and Christina Troiber (LMU) through fluorescent correlation spectroscopy.

Polymer	r_h [nm]
C-Y3-Stp_4-K(Stp_4-Y3-C)-PEG_{24}-FolA	2.8
C-K(K-$CapA_2$)-Stp_4-K(Stp_4-K(K-$CapA_2$)-C)-PEG_{24}-FolA	17
C-K(K-$SteA_2$)-Stp_4-K(Stp_4-K(K-$SteA_2$)-C)-PEG_{24}-FolA	160

The newly synthesized polymers including Cy7-labeled siRNA were injected intravenously and NIR imaging was performed. Figure 17 represents one mouse per group. The modification with tyrosine or alternatively caprylic acid induced a

liver accumulation and a delayed renal clearance (represented in a later kidney and bladder signal). Addition of stearic acid resulted in lung accumulation, leading to the death of the mouse during anesthesia.

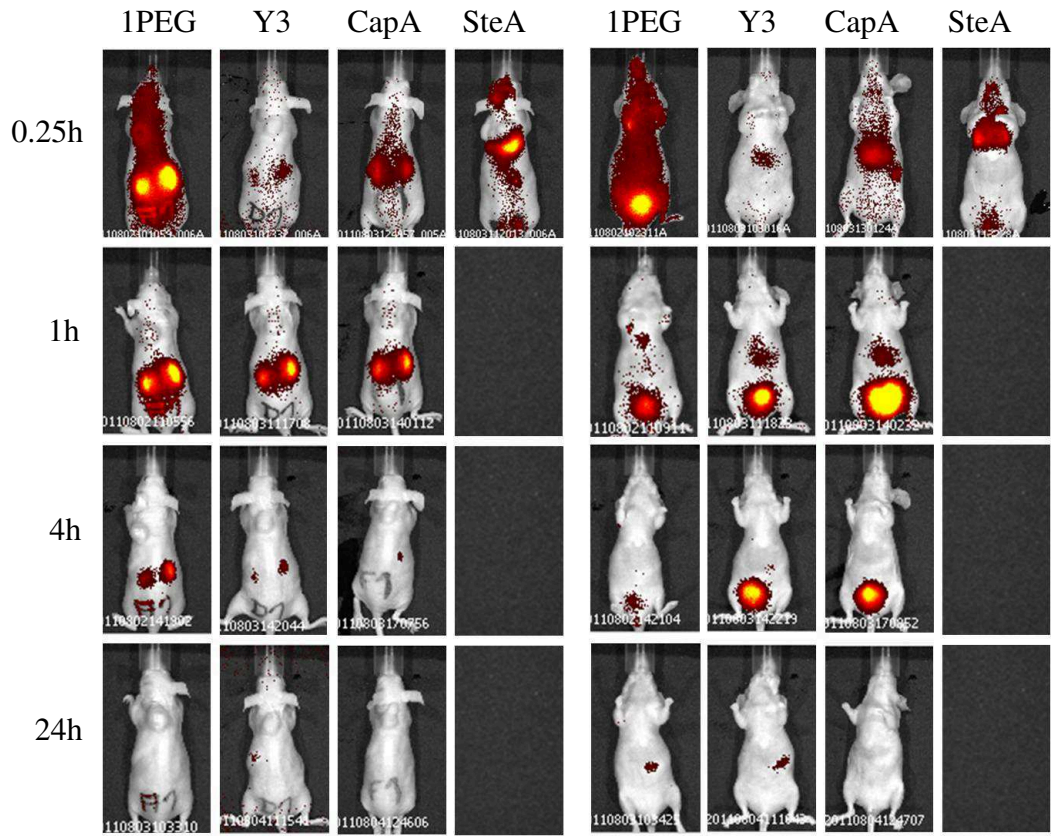

Figure 17: Biodistribution of i.v. injected siRNA in combination with hydrophobic modified polymers. Initial polymers were modified with additional tyrosines (Y3), caprylic acids (CapA) or stearic acids (SteA). Biodistribution is shown in ventral (left side) and dorsal (right side) position of one mouse per group over 24 h. The color scale had a minimum of 2.66e-7 and a maximum of 2.0e-6 fluorescent photons/incident excitation photon.

1.5. Stability of the polyplexes

Especially after i.v. injection, stability is essential for the polyplex efficacy. As the fluorescent stain Cy7 was covalently bound to the siRNA, a positive fluorescence signal only implicated the presence and distribution of siRNA, without saying anything about its complexation with the polymers. For evaluation of the stability, polyplexes with 1 PEG chain and with 8 PEG chains were analyzed in a gel shift assay (Figure 18). Using the polymer FolA-PEG_{24}-K(Stp_4-C)$_2$, siRNA remained complexed with an increase of polyplex stability with high N/P ratios. In comparison, A-PEG_{192}-K(Stp_4-C)$_2$ complexed with siRNA was less stable within every analyzed N/P ratio so that free siRNA was detectable.

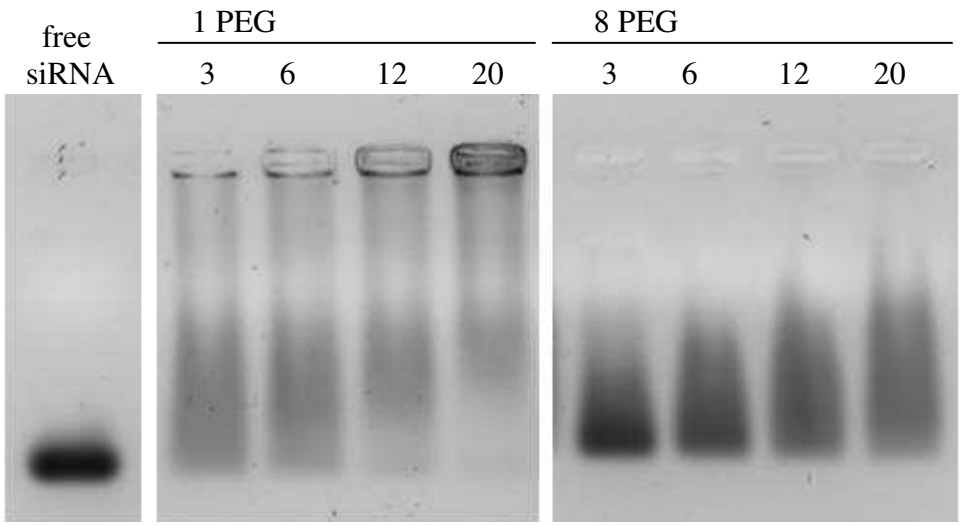

Figure 18: Gel electrophoresis of the polyplexes. Polyplexes containing 500 ng of siRNA in 20 µL HBG and loading buffer were placed into the sample pockets of an agarose gel in different N/P ratios. Free siRNA was used as control. Electrophoresis was performed at 120 V for 40 min. Experiment was performed by Christina Troiber (PhD student, LMU).

To investigate the polyplex stability after systemic application into the mice, urine samples were taken 4 h after intravenous injection of FolA-PEG_{24}-$K(Stp_4\text{-}C)_2$ complexed with siRNA, FolA-PEG_{72}-$K(Stp_4\text{-}C)_2$ complexed with siRNA or free siRNA and analyzed in an agarose gel with (+) or without (-) preincubation with the particle disruptive agents TCEP and heparin (Figure 19).

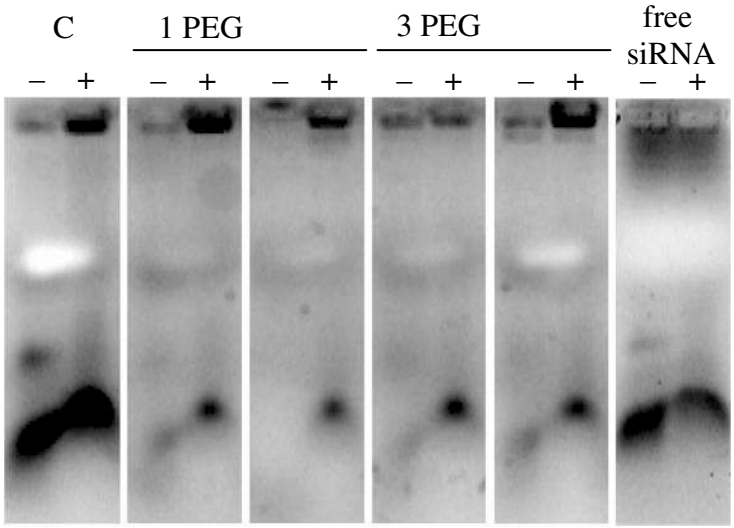

Figure 19: Gel electrophoresis of urine samples after i.v. polyplex injection. Polyplexes with 1 PEG or 3 PEG chains and free siRNA were injected intravenously into mice. 4 h after application, urine samples were taken and analyzed by gel electrophoresis. Free siRNA was used as control (C). Samples were analyzed without further treatment (-) or after incubation with TCEP and heparin (+). Experiment was performed by Dr. Christian Dohmen (LMU).

Without additional TCEP and heparin, polyplexes remained stable, as there was no free siRNA detectable in the gel.

1.6. Molecular biological activity of systemically injected polyplexes

Prolongation of FolA-PEG_{24}-$K(Stp_4\text{-}C)_2$ with 5 PEG_{24} spacers increased the distribution of the polyplex. However, most of the polyplex modifications did not achieve tremendous changes in the circulation time of the particles. Therefore, it was investigated if FolA-PEG_{24}-$K(Stp_4\text{-}C)_2$ causes gene silencing in the tumor tissue after i.v. injection, in spite of the weak fluorescence signal. For this purpose, the polymer was combined with Inf7-siEG5 and injected i.v. As controls, Inf7-siEG5 was injected in combination with the untargeted polymer A-PEG_{24}-$K(Stp_4\text{-}C)_2$ and the targeted carrier was injected, containing Inf7-siCtrl. Figure 20 shows DAPI stained tumor sections 24 h after the treatment. Both polyplexes containing Inf7-siEG5 led to mitotic figures in the tumor tissue, whereby the targeted polyplex caused about threefold more mitotic figures than the untargeted polyplex. In the control sections, no mitotic figures were detectable.

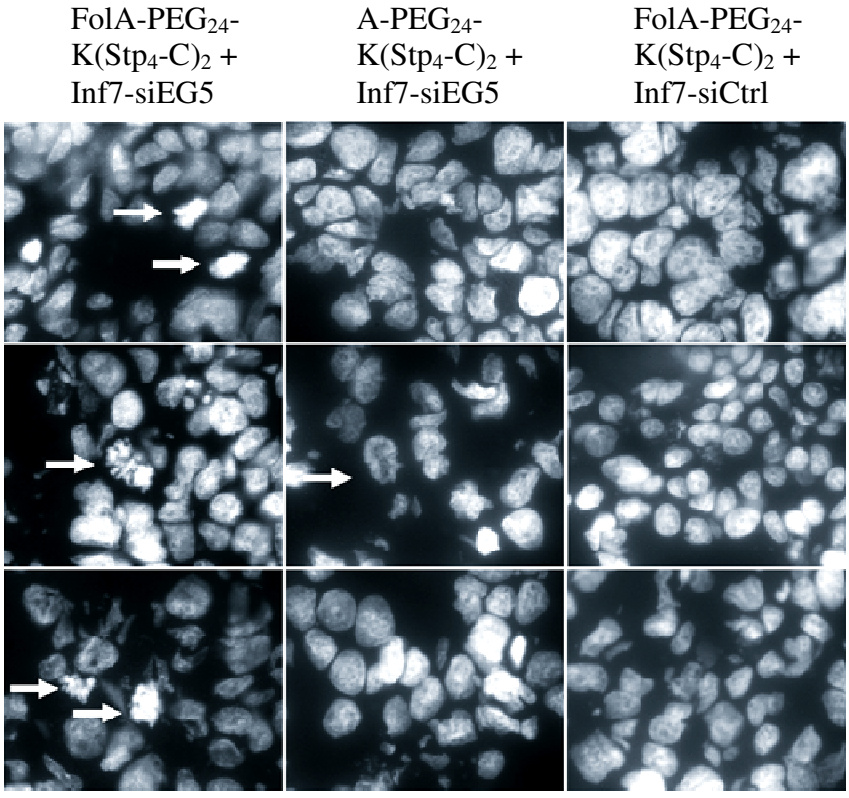

Figure 20: Gene silencing effect of i.v. injected, polymeric bound siRNA. DAPI stained tumor sections 24 h after application of FolA-PEG_{24}-$K(Stp_4\text{-}C)_2$ containing Inf7-siEG5 (left), A-PEG_{24}-$K(Stp_4\text{-}C)_2$ containing Inf7-siEG5 (middle) or FolA-PEG_{24}-$K(Stp_4\text{-}C)_2$ containing Inf7-siCtrl (right). Arrows highlight mitotic figures.

2. Efficiency of myxobacterial products in murine tumor models

In the following experiments, the efficiency of the myxobacterial compounds archazolid A, pretubulysin and chondramide B was analyzed *in vivo* concerning tumor cell colonization and tumor growth. These experiments were performed together with Rebekka Kubisch (PhD student, LMU). Previous cell culture assays had already shown the inhibitory effect of the compounds on cell proliferation and migration (DFG network Vollmar/Müller FOR 1406 "Exploiting the Potential of Natural Compounds: Myxobacteria as Source for Leads, Tools, and Therapeutics in Cancer Research").

2.1. Effects on tumor cell colonization

In the first experiment, we evaluated the V-ATPase inhibitor archazolid A. BALB/c mice (n = 20) were divided into two groups, one control group and one treatment group, and luciferase expressing syngeneic 4T1 breast tumor cells were injected intravenously. 24 h and 4 h before tumor inoculation, the treatment group had been medicated with 1 mg/kg archazolid A. Figure 21 represents the luciferin signals of the 4T1-Luc tumors at the end of the trial (day eight).

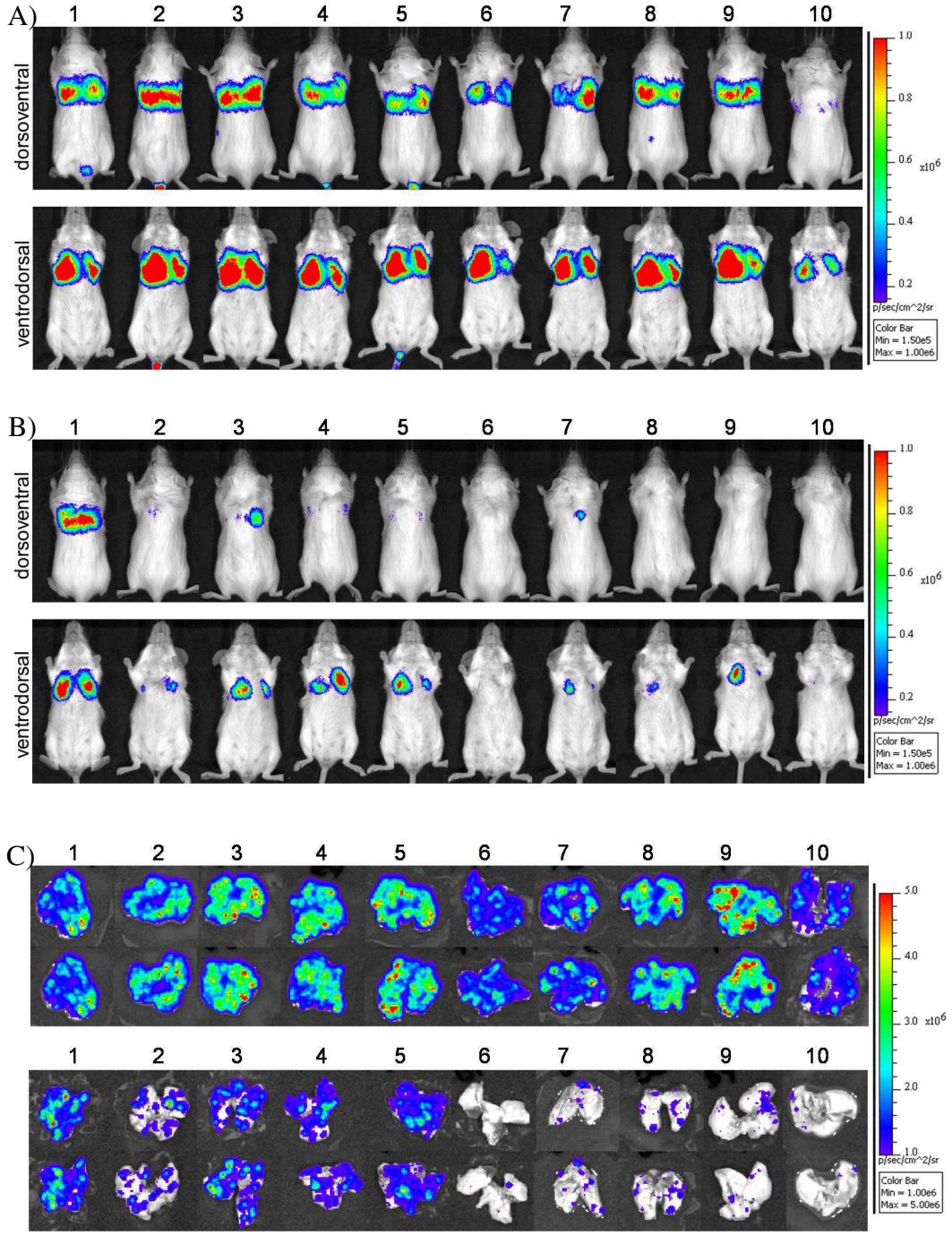

Figure 21: Bioluminescence images. A) Pictures of mice developing 4T1-Luc tumors (without pretreatment). The upper panel shows dorsoventral, the lower panel ventrodorsal images of the control mice. B) Pictures of the archazolid pretreated mice. The upper panel shows dorsoventral, the lower panel ventrodorsal images of the pretreated mice. C) Images of the harvested lungs. Upper panel shows the tumor burden of the lungs of the group without pretreatment, the lower panel the lungs of the pretreated group. Each lung was pictured from dorsal and ventral side.

All mice of the group without archazolid medication had a thoracic luminescence signal, displaying the lung tumor burden of each mouse. Nine of ten control mice had a very strong signal, showing the development of a high number of tumor cells. The strongest signals were seen, when mice lay in dorsal position. The archazolid A treated mice had much weaker signals than the control mice. Within these settings, two of these animals even had no luciferin signal at all. For the definite localization of the signals, lungs were harvested and imaged separately (Figure 21 C). Two pictures (dorsal and ventral side) were taken per organ. The results comply with the images of the animals, as the control lungs had much higher luciferin signals than the lungs of the archazolid A pretreated mice. During the trial, all mice were in good general condition and did not show any weight loss (Figure 22).

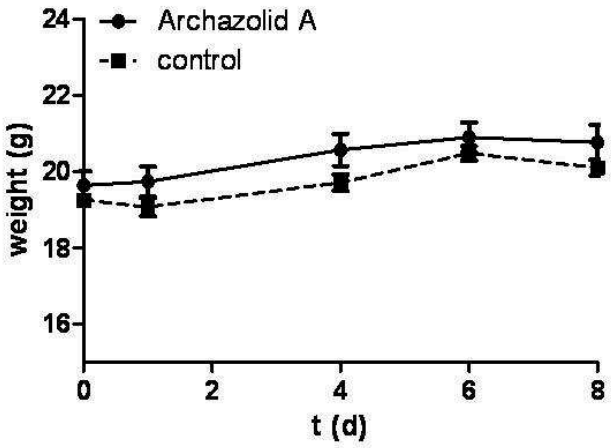

Figure 22: Weight of mice. Weight of the archazolid A pretreated and of the untreated (control) mice, starting with tumor cell inoculation (day 0), ending with euthanasia (day 8). Mean ± S.E.M. of ten mice per group.

For quantification of the tumor burden, the bioluminescence signals of the lungs were calculated as photons/second/cm^2 (total flux/area). The mean ± S.E.M. is represented in Figure 23 A. The average luminescence signal in the pretreated group was significant lower than in the control group. After imaging, lungs were weighed. Figure 23 B represents the mean weight ± S.E.M. of ten lungs per group. Lungs of the control group were significant heavier compared to the pretreated group, caused by their higher tumor burden.

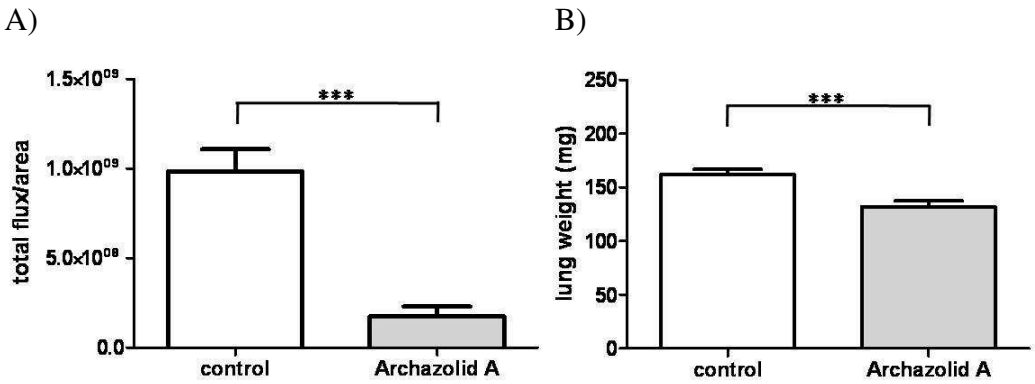

Figure 23: Quantification of the tumor burden in the lungs. A) The luciferin signal of the harvested lungs was calculated as photons/second/cm^2 (total flux/area). Bars represent the mean ± S.E.M. (***p<0.0001 (t-test)). B) Lungs were weighed. Bars represent the mean ± S.E.M. of ten lungs per group (***p<0.0001 (t-test)).

Subsequent to the archazolid experiment, the effect of pretubulysin (0.1 mg/kg) and chondramide B (0.5 mg/kg) on tumor cell colonization was analyzed with analogous experimental setups. Figure 24 presents the tumor burden of the mice, revealed through the bioluminescence signals of the 4T1-Luc tumor cells.

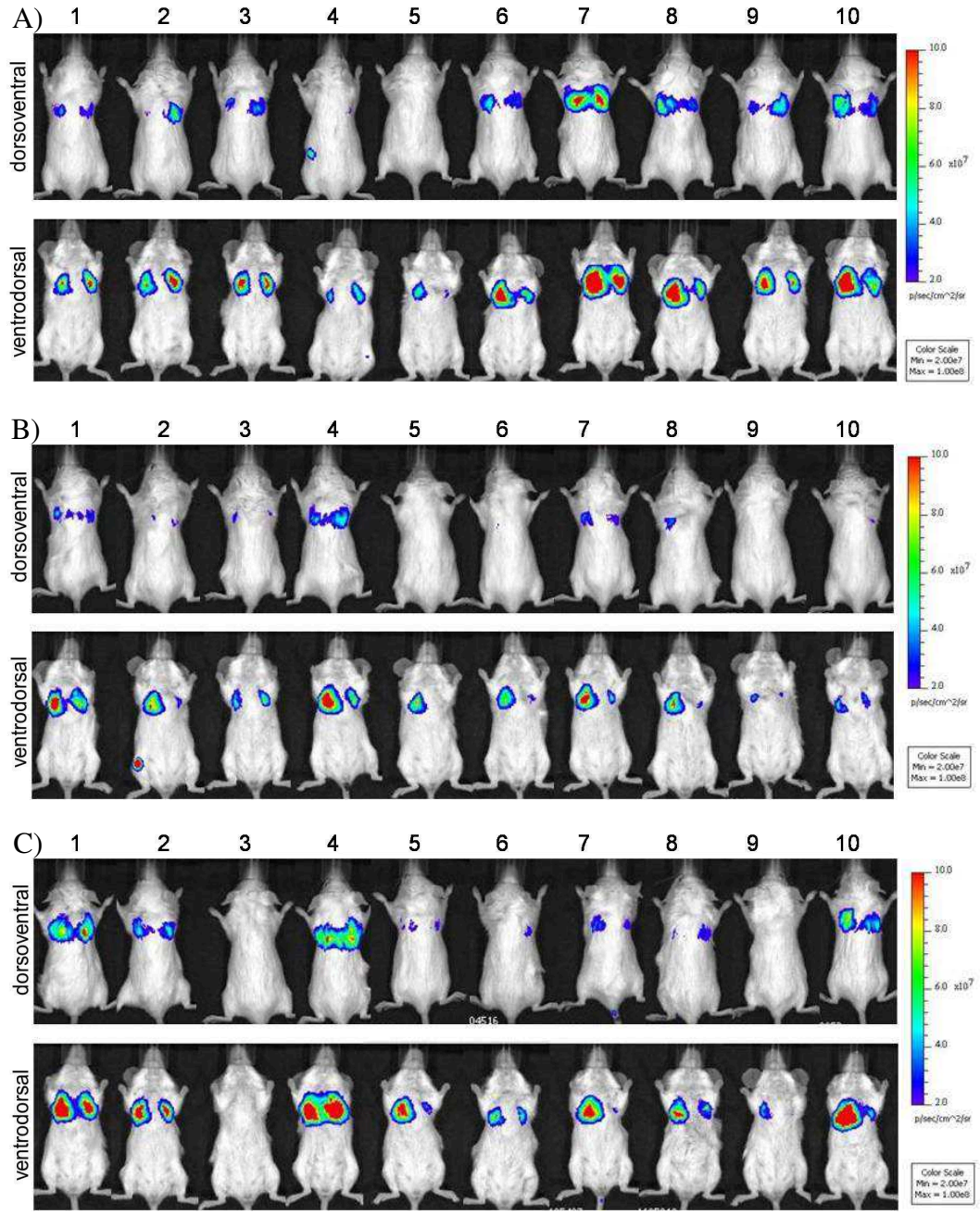

Figure 24: Bioluminescence images. A) Pictures of the mice without pretreatment (control). B) Pictures of the pretubulysin pretreated mice. C) Pictures of the chondramide B pretreated mice. The upper panel of each graphic shows the mice in ventral, the lower panel in dorsal position.

The control mice (Figure 24 A) had the strongest luciferin signal. Ten of ten mice had developed visible lung tumors like in the pretubulysin treated group (Figure 24 B). One of the chondramide B treated mice (Figure 24 C) did not have a luciferin signal within these settings. Nevertheless, in average, the pretubulysin group had optically the smallest tumor burden in the lungs, followed by the chondramide B treated mice. The difference in signal strength between the

chondramide B pretreated and the control mice was visually assumable, but not absolute clear. After euthanasia of the animals, lungs were harvested and imaged separately (Figure 25). The results represent the findings of the previous pictures, indicating a higher anti-colonization effect of pretubulysin compared to chondramide B.

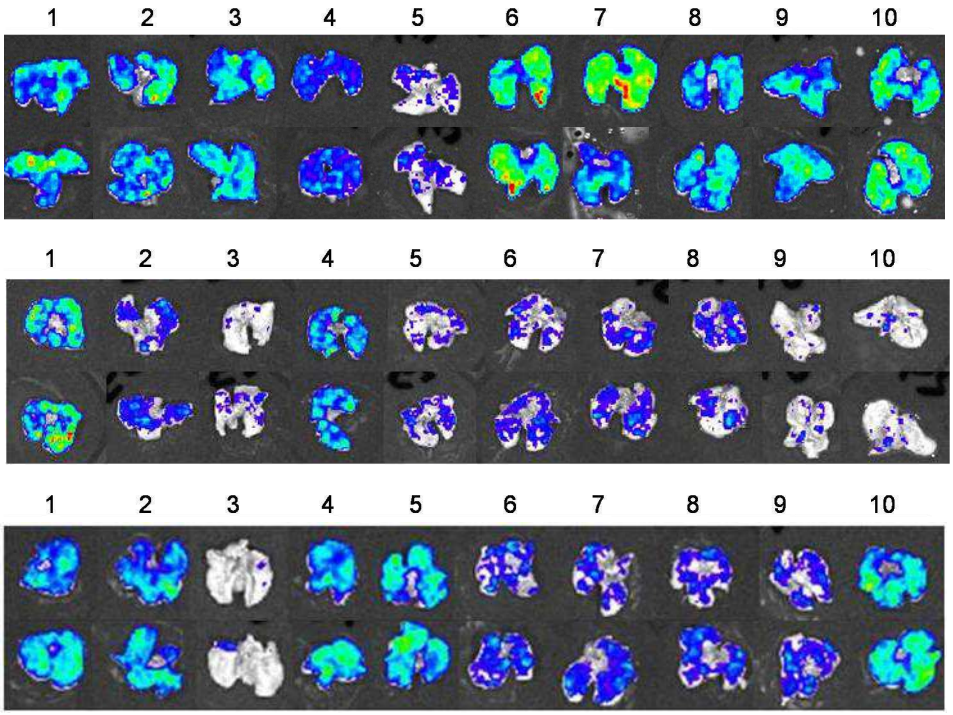

Figure 25: Bioluminescence images of the harvested lungs. The upper panel shows the lungs of the control mice without pretreatment, the middle panel the lungs of the pretubulysin pretreated mice and the lower panel the lungs of the chondramide B pretreated mice. Each lung was pictured from dorsal and ventral side.

To quantify the luminescence, signals of the lungs were again calculated as total flux/area (Figure 26 A). This analysis proved the optical impression of the pictures. Pretubulysin and chondramide B treated mice had a significant lower tumor burden than the control mice, whereby pretubulysin had a higher efficacy than chondramide B. Figure 26 B demonstrates the weight of the lungs.

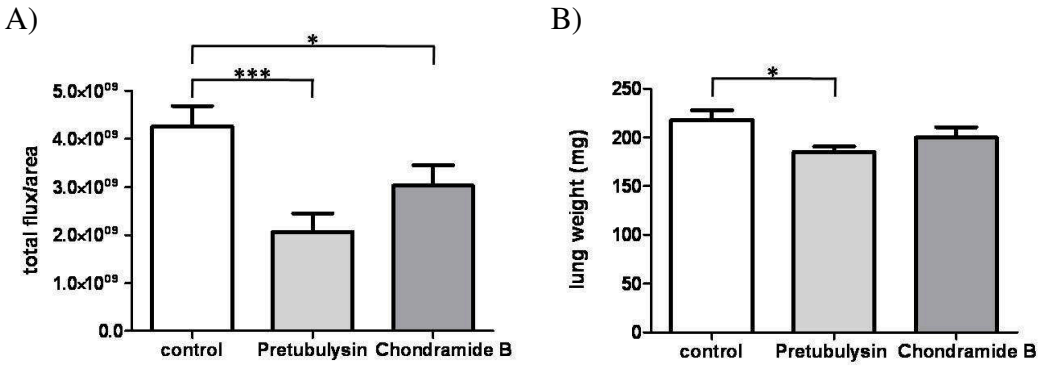

Figure 26: Quantification of the tumor burden in the lungs. A) The luciferin signal of the harvested lungs was calculated as photons/second/cm^2 (total flux/area). Bars represent the mean ± S.E.M. (***p<0.0001 (t-test)). B) Lungs were weighed. Bars represent the mean ± S.E.M. of ten lungs per group (***p<0.0001 (t-test)).

While pretubulysin had a significant effect using this evaluation method, chondramide B did not reduce the weight of the lungs significantly. Compared to archazolid, pretubulysin had a weaker anti-colonization efficacy and chondramide B even less. Mice were in good general condition during the experiment and none of them lost remarkable weight. Figure 27 shows the average weight of the groups over time.

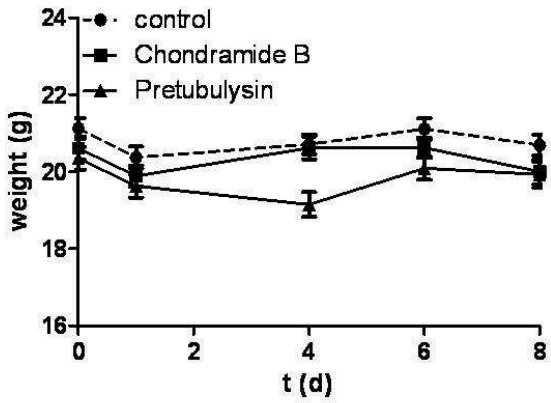

Figure 27: Weight of mice. Weight of the pretubulysin and chondramide B pretreated and of the untreated (control) mice, starting with tumor cell inoculation (day 0), ending with euthanasia (day 8). Represented is the mean ± S.E.M. per group over time.

2.2. Influence on tumor growth

Besides the impact of the three compounds on cell colonization, we were also interested in their effect on hampering tumor growth. Therefore, we investigated archazolid A, pretubulysin and chondramide B in a subcutaneous tumor model

with 4T1-Luc cells. Tumor bearing mice were treated intravenously with the myxobacterial compounds or PBS for 7 times between day 3 and 17 after tumor inoculation. Archazolid A was injected within a concentration of 3 mg/kg, whereas the concentrations of pretubulysin and chondramide B remained the same as in the colonization experiment (0.1 mg/kg and 0.5 mg/kg). Four of eight animals of the archazolid treated group had to be taken out of the experiment after the second application, as the injection sites became oedematous and inflammatory. In a growth curve (Figure 28 A), groups show a similar increase in tumor volume. The only compound, which could hamper tumor growth at least temporarily within this trial, was archazolid A (Figure 28 B).

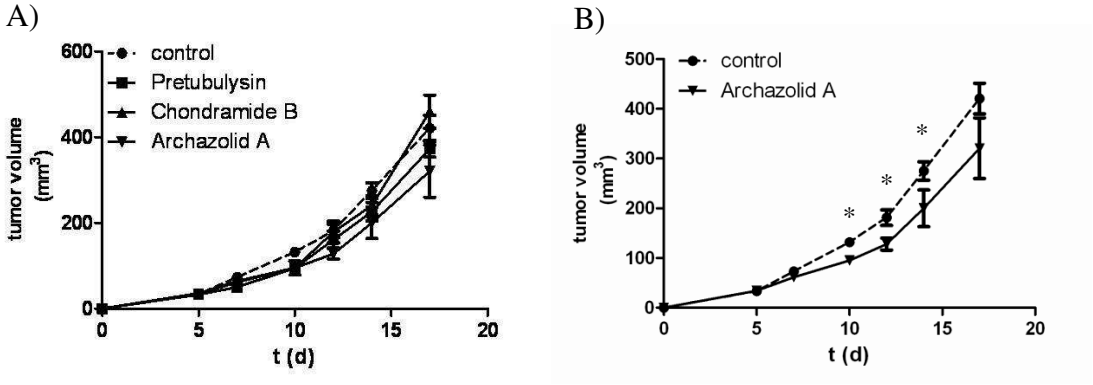

Figure 28: Tumor volume over time. BALB/c mice bearing subcutaneous 4T1-Luc tumors upon seven intravenous treatments (day 3, 5, 7, 10, 12, 14 and 17) with PBS (control), 3 mg/kg archazolid A, 0.1 mg/kg pretubulysin or 0.5 mg/kg chondramide B. A) Average tumor volumes of the four groups (mean ± S.E.M.) over time. B) Average tumor volumes of the archazolid A treated group, compared to the control group (mean ± S.E.M. per group, *$p<0.05$ (t-test)).

As the effect of tumor growth retardation by archazolid A was not significant at the end, a second trial with modified settings was carried out. This time, archazolid A was the only evaluated compound and already injected the first time on day two. Treatment was continued every 24 h for several days and repeated at the end of the trial. In total, the compound was injected eight times instead of seven times as in the previous trial. Figure 29 shows the growth curve of the tumors. Again, archazolid A reduced tumor growth only slightly. In this experiment, the difference was not significant at any points in time.

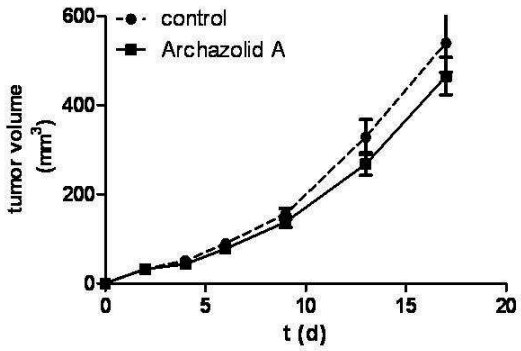

Figure 29: Tumor volume over time. BALB/c mice bearing subcutaneous 4T1-Luc tumors upon eight intravenous treatments (day 2, 3, 4, 5, 6, 9, 13 and 17) with PBS (control) or 3 mg/kg archazolid A. Average tumor volumes (mean ± S.E.M. per group) are presented over time.

3. Efficacy of polymer-melphalan formulations

To evaluate the improvement of the therapeutic effect of melphalan due to its polymeric immobilization, the three novel polymeric melphalan formulations were analyzed concerning their impact on cell viability and proliferation. Basing on the *in vitro* results, a short-time *in vivo* experiment was performed, comparing Conjugate 1 with the equivalent amounts of unmodified melphalan. In a mainly analogous, but more extensive animal experiment, these two treatment groups were compared to two control groups over a longer period of time. Dr. Anita Bogomilova synthesized the polyphosphoesters and the melphalan formulations.

3.1. Effect on cell viability and proliferation

To analyze the antitumoral activity of the three synthesized melphalan formulations *in vitro*, both metabolic activity of cells by MTT assay, representing enzymatic protein activity of tumor cells, and proliferation activity, representing the amount of tumor cell chromatin, was determined. The polymer-bound formulations were compared with equivalent doses of unmodified melphalan. Untreated and pure polymer treated cells were used as control.

On HuH7 cells, pure melphalan had a higher potency in the MTT assay (Figure 30 A, C, E) than polymer bound melphalan at the medium dose of 50 µg/mL. However, at a concentration of 100 µg/mL, the immobilization of melphalan led to a strong antitumoral activity, comparable to pure melphalan. In total, the efficacy of Conjugate 1 was a bit weaker in comparison to Complex 2 and Complex 3, but within the highest concentration (100 µg/mL) Conjugate 1

also had a strong effect on hampering cell metabolism.

In the proliferation assay on HuH7 cells (Figure 30 B, D, F), the melphalan formulations reached an equal or almost equal reduction of tumor DNA as unmodified melphalan. Within the highest concentration, cell proliferation was decreased to about 20% of the control cells.

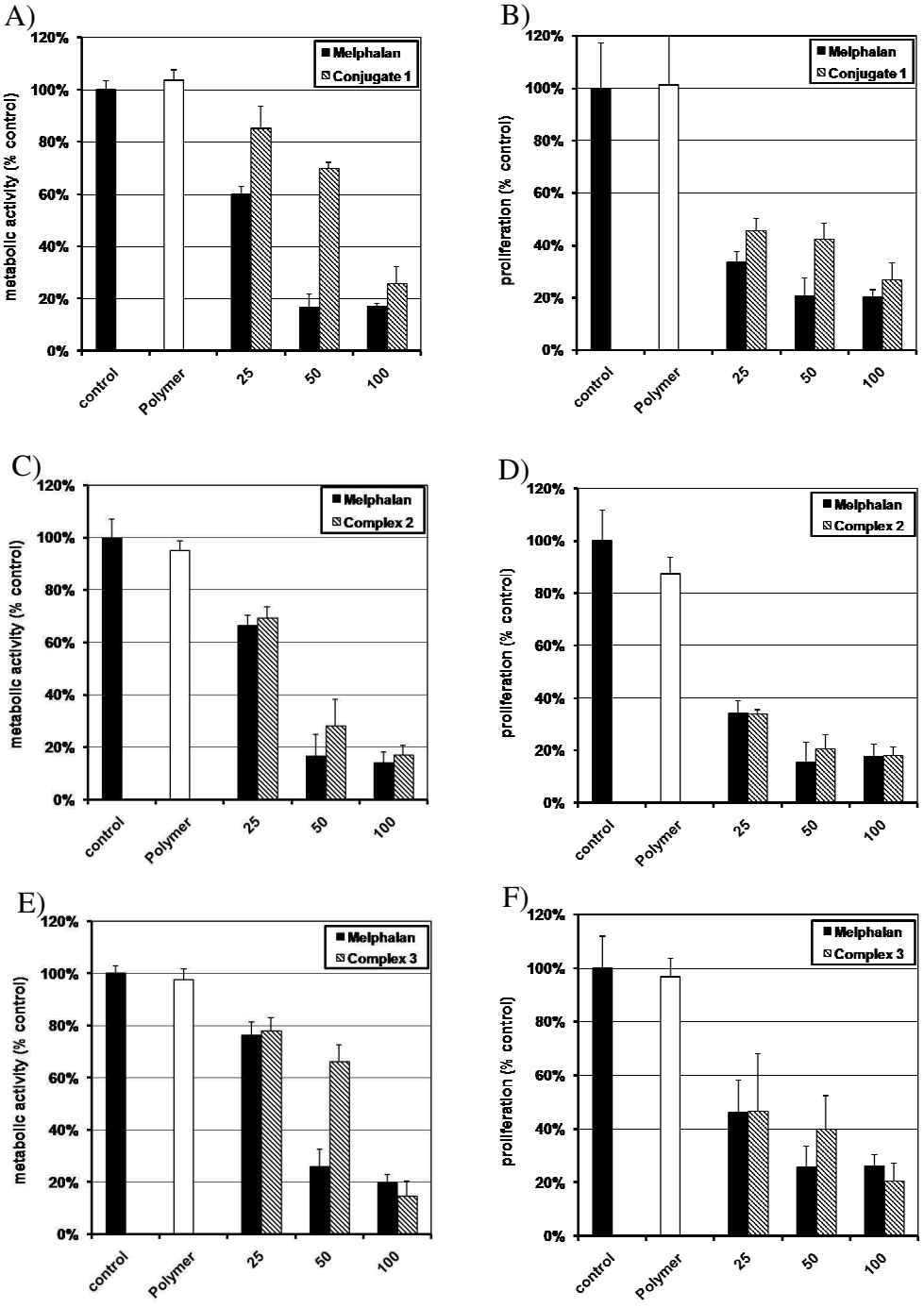

Figure 30. Treatment of HuH7 cell cultures with indicated concentrations (µg/mL melphalan equivalents) of unmodified melphalan, Conjugate 1, Complex 2, Complex 3, or 200 µg/mL free polymer. After 3 days culture under standard conditions, MTT assays for detection of cell metabolic activity (A, C, E) and H33342 dye staining for determining cell proliferation (B, D, F) were performed.

In the next experiments, SKBR3 cells were used. The MTT assay (Figure 31 A, C, E) showed similar results as before. Both, the melphalan formulations and pure melphalan had a comparable efficacy on cell viability, especially at a concentration of 100 µg/mL. Overall, the treatment was more effective than in HuH7 cells, reaching a reduction of metabolic activity of more than 90% with the highest melphalan concentration.

In the proliferation assay on SKBR3 cells (Figure 31 B, D, F), immobilized melphalan was as effective as pure melphalan. The treatment led to a very low amount of tumor cell chromatin (under 10% of control cells).

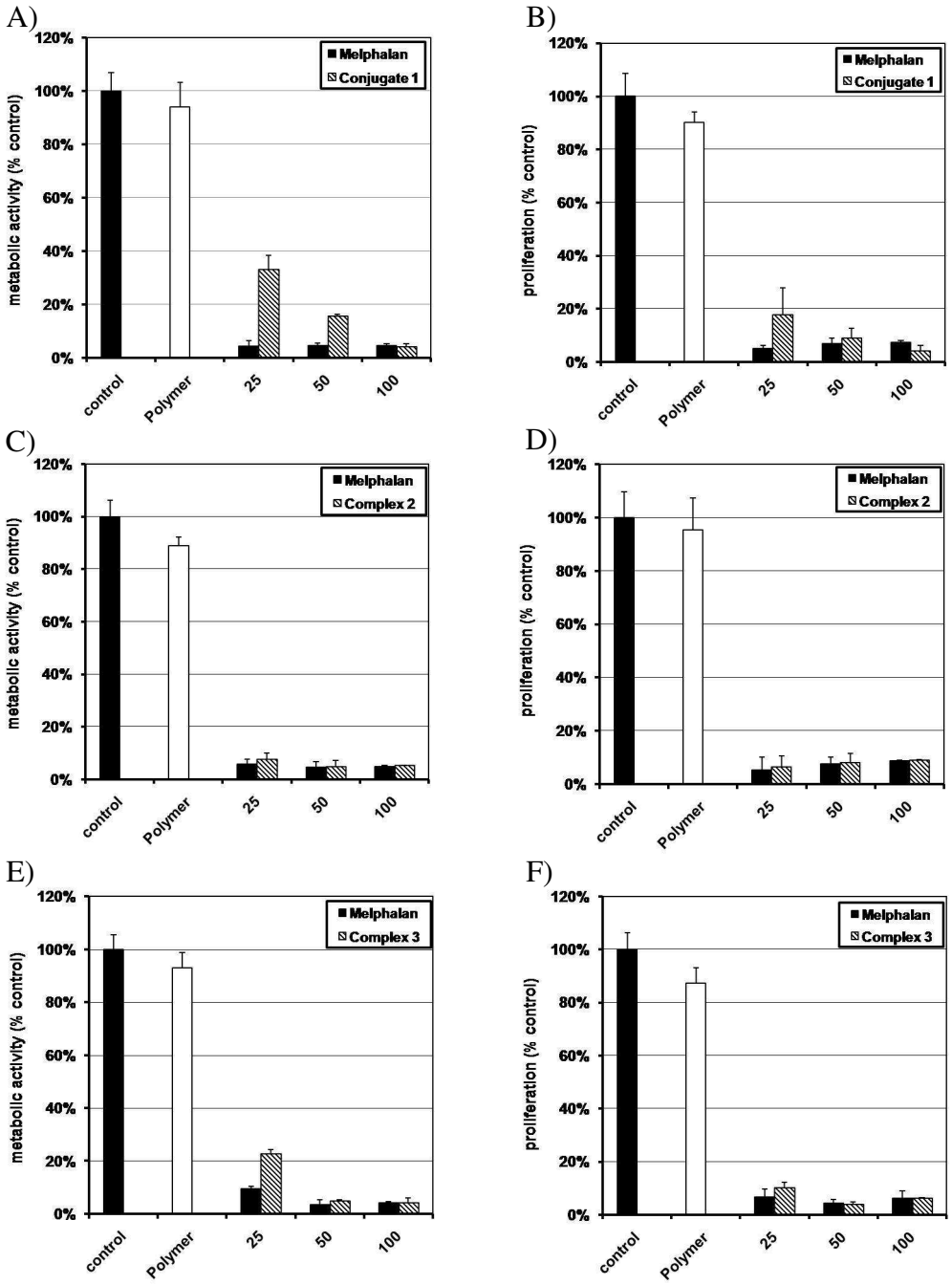

Figure 31. Treatment of SKBR3 cell cultures with indicated concentrations (µg/mL melphalan equivalents) of unmodified melphalan or Conjugate 1, Complex 2, Complex 3, or 200 µg/mL free polymer. After 3 days culture under standard conditions, MTT assays for detection of cell metabolic activity (A, C, E) and H33342 dye staining for determining cell proliferation (B, D, F) were performed.

In the following experiments, the antitumoral effects of the polymeric formulations were evaluated on U87MG cells. This cell line did not response as strong as HuH7 and SKBR3 cells to the treatment. However, the melphalan conjugate and the complexes reduced the metabolic activity (Figure 32 A, C, E)

and cell proliferation (Figure 32 B, D, F) comparable to pure melphalan.

Pure polymer (without incorporated melphalan) had no cytotoxic effect on the cells in all *in vitro* experiments.

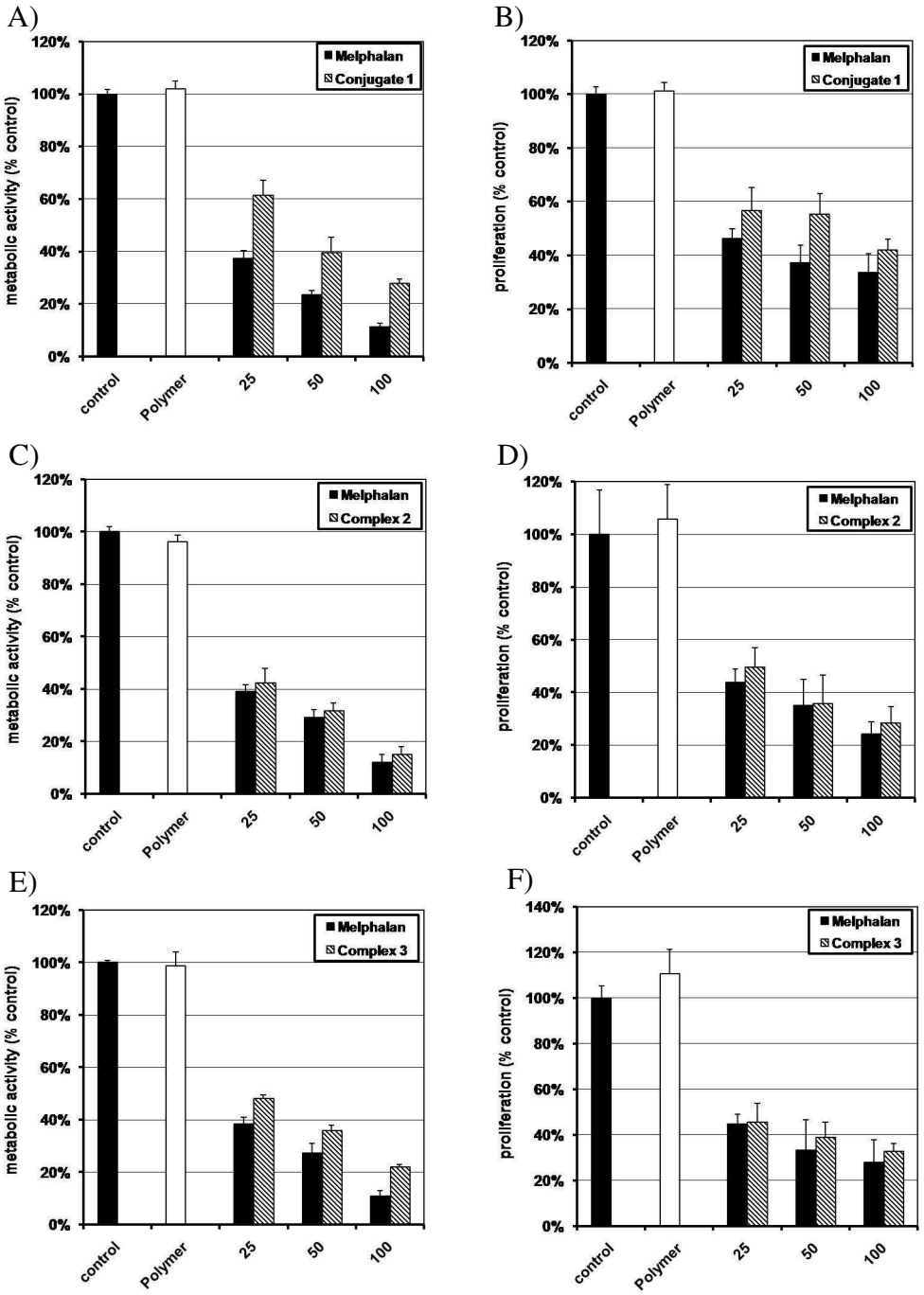

Figure 32. Treatment of U87MG cell cultures with indicated concentrations (µg/mL melphalan equivalents) of unmodified melphalan or the three polymer-incorporated forms, or 200 µg/mL free polymer. After 3 days culture under standard conditions, MTT assays for detection of cell metabolic activity (A, C, E) and H33342 dye staining for determining cell proliferation (B, D, F) were performed.

3.2. *In vivo* studies

Conjugate 1, which - due to covalent linkage - presents the most stable form of incorporation, and nevertheless displays high antitumoral activity *in vitro*, was selected for further *in vivo* evaluation in a subcutaneous HuH7 model in SCID mice.

3.2.1. Short-time experiment

A preliminary *in vivo* experiment was performed to determine the efficacy and toxicity of the conjugate. Mice were divided into two groups; one was treated with unmodified melphalan (6 mg/kg), one with the polymer-melphalan conjugate (equal dose of melphalan). HuH7 cells were injected subcutaneously and mice were treated intravenously 5 times from day 5 till day 14. The experiment was terminated on day 16 after measurement of the tumor volumes. Starting with the second treatment, the tumor growth in the Conjugate 1 treated group was hampered compared to the melphalan treated group (Figure 33 A). From day nine on, tumor growth stagnated in the Conjugate 1 treated group and tumors even decreased, whereas the tumors of the melphalan treated group showed a constantly increasing volume. From day twelve (fourth treatment) on, the mean tumor volume of the conjugate group was significant smaller than the tumor volume of the melphalan group (Figure 33 A and B). Beside the tumor specific effects, no obvious signs of toxicity, like weight loss of mice, were detected (Figure 33 C).

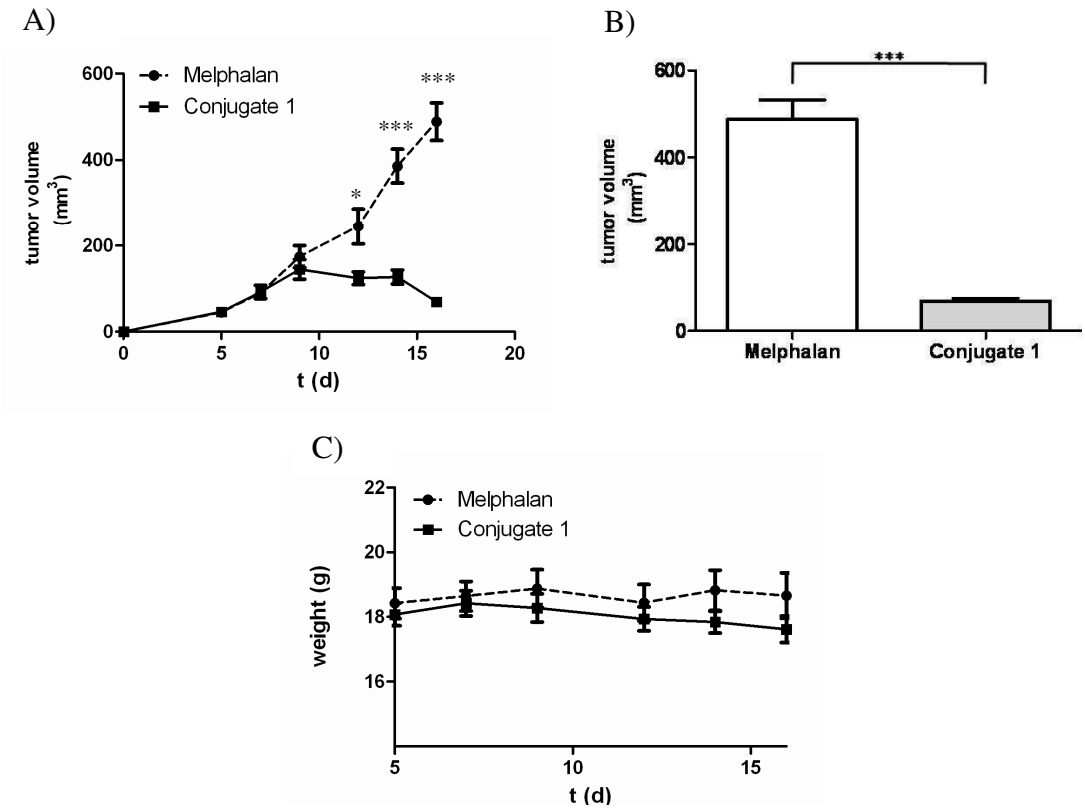

Figure 33: Tumor volume and weight of mice. SCID mice (n = 10) bearing subcutaneous HuH7 tumors upon five intravenous treatments (day 5, 7, 9, 12, 14) with pure melphalan or melphalan Conjugate 1 at a dosage of 6 mg/kg melphalan equivalent. A) Tumor volume over time and B) at the end of the experiment (day 16). Values represent the mean ± S.E.M. of five mice per group. ***p<0.0001 (t-test) C) Average weight of mice per group as mean ± S.E.M.

3.2.2. Long-term experiment

Basing on the previous *in vivo* results, a more comprehensive experiment including two control groups, was performed. Mice (n = 32) were divided into four groups and treated intravenously for six times (day 5, 7, 9, 12, 14, 16) with unmodified melphalan, conjugated melphalan, polymeric carrier alone or PBS. Tumor growth was monitored by caliper measurement. In this experiment, each tumor of the melphalan and Conjugate 1 treated group showed a complete regression after 27 days (Figure 34 A). In the same time, tumors of both control groups grew rapidly and mice had to be sacrificed between day 16 and 40. From day 42 on, regrowth of 4 melphalan treated tumors and 1 conjugate treated tumor was observed (Figure 34 A and B).

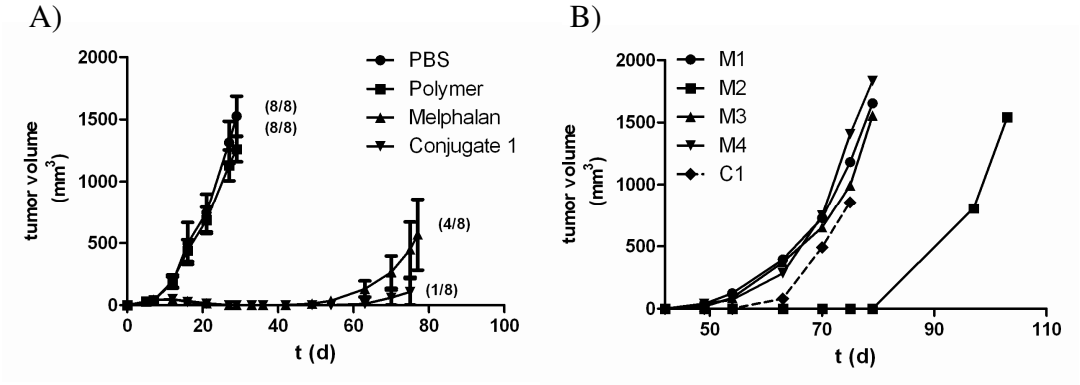

Figure 34: Tumor growth over time. SCID mice (8 per group) bearing subcutaneous HuH7 tumors upon 6 intravenous treatments (day 5, 7, 9, 12, 14, 16) with PBS, free polymer, pure melphalan or Conjugate 1 at a dosage of 6 mg/kg melphalan equivalent. A) Tumor volumes over time (measured until mice had to be sacrificed due to tumor burden). Number of tumor-developing mice at the end of the experiment (day 120) is indicated in brackets. B) Tumor regrowth (volumes) in the individual (4/8) melphalan (M1-M4) or (1/8) Conjugate 1 (C1) treated mice (average data shown in A).

Mice were weighed during the entire experiment to monitor their general condition. In the first 25 days, unspecific weight loss was detected, occurring in all groups (Figure 35 A). After this initial phase, mice gained weight again. For a better presentation, only the weight of both treatment groups is shown over the whole time (Figure 35 B). The experiment was terminated on day 120, when all heretofore survived animals, having a good general condition, were sacrificed.

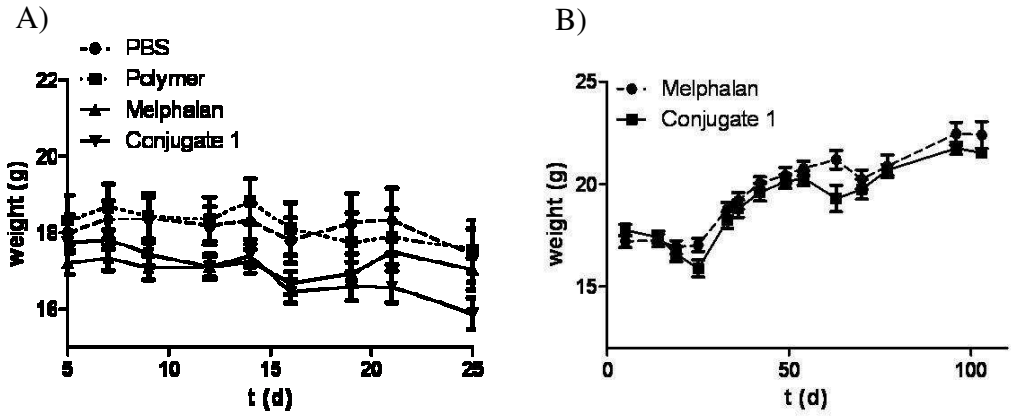

Figure 35: Weight of mice over time. A) Weight of mice of all groups in the first 25 days. Mean of eight mice per group ± S.E.M. B) Weight of mice, treated with pure melphalan or Conjugate 1, over the experimental time. Mean of eight mice per group ± S.E.M.

IV. DISCUSSION

1. Tumor targeted siRNA delivery

1.1. Mode of action of intratumoral injected polyplexes

In the first *in vivo* experiments, polyplexes were injected locally into subcutanous folate receptor overexpressing KB tumors. Within this experimental setup, we demonstrated that the polymer under investigation, FolA-PEG_{24}-$K(Stp_4\text{-}C)_2$, had a longer retention time in the tumor tissue than the untargeted polymer, A-PEG_{24}-$K(Stp_4\text{-}C)_2$ (Figure 12). As both polyplexes were identical apart from the folic acid ligand, this proves that folate enabled a tumor specific targeting through folate receptor binding.

Folate receptors are overexpressed in many tumor types,[139, 140] but have a limited normal tissue distribution[141] and thus, are a suitable and commonly used cell surface protein for targeted cancer therapy. Folic acid has a high affinity to folate receptors and its binding leads to receptor-mediated endocytosis, which circumvents cell penetration problems of charge neutral polyplexes.[142] Therefore, it was assumed that FolA-PEG_{24}-$K(Stp_4\text{-}C)_2$ was internalized through receptor binding, but this could not be proven within the NIR imaging (Figure 11).

The taken pictures only demonstrated the increased tumor retention of the polyplexes due to folic acid as targeting ligand, whereas no information about the polyplex internalization and the siRNA efficiency was given. Therefore, the gene silencing effect of the polyplexes was investigated by knocking down the mitotic kinosin EG5 encoding mRNA. The resulting number of mitotic figures demonstrated that the polyplexes did not remain in the extracellular space after application, but overcame all critical bottlenecks of local nucleic acid delivery (Figure 13). Due to the folic acid, FolA-PEG_{24}-$K(Stp_4\text{-}C)_2$ was able to attach to the tumor cells and was internalized. The next hurdle in the delivery process is the endosomal escape. To overcome this obstacle, the siRNA was conjugated to Inf7, an endosomolytic peptide based on the sequence of the amino-terminus of influenza virus hemagglutinin subunit 2 (HA-2). This lytic peptide was developed by Plank *et al*. in 1994.[43] Inf7 is only lytic at an acidic pH of 5.5, which prevents extracellular toxicity due to lytic activity. This is an advantage over pH-unspecific lytic peptides, like mellitin.[143] Additionally, endosomal escape due to Inf7 is

independent of the amount of polyplexes per endosome and is therefore more effective compared to the proton sponge effect. All these overcome obstacles represent big challenges in nucleic acid therapy[144, 145] and thus, these results are very promising for further siRNA delivery.

1.2. Biodistribution of systemic injected polyplexes

In most cases, a local application of cancer therapeutics is not possible. Therefore, a systemic injection is necessary to reach the tumor tissue. Thus, polyplexes were injected intravenously for further investigations. This method bears several additional bottlenecks in nucleic acid delivery. The nucleic acid needs to be protected from unwanted interactions with other cells. If the siRNA is not bound effectively, it can be degraded in the blood circulation, or polyplexes can accumulate in organs, typically the liver, spleen and lung. As a result, the nucleic acid loses its efficacy and strong toxic side effects through untargeted gene silencing may occur. Therefore, polyplexes were synthesized contained polyethylene glycol (PEG), an often used hydrophilic molecule for surface shielding of pharmaceuticals.[36, 146, 147]

In the following experiments, the initial polyplex was applicated intravenously. The injection of FolA-PEG_{24}-$K(Stp_4\text{-}C)_2$ complexed Cy7-labeled siRNA caused fluorescent signals in the tumor tissue, and the kidneys and bladder due to its renal clearance (Figure 14). No other tissue was targeted by the polyplexes, indicating that the pegylation led to a charge neutralization of the polyplexes, preventing unwanted interactions with untargeted organs. The good tolerability of systemic polyplex injection was proven by the absence of weight loss or reduced general condition. Additionally, the polyplexes were completely cleared, causing no residues in the body.

1.3. Modification of the polymers

The investigated polyplexes fulfilled all necessary prerequisites for the delivery process, but had a short circulation time. However, besides active targeting, passive tumor targeting is another method to increase the uptake of nucleic acids in tumor cells. This method underlies the so called EPR effect,[148] as described before. Nanoparticles may pass the leaky tumor endothel and accumulate in the tumor tissue due to its pure lymphatic drainage. A long circulation time can increase this effect.

To gain larger particles and thus, prolong the circulation time of the polyplexes due to a slower renal clearance, 1 PEG to 8 PEG spacers were added to the polycationic backbone. FolA-PEG_{48}-$K(Stp_4\text{-}C)_2$ and FolA-PEG_{72}-$K(Stp_4\text{-}C)_2$ had similar distribution characteristics like the initial polymer (Figure 15). This could be explained by their small radius of 3.2 nm and 4.4 nm (Table 1), resulting in a fast renal filtration.[149] In the following, polyplexes with 5 PEG and 8 PEG spacers, reaching a radius of 5.8 nm and 25.4 nm, were evaluated after systemic injection.

A-PEG_{120}-$K(Stp_4\text{-}C)_2$ including 5 PEG_{24} achieved a wider distribution in the body, improving the diffusion of the initial polyplex. This effect was caused by its increased size, leading to a delayed renal clearance. A-PEG_{120}-$K(Stp_4\text{-}C)_2$ even had a better distribution than A-PEG_{192}-$K(Stp_4\text{-}C)_2$ (Figure 16).

Further analysis by gel electrophoresis showed that this was probably caused by the increased instability of the 8 PEG chains containing polyplex (Figure 18). It is known, that relatively long PEG chains can destabilize pegylated polyplexes, especially under *in vivo* conditions.[150] With the distribution refinement of 5 PEG chains containing polyplexes, the amount of siRNA reaching the tumor tissue might be increased. On the other hand, the instability of A-PEG_{192}-$K(Stp_4\text{-}C)_2$ showed the limitation of the polyplex modification and enlargement by additional pegylation. Hence, polyplexes were altered using hydrophobic domains.

By short hydrophobic modification with tyrosines, no change of polymer size occurred, whereas additional caprylic or stearic acids led to particles with a hydrodynamic radius of 17 nm or 160 nm, respectively. Tyrosines and caprylic acids prolonged the half life of the polyplexes, which was visible in the delayed bladder and kidney signal of the mice (Figure 17). Unfortunately, this was not due to a better circulation but only due to liver accumulation of the particles. In this case, the pegylation could not shield the hydrophobic character of the new polyplexes. Modification with stearic acids dramatically increased the particle size and led to an accumulation in the lung of the mouse with lethal toxic side effect.

1.4. Stability of the polyplexes

The fluorescence signals in the biodistribution assays represented the diffusion of Cy7-labeled siRNA. Its stable binding to the polymers was assumed due to the targeted tumor accumulation, but had to be proven in another experiment. For the definite prove, gel electrophoresis of the polyplexes with 1 PEG, 3 PEG and

8 PEG chains was carried out. In the first gel shift (Figure 18), the initial polymer turned out to form more stable polyplexes, when compared with A-PEG_{192}-$K(Stp_4$-C). Basing on these results, the *in vivo* stability of FolA-PEG_{24}-$K(Stp_4$-$C)_2$ and FolA-PEG_{72}-$K(Stp_4$-$C)_2$ was evaluated by a gel electrophoresis of urine samples after i.v. polyplex injection (Figure 19). The fluorescence signal seen in the *in vivo* trials was produced by Cy7-linked, still polymer bound siRNA, as the polyplexes FolA-PEG_{24}-$K(Stp_4$-C) and FolA-PEG_{72}-$K(Stp_4$-C) remained stable. Thus, the pegylation could successfully reduce interactions with blood components and degradation by the reticuloendothelial system.

The hydrophobic modified polyplexes also remained stable in the blood circulation, obvious through the occurring fluorescent signal in the liver. Pure siRNA would not accumulate in the liver, but be quickly cleared by the kidneys.

1.5. Molecular biological effect after systemic polyplex application

FolA-PEG_{24}-$K(Stp_4$-$C)_2$ siRNA complexes had a good gene silencing effect after local application. However, its distribution characteristics after systemic injection indicated a small molecular biological effect due to a weak tumor fluorescence signal. Prolongation of the circulation time, which could increase the amount of delivered siRNA in the tumor, could be reached due to additional PEG spacers but was limited. Therefore it was important to evaluate the gene silencing efficacy of FolA-PEG_{24}-$K(Stp_4$-$C)_2$ bound Inf7-siRNA after systemic application.

The targeted polyplex was compared with the untargeted polyplex, both containing Inf7-siEG5. As a second control, the targeted polymer was injected in combination with Inf7-siCtrl. Both polyplexes containing Inf7-siEG5 led to mitotic figures in the tumor tissue through gene silencing, whereby the targeted polyplex caused an about threefold higher number of asters than the untargeted polyplex (Figure 20). This experiment showed that even though the amount of nanoparticles in the tumor after 24 h did not cause a visible fluorescence signal, enough polyplexes reached their target area for specific gene silencing.

2. Myxobacterial compounds

The three myxobacterial compounds archazolid, pretubulysin and chondramide were analyzed regarding their effect on tumor growth and tumor metastasis *in vivo*. For this purpose, murine 4T1 breast tumor cells were used. These cells have a good growth rate and can be inoculated into BALB/c mice, as they originate from and therefore are syngeneic with this mouse strain. To track tumor cell dissemination and tumor growth by bioluminescence imaging, we injected stable luciferase expressing 4T1 cells (4T1-Luc).

As none of the compounds had been evaluated concerning metastasis *in vivo* before, we decided to use simplified setups for this analysis. Thus, we did not inject cells subcutaneously or orthotopically to spontaneously metastasize, but we injected the cells intravenously, mimicking the process of vascular migration. Within these setups, the cells migrated out of the blood circulation and colonized a new tissue, which was almost without exception the lung. The drugs were injected before tumor cell inoculation, to imitate the situation of a treated primary tumor with the aim of preventing its metastasis.

The colonization experiments were terminated eight days after the injection of 4T1-Luc cells, as this time period was on the one hand long enough to evaluate the compounds through bioluminescence imaging and on the other hand short enough to maintain a good general condition of the mice. None of the animals showed any health problems in consequence of their pulmonary tumor burden.

In the subcutaneous tumor growth experiments, we terminated the trials within 18 days, as the 4T1-Luc tumors became necrotic after this time. Although the tumor volumes did not reach a critical size until these points in time, we stopped the experiments, as tumor necrosis would affect the bioluminescence signals and might lead to painful conditions for the animals.

2.1. Influence of archazolid on tumor growth and colonization

V-ATPases play an important role in tumor cell migration and metastasis. They regulate the microenvironment of tumors by acidifying the extracellular space. This enables tumor cells to be invasive and to migrate into other tissues.[151]

In 2005, Lu *et al.* had already demonstrated that the knockdown of ATP6L, a subunit of the V-ATPase complex, through siRNA suppresses the growth and metastasis of human hepatocellular carcinoma.[152] These findings strengthened the

assumption that archazolid can reduce tumor metastasis *in vivo*, caused by the inhibition of V-ATPases.

Indeed, two systemic injections of 1 mg archazolid A per kg body weight led to a reduced migration of 4T1-Luc cells out of the circulation into the lung and therefore, to a significant lower tumor burden, compared to the control group (Figure 21 and 23).

As archazolid had never been evaluated *in vivo* before, these first colonization results have been important and are very promising for further investigations of archazolid.

Previous cell culture studies had not only shown that archazolid hampers cell migration, but had also demonstrated that archazolid is highly effective in reducing cell proliferation of different mammalian cell lines *in vitro*.[71, 79] Therefore, we evaluated its effect on reducing tumor growth *in vivo* as well.

Unfortunately, multiple intravenous injections of 3 mg/kg archazolid A could only slightly decrease the growth of established subcutaneous 4T1-Luc tumors (Figure 28). There was no significant difference between the average tumor volume of the treated and untreated group at the end of the trial.

After gaining these results, we changed the experimental settings for a second tumor growth experiment. In this trial, we started the treatment earlier and shortened the intervals between each application at the beginning of the experiment. Overall, we injected archazolid once more (eight times), compared to the first settings. However, these alterations did not improve the antitumor efficacy of archazolid (Figure 29).

Ohta *et al.* has already published *in vivo* data of bafilomycin and concanamycin, two V-ATPase inhibitors that are *in vitro* as potent as archazolid. They found out that the daily subcutaneous injection of 1 mg/kg of these compounds led to a significant decrease in the growth of subcutaneous tumors after 21 days.[153]

In our tumor growth experiment, we injected the threefold amount of archazolid intravenously, but only for seven or eight times. The problem was that almost all of the subcutaneous 4T1-Luc tumors became necrotic after that time period. Therefore, we had to terminate the experiments on day 18 after tumor inoculation to guarantee a proper evaluation of the results and a good general condition of the mice. At that point in time, the tumors had been smaller than 600 mm^3 in average. As subcutaneous tumors are allowed to grow until they reach a volume of 1500 mm^3 in our experimental setups, they usually could have been monitored for

further days. Besides the problem of tumor necrosis, 4T1-Luc tumors had originally a poor blood supply. As a consequence, the experimental settings for further tumor growth experiments have to be improved and new tumor models have to be evaluated.

Using a higher archazolid concentration *in vivo* might be problematic, as it was already shown that multiple applications of bafilomycin and concanamycin in lower doses can lead to an insulin deficiency and therefore to a later risk of diabetes.[154] Additionally, when we injected a concentration of 3 mg/kg archazolid, we realized edema and inflammation at the injection side. Only minimal paravenous amounts of archazolid induced these side effects. It is known that chemotherapeutics can produce tissue necrosis and perivenous extravasation in different manifestations.[155, 156] When this problem occurred in the first tumor growth trial, we had to take four animals out of the experiment. Afterwards, there were no difficulties concerning this issue, as we injected archazolid even more carefully and thus prevented further complications. Beside this, no other toxicity occurred.

In summary, a clear effect on preventing colonization, but less effect on tumor growth was demonstrated.

2.2. Influence of pretubulysin on tumor growth and colonization

Microtubules targeting compounds gain more and more attention in cancer therapy and there are already several natural compounds like taxanes or vinca alkaloids part of tumor therapy[157] or in clinical trials.[158, 159]

In our experiments, we analyzed the *in vivo* efficacy of pretubulysin, a structural simplified precursor of the tubulin polymerization inhibitor tubulysin. To our knowledge, the collaborative work of our group and the Vollmar group, in which the anti-angiogenesis effect of pretubulysin was evaluated in a subcutaneous HuH7 tumor model (published by Rath *et al.*), was the first successful application of pretubulysin *in vivo*.[84]

In our colonization experiment, the pretreatment of the mice with 0.1 mg pretubulysin per kg body weight led to a significant reduction of colonized 4T1-Luc cells in the lungs, compared to the untreated group (Figure 24 – 26). Regarding the effect of pretubulysin on tumor cell migration, there had only been *in vitro*[49] but no *in vivo* data published before. Thus, these results prove for the first time that pretubulysin can hamper tumor cell colonization *in vivo*. This effect

is probably caused by the inhibition of tubulin polymerization, as microtubules play a crucial role in cell migration.

Concerning tumor growth, multiple i.v. injections of 0.1 mg/kg pretubulysin had no therapeutic effect within our experimental setups (Figure 28), whereas Rath *et al.* could already show that multiple intravenous treatments with 0.1 mg/kg pretubulysin did significantly reduce HuH7 tumor growth.[84] The HuH7 experiments proved that pretubulysin not only hampered tumor growth but also tumor angiogenesis. These findings explain the better efficacy of pretubulysin in HuH7 tumors compared to 4T1 tumors, as hepatocellular carcinomas such as HuH7 tumors, are the most vascularized solid tumors. Thus, they are strongly affected by anti-angiogenetic drugs. Moreover, there is a higher amount of pretubulysin reaching HuH7 tumors because of their good blood supply.

Tubulysin A has a very comparable *in vitro* efficacy as pretubulysin and has already been investigated in different *in vivo* experiments before.[160] It turned out to be toxic in a concentration of 0.1 mg/kg body weight, which was below its therapeutic dose. To reduce its toxicity, tubulysin A was bound to a polymeric backbone. The resulting complex led to a significant tumor growth delay of colon carcinoma, when injected intravenously three times a week in a concentration of 3 mg/kg tubulysin A. Furthermore, a semisynthetic analog of tubulysin B was already used to create a folate conjugate. This conjugate overcame the dose-limiting toxicities of tubulysin B and led to a significant reduction of tumor growth.[161]

Taking together these findings, 0.1 mg/kg pretubulysin reduced the growth of well vascularized HuH7 tumors, whereas the same concentration of the closely related compound tubulysin A did not impair the growth of less vascularized colon carcinoma. Therefore, the cause for the insufficient impact of pretubulysin in our growth experiments might have been the low amount of pretubulysin, reaching the poorly vascularized tumor tissue.

It was encouraging that multiple intravenous injections of 0.1 mg/kg pretubulysin did not cause any obvious side effects. However, as pretubulysin can probably be compared to tubulysin A, a higher dose might be toxic for the animals.

Summarizing, pretubulysin could reduce tumor colonization in the lungs at a low concentration. This concentration was however not high enough to impair solid tumor growth in our experiments. Pretubulysin might be comparable to tubulysin A and tubulysin B and therefore, a good candidate for targeted tumor delivery.

Polymeric immobilization of pretubulysin could possibly reduce the toxicity of higher pretubulysin doses and might target the compound to the tumor site. This could enhance its effectiveness and enable the treatment of rarely vascularized tumors, like the 4T1-Luc tumors, with a higher dose.

2.3. Influence of chondramide on tumor growth and colonization

Chondramide was the third myxobacterial product, we evaluated in animal experiments. In comparison to archazolid and pretubulysin, this actin polymerization promoter had the lowest antitumor efficacy *in vivo*. Nevertheless, chondramide still reduced the colonization of 4T1-Luc cells in the lungs of BALB/c mice significantly (Figure 24 - 26). Comparable to archazolid and pretubulysin, it had a weaker effect in the subcutaneous tumor model and could not affect tumor growth (Figure 28).

Chondramide had shown to impair the growth of different tumor cells *in vitro* before. As chondramide is structurally very closely related to jasplakinolide, their cytotoxic efficacy was compared and found out to be very similar.[69, 88, 162] Chondramide itself had not been tested in animal experiments before, but the *in vivo* information about jasplakinolides gave us a hint for choosing the chondramide dose for our experiment. 1.5 mg/kg jasplakinolide injected i.p. for multiple times had been shown to reduce tumor growth and metastasis of Lewis lung carcinoma in mice.[90] We decided to use a lower concentration of 0.5 mg/kg chondramide, but to inject it intravenously, as we did with archazolid and pretubulysin.

Fortunately, this dose did not cause any visible toxicity in the mice, but at the same time reduced the colonization of 4T1-Luc cells significantly. Actin is necessary for cell migration[163] and intervention in its polymerization process leads to dramatic migration defects. This might explain the reduction of tumor colonization in our animal experiments.

In the tumor growth experiment however, chondramide could not influence the proliferation of 4T1-Luc cells in a concentration of 0.5 mg/kg, although actin plays an important role in cell proliferation.

As mentioned before, the growth of solid 4T1-Luc tumors was already harder to influence comparing to tumor cell colonization with archazolid and pretubulysin. Apparently, the compounds reach the tumor cells in a higher amount, when cells are injected intravenously like the compounds themselves. Subcutaneous growing

tumors are difficult to target, especially when they are not well vascularized like the 4T1-Luc tumors.

At the moment, there is only little information about the characteristics of chondramide *in vivo*. Therefore, it will be difficult to improve this model within a short time. As chondramide was not toxic at all, the next step might be to increase the injection dose. Additionally, using another cell line that forms better vascularized tumors without becoming necrotic, could be successful.

3. Polymer linked melphalan

3.1. *In vitro* efficacy of polymer-melphalan formulations

In MTT and proliferation assays on different cell lines (HuH7, SKBR3 and U87MG), the three novel polymeric melphalan formulations had a comparable effect on cell viability and cell proliferation as equivalent amounts of pure melphalan (Figures 30 – 32). Low-molecular-weight drugs enter cells rapidly by crossing the plasma membrane, whereas conjugated drugs usually are internalized slower through endocytosis and have a delayed drug release within endosomes or lysosomes.[164, 165] As a result, conjugates are generally less cytotoxic *in vitro* than their free counterparts.[120] Therefore, the achievement of an equal cytostatic effect of the polyphosphoester bound melphalan compared to the pure melphalan was a promising result concerning further *in vivo* experiments.

An often occurring problem in polymer-drug conjugation is the toxicity of the synthesized polymers. Thus, the efficiency of the phosphoester polymers was tested without melphalan incorporation, too. The results of MTT and proliferation assays showed that pure polymer did neither influence the metabolic activity, nor the proliferation of the cells (Figures 30 – 32). This finding is well consistent with the previously published high biocompatibility of phosphoester polymers. It proves that the evaluated polymers did not cause any cell toxicity and were not the reason for the cytotoxicity of polymer linked melphalan. Additionally, the polymer increased the water solubility of melphalan, leading to a simplified preparation of the injection solution. Gaining these promising *in vitro* results, we planned further evaluations in animal experiments.

For *in vivo* trials, one cell line and one polymeric system, evaluated in the *in vitro* assays, were chosen. Although SKBR3 cells were the most sensitive cell line, the also responsive HuH7 cells were used in the following animal experiments.

Investigations in previous trials had shown that this well established cell line has a better growth rate and blood supply than SKBR3 or U87MG cells. Amongst the polymeric formulations, melphalan was covalently bond to a polymer (poly(oxyethylene H-phosphonate)) only in one case (by P-O or P-N bonds), forming Conjugate 1. In Complex 2, the negatively charged phosphodiester polymer poly(hydroxyoxyethylene phosphate) was complexed to positively charged melphalan through ionic bonds, in Complex 3 the neutral phosphotriester (poly(methyloxyethylene phosphate) binds melphalan through hydrogen bonding. The *in vitro* efficacy of the three systems had been very comparable. Conjugate 1 was the only formulation with a covalent bond, which is more stable than the ionic and hydrogen bonds of the two complexes. It was remarkable that Conjugate 1 had almost equal cytotoxic effects as Complex 2 and Complex 3, despite melphalan was covalently immobilized on the polymer. *In vivo*, this tight bonding protects melphalan from dissociation in the blood circulation. For this reason, Conjugate 1 was chosen for animal experiments.

3.2. *In vivo* efficacy of the polymer-melphalan conjugate

In the first *in vivo* experiment, polymer-melphalan conjugate (Conjugate 1) treated mice developed significant smaller tumors than mice treated with the equal amount of pure melphalan (Figure 33 A and B). After a first delay of tumor growth, the tumor volumes stagnated during the treatment with the polymer conjugated melphalan. Tumors treated with an equivalent dose of pure melphalan grew significantly faster. Thus, this trial showed that polymeric conjugation of melphalan to the synthesized poly(oxyethylene H-phosphonate) led to a strong improvement of its therapeutic efficacy *in vivo*.

The enhanced therapeutic effect of Conjugate 1 treated mice occurred only short time after the first injection and was presumably caused by the EPR effect.[96] By conjugating melphalan to the polyphosphoester, the low-molecular-weight drug achieved a macromolecular size. This probably enabled the drug to passively target the tumor and to accumulate in the tumor tissue. Thus, a higher amount of melphalan might have reached the tumor compared to the pure drug, increasing the efficacy of the conjugate. Therefore, the novel polymeric analogue could have overcome the lack of tumor selectivity, a major limitation of most conventional anticancer chemotherapeutics.[166]

Beside the tumor toxicity, no other side effects like weight loss (Figure 33 C) or a

reduced general condition occurred, indicating the tolerability of the conjugate treatment. Usually, the passive targeting to the tumor site and the decreased body dissemination of conjugated cytostatic drugs reduces toxic side effects. As the dose of melphalan was relatively low and did not cause any visible toxicity under the experimental conditions, this effect could not be shown in this experimental setup.

In the following more comprehensive animal experiment, the two treatment groups were compared to a PBS and a pure polymer injected group. This was done to analyze the *in vivo* toxicity of the pure polymer and to compare the results to a control group. In this experiment, all tumors treated with polymer-melphalan conjugate or pure melphalan showed a complete growth regression within the first 27 days (Figure 34 A). When mice were treated on day five for the first time, tumors had an average volume of 50 mm^3 and thus, they were 20 mm^3 smaller than tumors in the first *in vivo* trial at that time. This could be the reason for the stronger therapeutic response of these tumors compared to the tumors of the first experiment. Because of the nice complete regression of the treated tumors, no difference was seen in antitumor efficacy between melphalan and the polymer-melphalan conjugate at this occasion.

However, as tumor relapse plays an important role in cancer therapy,[167] mice were monitored for tumor regrowth over 120 days. Animals of both control groups showed a rapid tumor growth, leading to their early euthanasia between day 16 and 40. In the following days, four of eight tumors of the melphalan treated group and only one of eight tumors of the conjugate treated group regrew (Figure 34 B). This could have had different causes.

The decreased tumor regrowth in the conjugate treated mice could be caused by an increased initial cytostatic efficacy of the conjugate. Through polymeric conjugation, a higher amount of melphalan could have reached the tumor site because of the EPR effect. In the tumor tissue, the enhanced drug concentration could then affect more tumor cells compared to the pure melphalan. As a result, fewer tumors were able to regrow.

The EPR effect not only leads to passive targeting for short-term tumor delivery, but it induces a prolonged drug retention, up to several weeks or longer.[105] Polymers are able to release a drug controlled over time. Thus, polyphosphoester conjugation could have prolonged the therapeutic effect of melphalan up to more than 100 days. Therefore, melphalan conjugates could enable a more convenient

therapy for patients, prolonging the intervals between cytostatic treatments. This controlled release of anticancer drugs is already successfully utilized within the application of polymer conjugates in prostate cancer therapy.[168, 169]

Another hope in the use of polymers is the possible circumvention of drug resistance. One cause of multidrug resistance is the efflux of drugs out of the cells through different ABC transporters, for example P-glycoprotein.[170-172] Miyamoto *et al.* described the hampered efflux of polymer conjugated drugs compared to free drugs, which was probably caused by a reduced binding of the polymeric drug to P-glycoprotein. Macromolecular drugs do not seem to interact with the ABC transporter system.[173, 174] In case the tumor contains already multidrug-resistant tumor cell clones, this might be an additional reason for the reduced amount of tumor regrowth after six treatments with the conjugated drug (one of eight tumors), compared to the higher regrowth rate after pure melphalan injections (four of eight tumors).

In the first 25 days of the experiment, the mice lost some weight (Figure 35 A). As most of the mice were affected, whether belonging to the treatment groups or to the control groups, this was an unspecific side effect, being reducible to the application distress. None of these mice lost more than 10% of its body weight. After this initial time period, mice started to gain weight again (Figure 35 B). Neither mice of the treatment groups nor of the pure polymer injected group showed any signs of reduced general condition. The polymer itself was non-toxic for the animals.

V. SUMMARY

Cancer is a leading cause of death worldwide. Although several common treatment options exist, there is an urgent need for improved tumor therapeutics. Therefore, we evaluated three innovative anticancer approaches *in vivo*. These were newly synthesized siRNA polyplexes, novel myxobacterial anticancer compounds, and innovative polymeric melphalan formulations.

We evaluated the *in vivo* characteristics of polymeric bound siRNA. We could demonstrate that the polymer FolA-PEG_{24}-$K(Stp_4\text{-}C)_2$ is an efficient carrier for targeting siRNA to the folate receptor expressing tumor tissue of mice. Moreover, the siRNA was able to enter tumor cells and led to specific gene silencing. After systemic injection, the polyplexes did neither cause any toxic side effects nor accumulate in any healthy organ. With only 6 nm average diameter, polyplexes were very small, resulting in fast removal from blood circulation by renal clearance. Addition of larger PEG spacers to the initial polyplex led to an increased polyplex size. As a result, the renal clearance was decreased, and polyplex distribution in the body was optimized. These results show that the *in vivo* hurdles of siRNA delivery can be overcome by binding siRNA to the precise and multifunctional polymers.

Natural compounds have broad therapeutic effects, and are basis for the production of various anticancer drugs. Myxobacterial products often target cell structures which are rarely targeted by other metabolites, and they exert novel modes of action. Therefore, they are of particular importance for the development of new anticancer drugs. In this thesis, we evaluated three novel myxobacterial compounds *in vivo*. Within our experimental settings, we could demonstrate for the first time that archazolid, pretubulysin and chondramide can impair the migration and colonization of breast cancer cells in mice. Concerning their impact on tumor growth reduction, the compounds have promising characteristics, but the experimental setups need further improvement.

Cytostatic drugs, like melphalan play an important role in cancer therapy, but bear problems, such as a low therapeutic efficacy and strong toxic side effects. Immobilization of chemotherapeutics on polymers is an interesting option to reduce their toxicity and enhance their efficacy, mainly by passive tumor targeting. We evaluated three innovative polymer-melphalan formulations in cell

viability and proliferation assays. The covalent conjugate of poly(oxyethylene H-phosphonate) with melphalan was additionally investigated *in vivo*. This polymeric immobilization of melphalan led to an improved therapeutic effect compared to the pure cytostatic drug, as the growth and regrowth of HuH7 tumors could be hampered effectively.

In conclusion, this thesis deals with the *in vivo* evaluation of innovative cancer therapeutics, which were successfully investigated in murine tumor models. The results with the experimental agents, based on siRNA, polymers or biogenic drugs, are encouraging starting points for further anticancer research.

VI. ZUSAMMENFASSUNG

Krebserkrankungen gehören zu den weltweit häufigsten Todesursachen. Dies verdeutlicht, dass es trotz der vielfältigen bestehenden Behandlungsmethoden einer Verbesserung in der Krebstherapie bedarf. Aus diesem Grund haben wir drei innovative Therapieansätze in Tumormausmodellen analysiert. Dazu zählen neu synthetisierte siRNA Polyplexe, myxobakterielle Naturstoffe und innovative auf Polymeren basierende Melphalan Formulierungen.

Mit der tierexperimentellen Evaluierung von an Polymere gebundener siRNA konnten wir zeigen, dass FolA-PEG_{24}-$K(Stp_4\text{-}C)_2$ ein effizienter Vektor ist, um siRNA zu Folsäurerezeptor exprimierenden Tumorzellen zu transportieren. Darüber hinaus konnte die an das Polymer gebundene siRNA in die Tumorzellen eindringen und die Expression der entsprechenden Gene hemmen. Die Polyplexe akkumulierten weder in Organen noch führte ihre systemische Injektion zu toxischen Nebenwirkungen. Sie wurden schnell über die Nieren ausgeschieden, da sie einen Durchmesser von nur 6 nm haben. Die Vergrößerung der Polyplexe über weitere PEG Einheiten erhöhte ihre Halbwertszeit und führte zu einer optimierten Verteilung im Körper. Die Schwierigkeiten des gezielten *in vivo* siRNA Transportes konnten durch den Einsatz der Polymere überwunden werden.

Naturstoffe haben ein breites Wirkungsspektrum und spielen eine große Rolle in der Entwicklung von Zytostatika. Myxobakterielle Stoffwechselprodukte besitzen oft neuartige Wirkungsmechanismen, da sie an Zellstrukturen angreifen, die das Ziel von nur wenigen anderen Naturstoffen sind. Aus diesem Grund sind sie von großem Interesse für die Entwicklung neuer Krebstherapeutika. Wir haben die Eigenschaften von drei myxobakteriellen Sekundärmetaboliten *in vivo* untersucht. Unsere Ergebnisse zeigen zum ersten Mal, dass Archazolid, Pretubulysin und Chrondramid die Migration von murinen Tumorzellen in der Maus hemmen. Die analysierten Naturstoffe sind zudem vielversprechend bezüglich ihrer Wirkung auf das Wachstum solider Tumore. Um diesen Effekt *in vivo* zu verdeutlichen, müssen die Versuchsbedingungen jedoch weiter optimiert werden.

Chemotherapeutika, wie zum Beispiel Melphalan, werden häufig in der Krebstherapie angewendet. Ihr Einsatz ist jedoch mit starken Nebenwirkungen und einer nur bedingten Wirksamkeit verbunden. Durch die Bindung an Polymere können Zytostatika gezielter ins Tumorgewebe transportiert werden. Dies

verstärkt ihre Wirksamkeit und reduziert gleichzeitig ihre Toxizität. Wir haben Melphalan an drei innovative Polymere gekoppelt und die Wirksamkeit dieser Formulierungen *in vitro* getestet. Zusätzlich wurde die Wirkung des aus Melphalan und poly(Oxyethylene H-phosphonat) hergestellten Konjugates *in vivo* untersucht. In Wachstumsversuchen mit HuH7 Tumoren zeigte das Konjugat eine stärkere zytostatische Wirkung als pures Melphalan. Im Hinblick auf die Entstehung von Tumorrezidiven war das Konjugat ebenfalls wirksamer als pures Melphalan.

Zusammenfassend haben wir uns in dieser Arbeit mit der *in vivo* Evaluierung innovativer Krebstherapeutika in Tumormausmodellen beschäftigt. Die erzielten Ergebnisse mit den auf siRNA, Polymeren oder Naturstoffen basierenden Therapeutika stellen einen vielversprechenden Ausgangspunkt für weitere Forschungsarbeiten dar.

VII. REFERENCES

(1) Ferlay, J., Shin, H. R., Bray, F., Forman, D., Mathers, C., and Parkin, D. M. (2010) Estimates of worldwide burden of cancer in 2008: GLOBOCAN 2008. *Int J Cancer 127*, 2893-917.
(2) Jemal, A., Bray, F., Center, M. M., Ferlay, J., Ward, E., and Forman, D. (2011) Global cancer statistics. *CA: a cancer journal for clinicians 61*, 69-90.
(3) Bray, F., Jemal, A., Grey, N., Ferlay, J., and Forman, D. (2012) Global cancer transitions according to the Human Development Index (2008-2030): a population-based study. *The lancet oncology*.
(4) Wagner, E. (2012) Functional Polymer Conjugates for Medicinal Nucleic Acid Delivery, in *Advances in Polymer Science* pp 1-29.
(5) Dzau, V. J., Beatt, K., Pompilio, G., and Smith, K. (2003) Current perceptions of cardiovascular gene therapy. *The American journal of cardiology 92*, 18N-23N.
(6) Tuszynski, M. H. (2007) Nerve growth factor gene therapy in Alzheimer disease. *Alzheimer disease and associated disorders 21*, 179-89.
(7) Bunnell, B. A., and Morgan, R. A. (1998) Gene therapy for infectious diseases. *Clinical microbiology reviews 11*, 42-56.
(8) Lew, D., Parker, S. E., Latimer, T., Abai, A. M., Kuwahara, R., Doh, S. G., Yang, Z. Y., Laface, D., Gromkowski, S. H., and Nabel, G. J. (1995) Cancer gene therapy using plasmid DNA: pharmacokinetic study of DNA following injection in mice [see comments] 389. *Hum Gene Ther 6*, 553-564.
(9) Harrington, K. J., Spitzweg, C., Bateman, A. R., Morris, J. C., and Vile, R. G. (2001) Gene therapy for prostate cancer: current status and future prospects 1. *J.Urol. 166*, 1220-1233.
(10) http://www.wiley.com/legacy/wileychi/genmed/clinical/.
(11) Nathwani, A. C., Tuddenham, E. G., Rangarajan, S., Rosales, C., McIntosh, J., Linch, D. C., Chowdary, P., Riddell, A., Pie, A. J., Harrington, C., O'Beirne, J., Smith, K., Pasi, J., Glader, B., Rustagi, P., Ng, C. Y., Kay, M. A., Zhou, J., Spence, Y., Morton, C. L., Allay, J., Coleman, J., Sleep, S., Cunningham, J. M., Srivastava, D., Basner-Tschakarjan, E., Mingozzi, F., High, K. A., Gray, J. T., Reiss, U. M., Nienhuis, A. W., and Davidoff, A. M. (2011) Adenovirus-associated virus vector-mediated gene transfer in hemophilia B. *The New England journal of medicine 365*, 2357-65.
(12) Ashtari, M., Cyckowski, L. L., Monroe, J. F., Marshall, K. A., Chung, D. C., Auricchio, A., Simonelli, F., Leroy, B. P., Maguire, A. M., Shindler, K. S., and Bennett, J. (2011) The human visual cortex responds to gene therapy-mediated recovery of retinal function. *J Clin Invest 121*, 2160-8.
(13) Verma, I. M., and Somia, N. (1997) Gene therapy -- promises, problems and prospects. *Nature 389*, 239-42.
(14) Fire, A., Albertson, D., Harrison, S. W., and Moerman, D. G. (1991) Production of antisense RNA leads to effective and specific inhibition of gene expression in C. elegans muscle. *Development (Cambridge, England) 113*, 503-14.
(15) Fire, A., Xu, S., Montgomery, M. K., Kostas, S. A., Driver, S. E., and Mello, C. C. (1998) Potent and specific genetic interference by double-stranded RNA in Caenorhabditis elegans. *Nature 391*, 806-811.
(16) Elbashir, S. M., Harborth, J., Lendeckel, W., Yalcin, A., Weber, K., and Tuschl, T. (2001) Duplexes of 21-nucleotide RNAs mediate RNA interference in cultured mammalian cells. *Nature 411*, 494-8.

(17) Bumcrot, D., Manoharan, M., Koteliansky, V., and Sah, D. W. (2006) RNAi therapeutics: a potential new class of pharmaceutical drugs. *Nature chemical biology 2*, 711-9.
(18) Matranga, C., Tomari, Y., Shin, C., Bartel, D. P., and Zamore, P. D. (2005) Passenger-strand cleavage facilitates assembly of siRNA into Ago2-containing RNAi enzyme complexes. *Cell 123*, 607-20.
(19) Ameres, S. L., Martinez, J., and Schroeder, R. (2007) Molecular basis for target RNA recognition and cleavage by human RISC. *Cell 130*, 101-12.
(20) McCaffrey, A. P., Meuse, L., Pham, T. T., Conklin, D. S., Hannon, G. J., and Kay, M. A. (2002) RNA interference in adult mice. *Nature 418*, 38-9.
(21) Turner, J. J., Jones, S. W., Moschos, S. A., Lindsay, M. A., and Gait, M. J. (2007) MALDI-TOF mass spectral analysis of siRNA degradation in serum confirms an RNAse A-like activity. *Molecular bioSystems 3*, 43-50.
(22) Xie, F. Y., Woodle, M. C., and Lu, P. Y. (2006) Harnessing in vivo siRNA delivery for drug discovery and therapeutic development. *Drug Discov Today 11*, 67-73.
(23) Anderson, W. F. (1998) Human gene therapy. *Nature 392*, 25-30.
(24) Braasch, D. A., Paroo, Z., Constantinescu, A., Ren, G., Oz, O. K., Mason, R. P., and Corey, D. R. (2004) Biodistribution of phosphodiester and phosphorothioate siRNA. *Bioorganic & medicinal chemistry letters 14*, 1139-43.
(25) Pack, D. W., Hoffman, A. S., Pun, S., and Stayton, P. S. (2005) Design and development of polymers for gene delivery. *Nat.Rev.Drug Discov. 4*, 581-593.
(26) Li, S. D., and Huang, L. (2007) Non-viral is superior to viral gene delivery. *J Control Release 123*, 181-3.
(27) Tatsis, N., and Ertl, H. C. (2004) Adenoviruses as vaccine vectors. *Mol Ther 10*, 616-29.
(28) Gao, K., and Huang, L. (2009) Nonviral methods for siRNA delivery. *Mol Pharm 6*, 651-8.
(29) Wagner, E. (2008) Converging Paths of Viral and Non-viral Vector Engineering. *Mol Ther 16*, 1-2.
(30) Zuber, G., Dauty, E., Nothisen, M., Belguise, P., and Behr, J. P. (2001) Towards synthetic viruses. *Adv.Drug Deliv.Rev. 52*, 245-253.
(31) Wagner, E. (2004) Strategies to improve DNA polyplexes for in vivo gene transfer: will "artificial viruses" be the answer? *Pharm.Res. 21*, 8-14.
(32) Hughes, J., Yadava, P., and Mesaros, R. (2010) Liposomal siRNA delivery. *Methods Mol Biol 605*, 445-59.
(33) Parker, A. L., Newman, C., Briggs, S., Seymour, L., and Sheridan, P. J. (2003) Nonviral gene delivery: techniques and implications for molecular medicine. *Expert.Rev.Mol.Med. 5*, 1-15.
(34) Ogris, M., Steinlein, P., Carotta, S., Brunner, S., and Wagner, E. (2001) DNA/polyethylenimine transfection particles: Influence of ligands, polymer size, and PEGylation on internalization and gene expression. *AAPS.PharmSci. 3*, E21.
(35) Behr, J. P. (1997) The proton sponge: A trick to enter cells the viruses did not exploit. *Chimia 51*, 34-36.
(36) Plank, C., Mechtler, K., Szoka, F. C., Jr., and Wagner, E. (1996) Activation of the complement system by synthetic DNA complexes: a potential barrier for intravenous gene delivery. *Hum.Gene Ther 7*, 1437-1446.
(37) Ogris, M., and Wagner, E. (2002) Tumor-targeted gene transfer with DNA polyplexes. *Somat.Cell Mol Genet. 27*, 85-95.
(38) Fischer, D., Li, Y., Ahlemeyer, B., Krieglstein, J., and Kissel, T. (2003) In vitro cytotoxicity testing of polycations: influence of polymer structure on cell

viability and hemolysis. *Biomaterials 24*, 1121-1131.
(39) Wagner, E. (2012) Polymers for siRNA Delivery: Inspired by Viruses to be Targeted, Dynamic, and Precise. *Accounts of chemical research 45*, 1005-13.
(40) Schaffert, D., Troiber, C., Salcher, E. E., Fröhlich, T., Martin, I., Badgujar, N., Dohmen, C., Edinger, D., Kläger, R., Maiwald, G., Farkasova, K., Seeber, S., Jahn-Hofmann, K., Hadwiger, P., and Wagner, E. (2011) Solid-Phase Synthesized Sequence-Defined T-Shape, i-Shape and U-Shape Polymers for pDNA and siRNA Delivery. *Angew Chem Int Ed Engl*, Aug 11, 2011 [Epub ahead of print].
(41) Schaffert, D., Badgujar, N., and Wagner, E. (2011) Novel Fmoc-polyamino acids for solid-phase synthesis of defined polyamidoamines. *Org Lett 13*, 1586-9.
(42) Hartmann, L., Hafele, S., Peschka-Suss, R., Antonietti, M., and Borner, H. G. (2008) Tailor-Made Poly(amidoamine)s for Controlled Complexation and Condensation of DNA. *Chemistry. 14*, 2025-2033.
(43) Plank, C., Oberhauser, B., Mechtler, K., Koch, C., and Wagner, E. (1994) The influence of endosome-disruptive peptides on gene transfer using synthetic virus-like gene transfer systems. *J Biol.Chem. 269*, 12918-12924.
(44) Dohmen, C., Edinger, D., Frohlich, T., Schreiner, L., Lachelt, U., Troiber, C., Radler, J., Hadwiger, P., Vornlocher, H. P., and Wagner, E. (2012) Nanosized Multifunctional Polyplexes for Receptor-Mediated SiRNA Delivery. *ACS Nano 6*, 5198-208.
(45) Sneader, W. (1996) *Drug Prototypes and Their Exploitation*, Wiley, UK.
(46) Newman, D. J., Cragg, G. M., and Snader, K. M. (2000) The influence of natural products upon drug discovery. *Natural product reports 17*, 215-34.
(47) Harvey, A. L. (2008) Natural products in drug discovery. *Drug Discov Today 13*, 894-901.
(48) Clark, A. M. (1996) Natural products as a resource for new drugs. *Pharm Res 13*, 1133-44.
(49) Herrmann, J., Elnakady, Y. A., Wiedmann, R. M., Ullrich, A., Rohde, M., Kazmaier, U., Vollmar, A. M., and Muller, R. (2012) Pretubulysin: from hypothetical biosynthetic intermediate to potential lead in tumor therapy. *PLoS One 7*, e37416.
(50) Tan, L. T. (2007) Bioactive natural products from marine cyanobacteria for drug discovery. *Phytochemistry 68*, 954-79.
(51) Lam, K. S. (2006) Discovery of novel metabolites from marine actinomycetes. *Current opinion in microbiology 9*, 245-51.
(52) Fenical, W., and Jensen, P. R. (2006) Developing a new resource for drug discovery: marine actinomycete bacteria. *Nature chemical biology 2*, 666-73.
(53) Wenzel, S. C., and Muller, R. (2009) Myxobacteria--'microbial factories' for the production of bioactive secondary metabolites. *Molecular bioSystems 5*, 567-74.
(54) Iizuka, T., Jojima, Y., Fudou, R., and Yamanaka, S. (1998) Isolation of myxobacteria from the marine environment. *FEMS microbiology letters 169*, 317-22.
(55) Ravenschlag, K., Sahm, K., Pernthaler, J., and Amann, R. (1999) High bacterial diversity in permanently cold marine sediments. *Applied and environmental microbiology 65*, 3982-9.
(56) Velicer, G. J., and Vos, M. (2009) Sociobiology of the myxobacteria. *Annual review of microbiology 63*, 599-623.
(57) Reichenbach, H. (2001) Myxobacteria, producers of novel bioactive substances. *Journal of industrial microbiology & biotechnology 27*, 149-56.
(58) Nan, B., Chen, J., Neu, J. C., Berry, R. M., Oster, G., and Zusman, D. R.

(2011) Myxobacteria gliding motility requires cytoskeleton rotation powered by proton motive force. *Proc Natl Acad Sci U S A 108*, 2498-503.
(59) Shimkets, L. J. (1990) Social and developmental biology of the myxobacteria. *Microbiological reviews 54*, 473-501.
(60) Oxford, A. E. (1947) Observations Concerning the Growth and Metabolic Activities of Myxococci in a Simple Protein-free Liquid Medium. *Journal of bacteriology 53*, 129-38.
(61) Ringel, S. M., Greenough, R. C., Roemer, S., Connor, D., Gutt, A. L., Blair, B., Kanter, G., and von, S. (1977) Ambruticin (W7783), a new antifungal antibiotic. *The Journal of antibiotics 30*, 371-5.
(62) Reichenbach, H., and Hofle, G. (1993) Biologically active secondary metabolites from myxobacteria. *Biotechnology advances 11*, 219-77.
(63) Bode, H. B., and Muller, R. (2006) Analysis of myxobacterial secondary metabolism goes molecular. *Journal of industrial microbiology & biotechnology 33*, 577-88.
(64) Weissman, K. J., and Muller, R. (2010) Myxobacterial secondary metabolites: bioactivities and modes-of-action. *Natural product reports 27*, 1276-95.
(65) Weissman, K. J., and Muller, R. (2009) A brief tour of myxobacterial secondary metabolism. *Bioorganic & medicinal chemistry 17*, 2121-36.
(66) Gerth, K., Pradella, S., Perlova, O., Beyer, S., and Muller, R. (2003) Myxobacteria: proficient producers of novel natural products with various biological activities--past and future biotechnological aspects with the focus on the genus Sorangium. *Journal of biotechnology 106*, 233-53.
(67) Bollag, D. M., McQueney, P. A., Zhu, J., Hensens, O., Koupal, L., Liesch, J., Goetz, M., Lazarides, E., and Woods, C. M. (1995) Epothilones, a new class of microtubule-stabilizing agents with a taxol-like mechanism of action. *Cancer Res 55*, 2325-33.
(68) Sasse, F., Steinmetz, H., Heil, J., Hofle, G., and Reichenbach, H. (2000) Tubulysins, new cytostatic peptides from myxobacteria acting on microtubuli. Production, isolation, physico-chemical and biological properties. *The Journal of antibiotics 53*, 879-85.
(69) Kunze, B., Jansen, R., Sasse, F., Hofle, G., and Reichenbach, H. (1995) Chondramides A approximately D, new antifungal and cytostatic depsipeptides from Chondromyces crocatus (myxobacteria). Production, physico-chemical and biological properties. *The Journal of antibiotics 48*, 1262-6.
(70) Kunze, B., Jansen, R., Sasse, F., Hofle, G., and Reichenbach, H. (1998) Apicularens A and B, new cytostatic macrolides from Chondromyces species (myxobacteria): production, physico-chemical and biological properties. *The Journal of antibiotics 51*, 1075-80.
(71) Sasse, F., Steinmetz, H., Hofle, G., and Reichenbach, H. (2003) Archazolids, new cytotoxic macrolactones from Archangium gephyra (Myxobacteria). Production, isolation, physico-chemical and biological properties. *The Journal of antibiotics 56*, 520-5.
(72) Huss, M., Sasse, F., Kunze, B., Jansen, R., Steinmetz, H., Ingenhorst, G., Zeeck, A., and Wieczorek, H. (2005) Archazolid and apicularen: novel specific V-ATPase inhibitors. *BMC biochemistry 6*, 13.
(73) Izumi, H., Torigoe, T., Ishiguchi, H., Uramoto, H., Yoshida, Y., Tanabe, M., Ise, T., Murakami, T., Yoshida, T., Nomoto, M., and Kohno, K. (2003) Cellular pH regulators: potentially promising molecular targets for cancer chemotherapy. *Cancer treatment reviews 29*, 541-9.
(74) Sennoune, S. R., Luo, D., and Martinez-Zaguilan, R. (2004)

Plasmalemmal vacuolar-type H+-ATPase in cancer biology. *Cell biochemistry and biophysics 40*, 185-206.
(75) Sennoune, S. R., Bakunts, K., Martinez, G. M., Chua-Tuan, J. L., Kebir, Y., Attaya, M. N., and Martinez-Zaguilan, R. (2004) Vacuolar H+-ATPase in human breast cancer cells with distinct metastatic potential: distribution and functional activity. *American journal of physiology. Cell physiology 286*, C1443-52.
(76) Werner, G., Hagenmaier, H., Drautz, H., Baumgartner, A., and Zahner, H. (1984) Metabolic products of microorganisms. 224. Bafilomycins, a new group of macrolide antibiotics. Production, isolation, chemical structure and biological activity. *The Journal of antibiotics 37*, 110-7.
(77) Kinashi, H., Someno, K., and Sakaguchi, K. (1984) Isolation and characterization of concanamycins A, B and C. *The Journal of antibiotics 37*, 1333-43.
(78) Bowman, E. J., Siebers, A., and Altendorf, K. (1988) Bafilomycins: a class of inhibitors of membrane ATPases from microorganisms, animal cells, and plant cells. *Proc Natl Acad Sci U S A 85*, 7972-6.
(79) Wiedmann, R. M. (2011) in *Department of Chemistry and Pharmacy*, Ludwig-Maximilians-University, Munich.
(80) Wiedmann, R. M., von Schwarzenberg, K., Palamidessi, A., Schreiner, L., Kubisch, R., Liebl, J., Schempp, C., Trauner, D., Vereb, G., Zahler, S., Wagner, E., Muller, R., Scita, G., and Vollmar, A. M. (2012) The V-ATPase-inhibitor Archazolid abrogates tumor metastasis via inhibition of endocytic activation of the Rho-GTPase Rac1. *Cancer Res*.
(81) Ullrich, A., Chai, Y., Pistorius, D., Elnakady, Y. A., Herrmann, J. E., Weissman, K. J., Kazmaier, U., and Muller, R. (2009) Pretubulysin, a potent and chemically accessible tubulysin precursor from Angiococcus disciformis. *Angew Chem Int Ed Engl 48*, 4422-5.
(82) Steinmetz, H., Glaser, N., Herdtweck, E., Sasse, F., Reichenbach, H., and Hofle, G. (2004) Isolation, crystal and solution structure determination, and biosynthesis of tubulysins--powerful inhibitors of tubulin polymerization from myxobacteria. *Angew Chem Int Ed Engl 43*, 4888-92.
(83) Fornier, M. N. (2007) Ixabepilone, first in a new class of antineoplastic agents: the natural epothilones and their analogues. *Clinical breast cancer 7*, 757-63.
(84) Rath, S., Liebl, J., Furst, R., Ullrich, A., Burkhart, J. L., Kazmaier, U., Herrmann, J., Muller, R., Gunther, M., Schreiner, L., Wagner, E., Vollmar, A. M., and Zahler, S. (2012) Anti-angiogenic effects of the tubulysin precursor pretubulysin and of simplified pretubulysin derivatives. *British journal of pharmacology*.
(85) Gerth, K., Bedorf, N., Hofle, G., Irschik, H., and Reichenbach, H. (1996) Epothilons A and B: antifungal and cytotoxic compounds from Sorangium cellulosum (Myxobacteria). Production, physico-chemical and biological properties. *The Journal of antibiotics 49*, 560-3.
(86) Hagelueken, G., Albrecht, S. C., Steinmetz, H., Jansen, R., Heinz, D. W., Kalesse, M., and Schubert, W. D. (2009) The absolute configuration of rhizopodin and its inhibition of actin polymerization by dimerization. *Angew Chem Int Ed Engl 48*, 595-8.
(87) Sasse, F., Steinmetz, H., Hofle, G., and Reichenbach, H. (1993) Rhizopodin, a new compound from Myxococcus stipitatus (myxobacteria) causes formation of rhizopodia-like structures in animal cell cultures. Production, isolation, physico-chemical and biological properties. *The Journal of antibiotics*

46, 741-8.
(88) Sasse, F., Kunze, B., Gronewold, T. M., and Reichenbach, H. (1998) The chondramides: cytostatic agents from myxobacteria acting on the actin cytoskeleton. *Journal of the National Cancer Institute 90*, 1559-63.
(89) Scott, V. R., Boehme, R., and Matthews, T. R. (1988) New class of antifungal agents: jasplakinolide, a cyclodepsipeptide from the marine sponge, Jaspis species. *Antimicrobial agents and chemotherapy 32*, 1154-7.
(90) Takeuchi, H., Ara, G., Sausville, E. A., and Teicher, B. (1998) Jasplakinolide: interaction with radiation and hyperthermia in human prostate carcinoma and Lewis lung carcinoma. *Cancer chemotherapy and pharmacology 42*, 491-6.
(91) Leaf, C. (2004) Why we're losing the war on cancer (and how to win it). *Fortune 149*, 76-82, 84-6, 88 passim.
(92) Gabor Miklos, G. L. (2005) The human cancer genome project--one more misstep in the war on cancer. *Nat Biotechnol 23*, 535-7.
(93) Seymour, L. W., Ulbrich, K., Steyger, P. S., Brereton, M., Subr, V., Strohalm, J., and Duncan, R. (1994) Tumour tropism and anti-cancer efficacy of polymer-based doxorubicin prodrugs in the treatment of subcutaneous murine B16F10 melanoma. *British journal of cancer 70*, 636-41.
(94) Gianasi, E., Wasil, M., Evagorou, E. G., Keddle, A., Wilson, G., and Duncan, R. (1999) HPMA copolymer platinates as novel antitumour agents: in vitro properties, pharmacokinetics and antitumour activity in vivo. *European journal of cancer (Oxford, England : 1990) 35*, 994-1002.
(95) Duncan, R., and Spreafico, F. (1994) Polymer conjugates. Pharmacokinetic considerations for design and development. *Clinical pharmacokinetics 27*, 290-306.
(96) Fang, J., Nakamura, H., and Maeda, H. (2011) The EPR effect: Unique features of tumor blood vessels for drug delivery, factors involved, and limitations and augmentation of the effect. *Adv Drug Deliv Rev 63*, 136-51.
(97) Longley, D. B., and Johnston, P. G. (2005) Molecular mechanisms of drug resistance. *The Journal of pathology 205*, 275-92.
(98) Chien, A. J., and Moasser, M. M. (2008) Cellular mechanisms of resistance to anthracyclines and taxanes in cancer: intrinsic and acquired. *Seminars in oncology 35*, S1-S14; quiz S39.
(99) Coley, H. M. (2008) Mechanisms and strategies to overcome chemotherapy resistance in metastatic breast cancer. *Cancer treatment reviews 34*, 378-90.
(100) Gatti, L., and Zunino, F. (2005) Overview of tumor cell chemoresistance mechanisms. *Methods in molecular medicine 111*, 127-48.
(101) Matsumura, Y., and Maeda, H. (1986) A new concept for macromolecular therapeutics in cancer chemotherapy: mechanism of tumoritropic accumulation of proteins and the antitumor agent smancs. *Cancer Res. 46*, 6387-6392.
(102) Folkman, J. (1971) Tumor angiogenesis: therapeutic implications. *N.Engl.J Med. 285*, 1182-1186.
(103) Folkman, J. (1995) Angiogenesis in cancer, vascular, rheumatoid and other disease. *Nat.Med. 1*, 27-31.
(104) Fang, J., Sawa, T., and Maeda, H. (2003) Factors and mechanism of "EPR" effect and the enhanced antitumor effects of macromolecular drugs including SMANCS. *Adv Exp Med Biol 519*, 29-49.
(105) Maeda, H., Bharate, G. Y., and Daruwalla, J. (2009) Polymeric drugs for efficient tumor-targeted drug delivery based on EPR-effect. *Eur J Pharm Biopharm 71*, 409-19.

(106) Noguchi, Y., Wu, J., Duncan, R., Strohalm, J., Ulbrich, K., Akaike, T., and Maeda, H. (1998) Early phase tumor accumulation of macromolecules: a great difference in clearance rate between tumor and normal tissues. *Jpn.J Cancer Res 89*, 307-314.
(107) Maeda, H., and Matsumura, Y. (1989) Tumoritropic and lymphotropic principles of macromolecular drugs. *Critical reviews in therapeutic drug carrier systems 6*, 193-210.
(108) Greish, K., Fang, J., Inutsuka, T., Nagamitsu, A., and Maeda, H. (2003) Macromolecular therapeutics: advantages and prospects with special emphasis on solid tumour targeting. *Clinical pharmacokinetics 42*, 1089-105.
(109) Harrington, K. J., Mohammadtaghi, S., Uster, P. S., Glass, D., Peters, A. M., Vile, R. G., and Stewart, J. S. (2001) Effective targeting of solid tumors in patients with locally advanced cancers by radiolabeled pegylated liposomes. *Clin Cancer Res 7*, 243-54.
(110) Greish, K., Sawa, T., Fang, J., Akaike, T., and Maeda, H. (2004) SMA-doxorubicin, a new polymeric micellar drug for effective targeting to solid tumours. *J Control Release 97*, 219-30.
(111) Iyer, A. K., Greish, K., Seki, T., Okazaki, S., Fang, J., Takeshita, K., and Maeda, H. (2007) Polymeric micelles of zinc protoporphyrin for tumor targeted delivery based on EPR effect and singlet oxygen generation. *Journal of drug targeting 15*, 496-506.
(112) Duncan, R. (2003) The dawning era of polymer therapeutics. *Nat.Rev.Drug Discov. 2*, 347-360.
(113) Matsumura, Y., and Kataoka, K. (2009) Preclinical and clinical studies of anticancer agent-incorporating polymer micelles. *Cancer science 100*, 572-9.
(114) Haag, R., and Kratz, F. (2006) Polymer therapeutics: concepts and applications. *Angew Chem Int Ed Engl 45*, 1198-215.
(115) Ringsdorf, H. (1975) Structure and properties of pharmacologically active polymers. *Journal of Polymer Science: Polymer Symposia 51*, 135-153.
(116) Duncan, R., Vicent, M. J., Greco, F., and Nicholson, R. I. (2005) Polymer-drug conjugates: towards a novel approach for the treatment of endrocine-related cancer. *Endocrine-related cancer 12 Suppl 1*, S189-99.
(117) Meerum Terwogt, J. M., ten Bokkel Huinink, W. W., Schellens, J. H., Schot, M., Mandjes, I. A., Zurlo, M. G., Rocchetti, M., Rosing, H., Koopman, F. J., and Beijnen, J. H. (2001) Phase I clinical and pharmacokinetic study of PNU166945, a novel water-soluble polymer-conjugated prodrug of paclitaxel. *Anti-cancer drugs 12*, 315-23.
(118) Vasey, P. A., Kaye, S. B., Morrison, R., Twelves, C., Wilson, P., Duncan, R., Thomson, A. H., Murray, L. S., Hilditch, T. E., Murray, T., Burtles, S., Fraier, D., Frigerio, E., and Cassidy, J. (1999) Phase I clinical and pharmacokinetic study of PK1 [N-(2-hydroxypropyl)methacrylamide copolymer doxorubicin]: first member of a new class of chemotherapeutic agents-drug-polymer conjugates. Cancer Research Campaign Phase I/II Committee. *Clin Cancer Res 5*, 83-94.
(119) Yurkovetskiy, A. V., and Fram, R. J. (2009) XMT-1001, a novel polymeric camptothecin pro-drug in clinical development for patients with advanced cancer. *Adv Drug Deliv Rev 61*, 1193-202.
(120) Duncan, R. (2005) Targeting and intracellular delivery of drugs, in *Encyclopedia of Molecular Cell Biology and Molecular Medicine* (Meyers, R., Ed.), Wiley-VCH Verlag, Weinheim, Germany.
(121) Duncan, R. (2006) Polymer conjugates as anticancer nanomedicines. *Nat Rev Cancer 6*, 688-701.
(122) Seymour, L. W., Ferry, D. R., Anderson, D., Hesslewood, S., Julyan, P. J.,

Poyner, R., Doran, J., Young, A. M., Burtles, S., and Kerr, D. J. (2002) Hepatic drug targeting: phase I evaluation of polymer-bound doxorubicin. *Journal of clinical oncology : official journal of the American Society of Clinical Oncology 20*, 1668-76.
(123) Allen, T. M. (2002) Ligand-targeted therapeutics in anticancer therapy. *Nat Rev Cancer 2*, 750-63.
(124) Duncan, R. (2011) Polymer therapeutics as nanomedicines: new perspectives. *Current opinion in biotechnology 22*, 492-501.
(125) Nowotnik, D. P., and Cvitkovic, E. (2009) ProLindac (AP5346): a review of the development of an HPMA DACH platinum Polymer Therapeutic. *Adv Drug Deliv Rev 61*, 1214-9.
(126) Dipetrillo, T., Suntharalingam, M., Ng, T., Fontaine, J., Horiba, N., Oldenburg, N., Perez, K., Birnbaum, A., Battafarano, R., Burrows, W., and Safran, H. (2012) Neoadjuvant paclitaxel poliglumex, cisplatin, and radiation for esophageal cancer: a phase 2 trial. *American journal of clinical oncology 35*, 64-7.
(127) Seymour, L. W., Ferry, D. R., Kerr, D. J., Rea, D., Whitlock, M., Poyner, R., Boivin, C., Hesslewood, S., Twelves, C., Blackie, R., Schatzlein, A., Jodrell, D., Bissett, D., Calvert, H., Lind, M., Robbins, A., Burtles, S., Duncan, R., and Cassidy, J. (2009) Phase II studies of polymer-doxorubicin (PK1, FCE28068) in the treatment of breast, lung and colorectal cancer. *Int J Oncol 34*, 1629-36.
(128) Li, C., Yu, D. F., Newman, R. A., Cabral, F., Stephens, L. C., Hunter, N., Milas, L., and Wallace, S. (1998) Complete regression of well-established tumors using a novel water-soluble poly(L-glutamic acid)-paclitaxel conjugate. *Cancer Res 58*, 2404-9.
(129) Bissett, D., Cassidy, J., de Bono, J. S., Muirhead, F., Main, M., Robson, L., Fraier, D., Magne, M. L., Pellizzoni, C., Porro, M. G., Spinelli, R., Speed, W., and Twelves, C. (2004) Phase I and pharmacokinetic (PK) study of MAG-CPT (PNU 166148): a polymeric derivative of camptothecin (CPT). *British journal of cancer 91*, 50-5.
(130) Vicent, M. J., Ringsdorf, H., and Duncan, R. (2009) Polymer therapeutics: clinical applications and challenges for development. *Adv Drug Deliv Rev 61*, 1117-20.
(131) Gilman, A. (1963) The initial clinical trial of nitrogen mustard. *American journal of surgery 105*, 574-8.
(132) Sarosy, G., Leyland-Jones, B., Soochan, P., and Cheson, B. D. (1988) The systemic administration of intravenous melphalan. *Journal of clinical oncology : official journal of the American Society of Clinical Oncology 6*, 1768-82.
(133) Samuels, B. L., and Bitran, J. D. (1995) High-dose intravenous melphalan: a review. *Journal of clinical oncology : official journal of the American Society of Clinical Oncology 13*, 1786-99.
(134) Duncan, R., Hume, I., Yardley, H., Flanagan, P., Ulbrich, K., Subr, V., and Strohalm, J. (1991) Macromolecular prodrugs for use in targeted cancer chemotherapy: melphalan covalently coupled to N- (2-hydroxypropyl) methacrylamide copolymers. *J. Cont. Rel. 16*, 121-136.
(135) Shukla, G., Tiwari, A. K., Kumar, N., Sinha, D., Mishra, P., Chandra, H., and Mishra, A. K. (2008) Polyethylene glycol conjugates of methotrexate and melphalan: synthesis, radiolabeling and biologic studies. *Cancer biotherapy & radiopharmaceuticals 23*, 571-9.
(136) Zhao, Z., Wang, J., Mao, H. Q., and Leong, K. W. (2003) Polyphosphoesters in drug and gene delivery. *Adv Drug Deliv Rev 55*, 483-99.
(137) Pencheva, I., Bogomilova, A., Koseva, N., Obreshkova, D., and Troev, K. (2008) HPLC study on the stability of bendamustine hydrochloride immobilized

onto polyphosphoesters. *Journal of pharmaceutical and biomedical analysis 48*, 1143-50.
(138) Penczek, S., Pretula, J., and Kaluzynski, K. (2005) Poly(alkylene phosphates): from synthetic models of biomacromolecules and biomembranes toward polymer-inorganic hybrids (mimicking biomineralization). *Biomacromolecules 6*, 547-51.
(139) Hartmann, L. C., Keeney, G. L., Lingle, W. L., Christianson, T. J., Varghese, B., Hillman, D., Oberg, A. L., and Low, P. S. (2007) Folate receptor overexpression is associated with poor outcome in breast cancer. *Int J Cancer 121*, 938-42.
(140) Toffoli, G., Cernigoi, C., Russo, A., Gallo, A., Bagnoli, M., and Boiocchi, M. (1997) Overexpression of folate binding protein in ovarian cancers. *Int J Cancer 74*, 193-8.
(141) Weitman, S. D., Lark, R. H., Coney, L. R., Fort, D. W., Frasca, V., Zurawski, V. R., Jr., and Kamen, B. A. (1992) Distribution of the folate receptor GP38 in normal and malignant cell lines and tissues. *Cancer Res 52*, 3396-401.
(142) Kularatne, S. A., and Low, P. S. (2010) Targeting of nanoparticles: folate receptor. *Methods Mol Biol 624*, 249-65.
(143) Boeckle, S., Wagner, E., and Ogris, M. (2005) C- versus N-terminally linked melittin-polyethylenimine conjugates: the site of linkage strongly influences activity of DNA polyplexes. *J Gene Med 7*, 1335-1347.
(144) Elsabahy, M., Nazarali, A., and Foldvari, M. (2011) Non-viral nucleic acid delivery: key challenges and future directions. *Current drug delivery 8*, 235-44.
(145) Frohlich, T., and Wagner, E. (2010) Peptide- and polymer-based delivery of therapeutic RNA. *Soft Matter 6*, 226-234.
(146) Harris, J. M., and Chess, R. B. (2003) Effect of pegylation on pharmaceuticals. *Nat Rev Drug Discov 2*, 214-21.
(147) Merkel, O. M., Librizzi, D., Pfestroff, A., Schurrat, T., Buyens, K., Sanders, N. N., De Smedt, S. C., Behe, M., and Kissel, T. (2009) Stability of siRNA polyplexes from poly(ethylenimine) and poly(ethylenimine)-g-poly(ethylene glycol) under in vivo conditions: effects on pharmacokinetics and biodistribution measured by Fluorescence Fluctuation Spectroscopy and Single Photon Emission Computed Tomography (SPECT) imaging. *J Control Release 138*, 148-59.
(148) Maeda, H. (2001) The enhanced permeability and retention (EPR) effect in tumor vasculature: the key role of tumor-selective macromolecular drug targeting. *Adv Enzyme Regul 41*, 189-207.
(149) Choi, H. S., Liu, W., Misra, P., Tanaka, E., Zimmer, J. P., Itty Ipe, B., Bawendi, M. G., and Frangioni, J. V. (2007) Renal clearance of quantum dots. *Nat Biotechnol 25*, 1165-70.
(150) Merdan, T., Kunath, K., Petersen, H., Bakowsky, U., Voigt, K. H., Kopecek, J., and Kissel, T. (2005) PEGylation of poly(ethylene imine) affects stability of complexes with plasmid DNA under in vivo conditions in a dose-dependent manner after intravenous injection into mice. *Bioconjug Chem 16*, 785-92.
(151) Perez-Sayans, M., Garcia-Garcia, A., Reboiras-Lopez, M. D., and Gandara-Vila, P. (2009) Role of V-ATPases in solid tumors: importance of the subunit C (Review). *Int J Oncol 34*, 1513-20.
(152) Lu, X., Qin, W., Li, J., Tan, N., Pan, D., Zhang, H., Xie, L., Yao, G., Shu, H., Yao, M., Wan, D., Gu, J., and Yang, S. (2005) The growth and metastasis of human hepatocellular carcinoma xenografts are inhibited by small interfering RNA targeting to the subunit ATP6L of proton pump. *Cancer Res 65*, 6843-9.

(153) Ohta, T., Arakawa, H., Futagami, F., Fushida, S., Kitagawa, H., Kayahara, M., Nagakawa, T., Miwa, K., Kurashima, K., Numata, M., Kitamura, Y., Terada, T., and Ohkuma, S. (1998) Bafilomycin A1 induces apoptosis in the human pancreatic cancer cell line Capan-1. *The Journal of pathology 185*, 324-30.
(154) Hettiarachchi, K. D., Zimmet, P. Z., and Myers, M. A. (2006) The effects of repeated exposure to sub-toxic doses of plecomacrolide antibiotics on the endocrine pancreas. *Food and chemical toxicology : an international journal published for the British Industrial Biological Research Association 44*, 1966-77.
(155) Banerjee, A., Brotherston, T. M., Lamberty, B. G., and Campbell, R. C. (1987) Cancer chemotherapy agent-induced perivenous extravasation injuries. *Postgraduate medical journal 63*, 5-9.
(156) Seyfer, A. E., and Solimando, D. A., Jr. (1983) Toxic lesions of the hand associated with chemotherapy. *The Journal of hand surgery 8*, 39-42.
(157) Pasquier, E., and Kavallaris, M. (2008) Microtubules: a dynamic target in cancer therapy. *IUBMB life 60*, 165-70.
(158) Kingston, D. G. (2009) Tubulin-interactive natural products as anticancer agents. *Journal of natural products 72*, 507-15.
(159) Dumontet, C., and Jordan, M. A. (2010) Microtubule-binding agents: a dynamic field of cancer therapeutics. *Nat Rev Drug Discov 9*, 790-803.
(160) Schluep, T., Gunawan, P., Ma, L., Jensen, G. S., Duringer, J., Hinton, S., Richter, W., and Hwang, J. (2009) Polymeric tubulysin-peptide nanoparticles with potent antitumor activity. *Clin Cancer Res 15*, 181-9.
(161) Leamon, C. P., Reddy, J. A., Vetzel, M., Dorton, R., Westrick, E., Parker, N., Wang, Y., and Vlahov, I. (2008) Folate targeting enables durable and specific antitumor responses from a therapeutically null tubulysin B analogue. *Cancer Res 68*, 9839-44.
(162) Zhdanko, A., Schmauder, A., Ma, C. I., Sibley, L. D., Sept, D., Sasse, F., and Maier, M. E. (2011) Synthesis of chondramide A analogues with modified beta-tyrosine and their biological evaluation. *Chemistry (Weinheim an der Bergstrasse, Germany) 17*, 13349-57.
(163) Bunnell, T. M., Burbach, B. J., Shimizu, Y., and Ervasti, J. M. (2011) beta-Actin specifically controls cell growth, migration, and the G-actin pool. *Molecular biology of the cell 22*, 4047-58.
(164) Veronese, F. M., Schiavon, O., Pasut, G., Mendichi, R., Andersson, L., Tsirk, A., Ford, J., Wu, G., Kneller, S., Davies, J., and Duncan, R. (2005) PEG-doxorubicin conjugates: influence of polymer structure on drug release, in vitro cytotoxicity, biodistribution, and antitumor activity. *Bioconjug Chem 16*, 775-84.
(165) Duncan, R. (2005) N-(2-Hydroxypropyl)methacrylamide copolymer conjugates., in *Polymeric Drug Delivery Systems* (Kwon, G., Ed.), Marcel Dekker, New York.
(166) Greish, K. (2010) Enhanced permeability and retention (EPR) effect for anticancer nanomedicine drug targeting. *Methods Mol Biol 624*, 25-37.
(167) Lage, H. (2008) An overview of cancer multidrug resistance: a still unsolved problem. *Cellular and molecular life sciences : CMLS 65*, 3145-67.
(168) Tsukagoshi, S. (2002) [A new LH-RH agonist for treatment of prostate cancer, 3-month controlled-release formulation of goserelin acetate (Zoladex LA 10.8 mg depot)--outline of pre-clinical and clinical studies]. *Gan to kagaku ryoho. Cancer & chemotherapy 29*, 1675-87.
(169) Heyns, C. F., Simonin, M. P., Grosgurin, P., Schall, R., and Porchet, H. C. (2003) Comparative efficacy of triptorelin pamoate and leuprolide acetate in men with advanced prostate cancer. *BJU international 92*, 226-31.
(170) Gros, P., Croop, J., Roninson, I., Varshavsky, A., and Housman, D. E.

(1986) Isolation and characterization of DNA sequences amplified in multidrug-resistant hamster cells. *Proc Natl Acad Sci U S A 83*, 337-41.
(171) Ueda, K., Cardarelli, C., Gottesman, M. M., and Pastan, I. (1987) Expression of a full-length cDNA for the human "MDR1" gene confers resistance to colchicine, doxorubicin, and vinblastine. *Proc Natl Acad Sci U S A 84*, 3004-8.
(172) Juliano, R. L., and Ling, V. (1976) A surface glycoprotein modulating drug permeability in Chinese hamster ovary cell mutants. *Biochim Biophys Acta 455*, 152-62.
(173) Miyamoto, Y., Oda, T., and Maeda, H. (1990) Comparison of the cytotoxic effects of the high- and low-molecular-weight anticancer agents on multidrug-resistant Chinese hamster ovary cells in vitro. *Cancer Res 50*, 1571-5.
(174) Miyamoto, Y., and Maeda, H. (1991) Enhancement by verapamil of neocarzinostatin action on multidrug-resistant Chinese hamster ovary cells: possible release of nonprotein chromophore in cells. *Japanese journal of cancer research : Gann 82*, 351-6.

VIII. APPENDIX

1. Abbreviations

CapA	Caprylic acid
CCD	Charge-coupled Device
DAPI	4',6-diamidino-2-phenylindole
DMSO	Dimethyl sulfoxide
DNA	Deoxyribonucleic acid
dsRNA	Double-stranded ribonucleic acid
e.g.	exempli gratia (for example)
EDTA	Ethylenediaminetetraacetic acid
EG5	Eglin 5, or KSP, Kinesin spindle protein
EPR effect	Enhanced permeability and retention effect
FCS	Fluorescence correlation spectroscopy
FCS	Fetal calf serum
FolA	Folic acid
HA-2	Hemagglutinin subunit 2
HBG	Hepes buffered glucose
HEPES	N-(2-hydroxyethyl) piperazine-N'-(2-ethansulfonic acid)
i.p.	Intraperitoneal(ly)
i.v.	Intravenous(ly)
LCA	Leber congenital amaurosis
LPEI	Linear polyethylenimine
Luc	Luciferin
MDR	Multidrug resistance
mRNA	Messenger ribonucleic acid
MTT	3-(4,5-dimethylthiazol-2-yl)-2,5-diphenyltetrazolium bromide
N/P	Polymer nitrogen to nucleic acid phosphate ratio

NIR	Near infrared
PBS	Phosphate buffered saline
pDNA	Plasmid deoxyribonucleic acid
PEG	Polyethylene glycol
PEG_{24}	Polyethylene glycol with exactly 24 monomers (= “1 PEG”)
P-glycoprotein	Permeability glycoprotein
r_h	Hydrodynamic radius
RISC	Ribonucleic acid induced silencing complex
RNA	Ribonucleic acid
RNAi	Ribonucleic acid interference
ROI	Region of Interest
S.E.M.	Standard Error of the Mean
SCID	Severe combined immunodeficiency
siRNA	Small interfering ribonucleic acid
SteA	Stearic acid
Stp	Succinoyl-tetraethylenpentamine
TBE-buffer	Tris-Boric acid-EDTA-buffer
TCEP	Tris(2-carboxyethyl)phosphine
V-ATPase	Vacuolar-type H^+-ATPase
w/v	Weight per volume
Y3	Tyrosin-Tyrosin-Tyrosin (Tyrosin trimer)

2. Publications

2.1. Original papers

Rath S, Liebl J, Furst R, Ullrich A, Burkhart JL, Kazmaier U, Herrmann J, Muller R, Gunther M, Schreiner L, Wagner E, Vollmar AM, and Zahler S. (2012) **Anti-angiogenic effects of the tubulysin precursor pretubulysin and of simplified pretubulysin derivatives.** *British Journal Pharmacology*.

Dohmen C, Edinger D, Frohlich T, Schreiner L, Lachelt U, Troiber C, Radler J, Hadwiger P, Vornlocher HP, and Wagner E. (2012) **Nanosized Multifunctional Polyplexes for Receptor-Mediated SiRNA Delivery.** *ACS Nano* 6, 5198-5208.

Wiedmann R, Schwarzenberg K, Palamidessi A, Schreiner L, Kubisch R, Liebl J, Schempp C, Trauner D, Zahler S, Wagner E, Müller R, Scita G and Vollmar AM. **The V-ATPase-inhibitor Archazolid abrogates tumor metastasis via inhibition of endocytic activation of the Rho-GTPase Rac1.** *Cancer Research*.

Christina Troiber, Daniel Edinger, Petra Kos, Laura Schreiner, Raphaela Kläger, Annika Herrmann, Ernst Wagner. **Stabilizing effect of tyrosine trimers on pDNA and siRNA polyplexes.** *Biomaterials.*

Bogomilova A*, Hohn M, Gunther M. Troev K, Wagner E and Schreiner L*. **Phosphopolymer-immobilized Melphalan Conjugate and Complexes as Antitumoral Agents.** *Bioconjugate Chemistry* (*corresponding authors). Manuscript prepared.

2.2. Abstracts

Laura Schreiner, Rebekka Kubisch, Romina Wiedmann, Angelika M Vollmar, Ernst Wagner. **Archazolid reduces experimental breast cancer metastasis *in vivo*.** NAD 2012, Olomouc, Czech Rep.

Magdalena Menhofer, Verena Kretschmann, Laura Schreiner, Rebekka Kubisch, Ernst Wagner, Rolf Müller, Robert Fürst, Angelika Vollmar, Stefan Zahler. **The myxobacterial compound chondramide shows anti-angiogenic and anti-migratory potency.** NAD 2012, Olomouc, Czech Rep.

IX. ACKNOWLEDGEMENTS

It would not have been possible to write this doctoral thesis without the help and support of a lot of people.

First of all, I would like to thank Univ.-Prof. Dr. Ernst Wagner, my supervisor at the chair of pharmaceutical biotechnology of the Ludwig-Maximilians-University Munich. This thesis would not have been possible without his help and professional support. Furthermore, I want to thank him for his careful proofreading of this thesis.

I would like to express my gratitude to Univ.-Prof. Dr. Eckhard Wolf for being my veterinary supervisor and for accepting this doctoral thesis at the veterinary faculty.

I would like to thank Univ.-Prof. Dr. Angelika Vollmar for her intensive support and supervision concerning the FOR 1406 project. Being part of this DFG-research group was a great pleasure for me. Hence, I would like to thank all project members for their great scientific contributions and for the good time I had during our meetings.

Thanks a lot to Dr. Martina Rüffer for her help concerning the practical courses.

I would like to thank Dr. Anita Bogomilova for synthesizing the polyphosphoesters and the melphalan formulations.

Wolfgang Rödl deserves my deepest “PC-gratitude” for helping me, whenever I needed his technical support. More important, it was reassuring, having him as a professional first aider at our department.

My gratitude goes to Miriam Höhn for her great scientific support concerning the melphalan experiments and her dedicated administrative work.

I would like to thank Markus Kovac for looking after our mice and for his help and the good atmosphere in the animal facility.

Furthermore, I would like to thank Ursula Biebl and Anna Kulinyak for their work in the labs.

I would like to express my gratitude to Olga Brück for handling the administrative stuff in our working group.

My special thanks go to Raphaela Kläger for her teamwork in the animal facility and for discussing veterinary and non-veterinary problems with me. It was great, having you as a colleague.

I want to thank Rebekka Kubisch for her cooperation in all FOR experiments. I

thank her for the great scientific support but even more for her personal support and the great time we had together. One song will always remind me of this time.

Christian Dohmen answered all polyplex questions I had, synthesized the polymers and performed the *ex vivo* gel electrophoresis - thanks a lot for this huge support.

I would like to thank Daniel Edinger, who performed the siRNA *in vivo* experiments and aster evaluations together with me.

Thanks a lot to Christina Troiber for carrying out the fluorescence correlation spectroscopy and the gel electrophoresis. Thank you for proofreading this thesis and for the numerous coffee breaks during the last weeks.

I want to thank the whole "AK Wagner" for being an amazing team. I had a great time with you during my PhD.

I would like to express my deepest gratitude to my family. I appreciate the social backing and the emotional support, you show me at any time. Thank you for being there, when I need you.

Thank you, Oliver, for being who you are and accepting me as I am. Thank you for being by my side, especially in the last nerve-racking weeks.

All of you were of great importance, creating this doctoral thesis.